UNIVERSITÉ DE SHERBROOKE
Faculté de génie
Département de génie chimique et de génie biotechnologie

STUDY OF NITROUS OXIDE ADSORPTION BY ZEOLITIC IMIDAZOLATE FRAMEWORK-8 (ZIF-8): MOLECULAR MODELING AND COMPUTATIONAL CHEMISTRY

ÉTUDE DE L'ADSORPTION DE L'OXYDE NITREUX SUR LE *ZEOLITIC IMIDAZOLATE FRAMEWORK-8* (ZIF-8): MODÉLISATION MOLÉCULAIRE ET CHIMIE COMPUTATIONNELLE

Mémoire de maîtrise
Spécialité : génie chimique

Karen VILLEGAS DOMÍNGUEZ

Sherbrooke (Québec) Canada

Septembre 2021

JURY MEMBERS

Pr. Michèle HEITZ
_____

(Université de Sherbrooke)
Supervisor

Dr. Antonio AVALOS RAMIREZ
_____

(Centre National en Électrochimie et en Technologies Environnementales)
Co-supervisor

Pr. Satinder KAUR BRAR
_____

(York University)
Co-supervisor

Dr. Beatriz DELGADO CANO
_____

(Centre National en Électrochimie et en Technologies Environnementales)
External examiner

Dr. Alain WILKIN
_____

(Cégep de Shawinigan)
External examiner

Pr. Gervais SOUCY
_____

(Université de Sherbrooke)
Internal examiner and reporter

ABSTRACT

Nitrous oxide (N_2O) is a greenhouse gas (GHG) mainly issued from agriculture and waste management activities, such as the use of nitrogen-based fertilizers and livestock manure storage. This gas has a global warming potential 298 times higher than carbon dioxide (CO_2) and an atmospheric lifetime of 116 years. The N_2O capture, in order to remove it partially or completely from gas emissions, becomes necessary to act against global warming and climate change. Even if N_2O is mainly emitted under ambient average conditions of temperature and pressure, most of the available technologies to control N_2O emissions operate at medium/high pressure, being high energy-consuming technologies. Gas clean processes based on regenerative adsorption are a feasible techno-economical solution to control N_2O emissions. However, the challenge to develop N_2O adsorption processes is the production of highly specific adsorbents that can capture N_2O under atmospheric pressure.

The molecular modeling of adsorption phenomena is a helpful tool to develop engineered adsorbents and to save time and material resources. The development and validation of analytical informatics procedures to obtain thermodynamic and kinetics data about gas adsorption by molecular modeling can be done using representative and well-known adsorbent materials. Due to its easy and reproducible synthesis, its thermal stability, its flexible structure, its hydrophobic behavior, and its high adsorption capacity for a wide range of gases, including some GHGs, ZIF-8 (Zeolitic Imidazolate Framework-8) has been selected in this study as adsorbent.

In this research, the adsorption phenomenon refers to the gas capture (adsorbate, N_2O) on a solid surface (adsorbent, ZIF-8) as a result of the molecular interactions between both. The thermodynamic parameters of these interactions have been predicted by using molecular modeling and computational chemistry which include quantum mechanics simulations and molecular dynamics simulations. Mathematical methods such as Semi-Empirical Method and Density Functional Theory have been used to simulate the most probable gas-adsorbent interaction sites. The thermodynamic stability of these interactions trough the adsorption energy has been analyzed to select the most stable adsorption site. The Molecular Mechanics 3 force field, adapted for porous materials like ZIF-8, has been used to simulate the gas-adsorbent molecular interactions over time. The adsorption capacity of the adsorbent material has been studied through adsorption isotherms curves to analyze the performance of the material under certain conditions.

Finally, a thermogravimetric adsorption-desorption technique has been used to validate the molecular simulation study performed for CO_2. A method for calculating experimentally the adsorption capacity of ZIF-8 with CO_2 has been developed based on this study and data issued from scientific literature. The use of molecular modeling and computational chemistry has helped to have a better understanding of gas adsorption process under different operating conditions and different adsorbent materials. This has allowed to optimize resources and to establish the basis to study other physicochemical processes in which the adsorption technique is part of them.

Keywords:
Nitrous oxide, Greenhouse gases, Zeolitic Imidazolate Framework-8, Molecular modeling, Gas adsorption

RÉSUMÉ

L'oxyde nitreux (N_2O) est un gaz à effet de serre (GES) issu, majoritairement, des activités agricoles telles que l'utilisation d'engrais à base d'azote et l'élevage intensif, ainsi que des activités de gestion des déchets. Ce gaz a un potentiel de réchauffement global 298 fois plus élevé que celui du dioxyde de carbone (CO_2) et une durée de vie atmosphérique de 116 années. Par conséquent, la capture ou l'élimination du N_2O des émissions gazeuses est fondamentale pour agir contre le réchauffement planétaire et les changements climatiques. Même si le N_2O est émis principalement, sous des conditions de température et de pression ambiantes, les technologies disponibles pour contrôler les émissions de N_2O fonctionnent à moyenne ou à haute pression parce qu'elles sont énergivores. Les procédés d'épuration des gaz basés sur l'adsorption régénérative sont des technologies économiques et faisables pour contrôler les émissions de N_2O. Cependant, le défi consiste à produire des adsorbants spécifiques capables de capturer le N_2O sous une pression atmosphérique.

La modélisation moléculaire pour le procédé d'adsorption est un outil pratique pour développer des adsorbants, en économisant, à la fois, des ressources et du temps. Le développement et la validation de procédures d'analyses informatiques pour obtenir des données thermodynamiques et cinétiques sur l'adsorption de gaz par modélisation moléculaire peuvent être réalisés à l'aide de matériaux adsorbants représentatifs et bien connus. En raison de sa synthèse facile et reproductible, sa stabilité thermique, sa structure flexible, son comportement hydrophobe et ses capacités d'adsorption élevées pour une grande gamme de gaz, incluant certains GES, le ZIF-8 (*Zeolitic Imidazolate Framework*-8) a été choisi comme adsorbant pour étudier l'adsorption du N_2O.

Dans cette étude, le phénomène d'adsorption fait référence à la capture du gaz (adsorbat, N_2O) présent à la surface du solide (adsorbant, ZIF-8) grâce à des interactions moléculaires entre l'adsorbat et l'adsorbant. Les paramètres thermodynamiques des interactions ont été prédits par la modélisation moléculaire et la chimie computationnelle qui incluent des simulations de mécanique quantique et des simulations de dynamique moléculaire. Des méthodes mathématiques telles que le *Semi-Empirical Method* et le *Density Functional Theory* ont été utilisées pour simuler les sites d'interaction gaz-adsorbant. La stabilité thermodynamique de ces interactions, obtenue par l'énergie d'adsorption, a été analysée pour sélectionner le site d'adsorption le plus stable. Le champ de force *Molecular Mechanics 3*, adapté aux matériaux poreux comme le ZIF-8, a été utilisé pour simuler les interactions moléculaires gaz-adsorbant au fil du temps. La capacité d'adsorption du matériau adsorbant a été étudiée en construisant des isothermes d'adsorption pour analyser la performance du matériau sous certaines conditions.

Finalement, une technique d'adsorption-désorption thermogravimétrique a été utilisée pour valider l'étude de simulation moléculaire réalisée pour le CO_2. Une méthode de calcul expérimentale de la capacité d'adsorption du CO_2 sur le ZIF-8 a été développée en se basant sur ces données et sur des données issues de la littérature scientifique. L'utilisation de la modélisation moléculaire et la chimie computationnelle a permis de mieux comprendre le procédé d'adsorption de gaz sous des conditions de température et pression ambiante et en utilisant différents matériaux adsorbants. Cette méthode a également permis d'optimiser les ressources et d'établir les bases pour étudier d'autres procédés physico-chimiques dans lesquels la technique d'adsorption fait partie d'eux.

Mots-clés: Oxyde nitreux, Gaz à effet de serre, Zeolitic Imidazolate Framework-8, Modélisation moléculaire, Adsorption de gaz

I dedicate this work to my family and friends. A special feeling of gratitude to my loving parents, Angélica and Bernardo, who have been a constant source of support and encouragement and whose good examples have taught me to work hard for the things I aspire to achieve. To my brother Bernardo for being there for me throughout the entire process and never leave my side. To my friends who have supported me and have been my cheerleaders to pursue my dreams and make them come true.

ACKNOWLEDGEMENTS

Getting through my master's studies required more than academic support, and I wish to express my sincere thanks to all my special friends. I am extremely thankful to Antonio and Luc who opened both their homes and hearts to me when I first arrived at Shawinigan and Sherbrooke, and who offered me unconditional support, and overwhelming generosity. I would also like to thank Beatriz and Carlos for sharing their expertise and extending their valuable guidance and encouragement to me. A huge thank you to Mariana and Aimeric for offering me a priceless friendship and for constantly listening and being there for me during difficult times. For many memorable evenings out and in, I thank everyone above.

Finally, my warm and heartfelt thanks go to my family for their constant love and confidence. I would like to express my endless gratitude to my parents for providing me with unfailing support and encouragement throughout this venture. My father for teaching me the value of perseverance and determination, my mother for teaching me the value of generosity and what is important in life, and my brother for teaching me to be brave. I am also grateful to my grandmothers Cornelia and Heriberta, my aunts María Félix, Nayely and Enriqueta, my uncles Arnoldo and Óscar, and my cousin Rommel, who directly and indirectly lent their hand to fulfill one of my dreams.

This accomplishment would not have been possible without all of them. Thank you!

TABLE OF CONTENTS

LIST OF TABLES

LIST OF FIGURES

LIST OF ACRONYMS

AIM	Atoms in molecules theory
AlN	Aluminum Nitrite Nanotube
AM1	Austin Model 1
AMBER	Assisted Model Building with Energy Refinement
BEA	Beta zeolite
$C_3H_5NaOS_2$	Ethyl xanthate
C_3H_6	Propylene
C_3H_8	Propane
$C_4H_6N_2$	2-methylimidazole, 2-mIm
CH_4	Methane
CHARMM	Chemistry at Harvard Macromolecular Mechanics
CHO	Aldehyde
CNDO	Complete Neglect of Differential Overlap
CO_2	Carbon dioxide
Cs	Cesium
DFT	Density Functional Theory
ED	Ethylenediamine
Fs	Femtosecond
G	Graphene
Ga	Gallium
GCMC	Grand Canonical Monte Carlo
GHG	Greenhouse gas
GWP	Global Warming Potential
HCl	Hydrochloric acid
HF	Hartree-Fock
MC	Monte Carlo
MD	Molecular Dynamics

MM	Molecular Mechanics
MM3	Molecular Mechanics 3
MOF	Metal-Organic Framework
N_2O	Nitrous oxide
NaOH	Sodium hydroxide
NBO	Natural Bond Orbital
NH_2	Azanide
NH_3	Ammonia
ONIOM	Our own N-layered Integrated molecular Orbital and Molecular Mechanics
PCPs	Porous Coordination Polymers
Pd-CNT	Palladium-doped single walled Carbon Nanotube
PM3	Parametric Method 3
PM6	Parametric Method 6
QM	Quantum Mechanics
SO_2	Sulfur dioxide
SP-DFT	Spin-Polarized Density Functional Theory
TGA	Thermo-Gravimetric Analysis
TPD	Temperature-Programmed Desorption
UFF	Universal Force Field
$Y(NO_3)_3$	Yttrium nitrate
ZAPS	Erionite
ZIF	Zeolitic Imidazolate Framework
ZnO (0001)-G	Zinc oxide doped graphene
ZNT	Mordenite
ZSL	Clinoptilolite
ZSM-5	Zeolite Socony Mobil-5

LIST OF SYMBOLS

E_{ads}	Adsorption energy	(kJ/mol)
T_{max}	Temperature maximum	(K)
ΔH_{ads}	Adsorption enthalpy	(kJ/mol)
E_{total}	Total potential energy in a force field	(kcal/mol)
E_{bonded}	Energy due to intramolecular forces in a molecule	(kcal/mol)
$E_{nonbonded}$	Energy due to intermolecular forces between molecules	(kcal/mol)
E_{bond}	Bond stretching energy	(kcal/mol)
E_{angle}	Angle bending energy	(kcal/mol)
$E_{dihedral}$	Dihedral torsion energy	(kcal/mol)
E_o	Out-of-plane bending coordinate	(kcal/mol)
E_{vdW}	Dispersion-repulsion energy due to van der Waals forces	(kcal/mol)
$E_{electrostatic}$	Energy due to coulomb electrostatic interactions	(kcal/mol)

GLOSSARY

/6-31G, /6-31G*, /6-311++G	A basis set of functions used in theoretical and computational chemistry (Hartree–Fock method or Density Functional Theory (DFT)) to represent the electronic wave function. Each figure represents the number of Gaussian functions used to imitate the atomic orbitals. The letter G corresponds to Gaussian.
46T ONIOM2	Hybrid method with 46T quantum clusters that enable different ab initio or semi-empirical methods to be applied to different parts of a molecule/system and combined to produce reliable geometry and energy at a reduced computational time. The 46T is the number of the main atoms that form the structure and in the framework of ONIOM2, the system is divided into two layers and treated at two different levels of theory.
5T quantum cluster	5T is the number of the main atoms that form the structure, and the quantum cluster is a computational method to study the ensemble of bound atoms or molecules that represent a fragment of the whole system.
Ab initio	A quantum mechanical calculation that may use mathematical approximations but does not utilize any experimental chemical data.
Aging	The undesirable change of the chemical and/or physical structures of a polymer with respect of time, mostly under atmospheric conditions.
$AlSi_2O_4H_8$	Zeolite's name (also known as 3T cluster), where 3T is the number of the main atoms that form the structure (tetrahedral Al and Si atoms), and the cluster is an ensemble of bound atoms or molecules that is intermediate in size between a molecule and a bulk solid.
$AlSi_9O_{16}H_{20}$	Zeolite's name (also known as 10T cluster), where 10T is the number of principal atoms that form the structure (tetrahedral Al and Si atoms), and the cluster is an ensemble of bound atoms or molecules that is intermediate in size between a molecule and a bulk solid.
B3LYP	Hybrid functional developed in the late 80s. It belongs to Density Functional Theory (DFT) and Hartree-Fock based methods to recover electron correlation. B3 is Becke's 3

parameter exchange correlation functional which uses 3 parameters to mix in the exact Hartree-Fock exchange-correlation and LYP is the Lee Yang and Parr correlation functional that recovers dynamic electron correlation.

Cut-off (for adsorption)	An arbitrary maximal value of length used to determine that molecules with larger values than this physical quantity are ignored in some calculations of adsorption. It is usually represented within a particular length scale such as angstrom (Å) units.
Dissociation	A general process in which molecules, ionic compounds or complexes separate or split into smaller particles such as atoms, ions, or radicals, usually in a reversible manner.
Electron correlation	Interaction between electrons in the electronic structure of a system where the correlation energy can be measured to know how much the movement of one electron is influenced by the presence of other electrons.
Fe(111)	Specific surface of iron (Fe) structure where the N_2O adsorption will occur.
Hamiltonian	Operator, in quantum mechanics, that corresponds to the sum of the kinetic energies plus the potential energies for all the particles in the system for calculating the total energy of the system. It is usually denoted by H, $\hat{H}$ or $\check{H}$.
Hypervalent molecules	Contain one or more main group elements which have more than eight electrons in their valence shells, being able to have five or more bonds.
Silicalite-1	All-silica zeolite that only contains silicon (Si), oxygen (O) and hydrogen (H) in the framework. It has high-temperature resistance, strong hydrophobic and oil-wet properties, due to the absence of aluminum in its structure.
Wave function	Mathematical description, in quantum mechanics, of electron distribution. The square of the wave function gives the probability of finding an electron. The most common symbols for a wave function are the Greek letters ψ and Ψ.
WB97XD	The latest functional from Head-Gordon and coworkers which is a new class of DFT functional known as range-separated functional. It includes empirical dispersion and can capture both short-range and long-range interactions. The WB97 and WB97X variations are also available.

CHAPTER 1. INTRODUCTION

1.1. Environmental issues

Environmental pollution levels have been rising rapidly in the last years. This uncontrolled increase of pollutants is due to strong industrialization, rapid population growth, overexploitation of natural resources and dependence on fossil fuels [1]. Because of high levels of greenhouse gases emissions, some other problems have been produced like climate change, global warming and ozone layer depletion which endanger the health and the quality of life of all living beings. Finding new solutions to control all these environmental problems is therefore very important to stop ecological imbalance and the technological and economic issues associated to them [2].

1.2. Greenhouse gases

Greenhouse gases (GHGs) are among the main atmospheric pollutants. They are associated to global warming and consequently to climate change. GHGs are generated naturally, but also by human activities such as industrial activities which increase the concentration of these gases. Humans are introducing these gases to the atmosphere at a rate much faster than earth's systems can remove them [3]. Because GHGs capture infrared radiation in the atmosphere, in their energized state, these gases become unstable, transforming solar radiation into heat and thus increasing the temperature on earth [4]. The three main GHGs are carbon dioxide (CO_2), methane (CH_4) and nitrous oxide (N_2O). From 1750 to 2019, the concentration of CO_2 in the atmosphere increased by 48 % (from 278 to 410.5 ppm), while the concentrations of CH_4 and N_2O increased by 160 % (from 722 to 1877 ppb) and 23 % (270 to 332 ppb), respectively [5].

1.3. N_2O gas

Nitrous oxide (N_2O) is a gas, commonly known as laughing gas. It is one of the gases that causes the ozone layer depletion in the stratosphere [6]. The molecular size of this gas is 2.5 Å. The molecular structure of N_2O has been shown to resonate between two bonding configurations with opposing dipole moments: $^-N{=}N^+{=}O \leftrightarrow N{\equiv}N^+{-}O^-$ [7]. Specifically, N_2O has a global warming potential (GWP) 298 times higher than CO_2 (GHG of reference) and an atmospheric lifetime of 116 years [8]. The annual global emissions of N_2O are equivalent to 5.1 % of total GHG emissions (15,219.27 Mt CO_2 eq.) [9]. About 40 % of total N_2O emissions come from human activities, arising from agricultural activities which are the main source of N_2O due to the use of nitrogen-based

fertilizers and livestock. Other sources of N_2O come from industrial activities such as adipic acid and nitric acid production. Fossil fuel combustion and waste management also constitute important sources of N_2O emissions [10]. Unfortunately, unlike CO_2 and CH_4 emissions, treatment solutions for N_2O emissions continue to be studied and developed [9].

1.4. Gas treatment

The control and quantification of N_2O emissions require technologies to capture, concentrate and degrade the gas. This type of technologies to control N_2O emissions are poorly known, even though this gas has shown a big environmental impact. For example, the conversion of N_2O when it is at low concentration in effluents is one of these technologies. It includes direct decomposition and selective catalytic reduction, into environmentally friendly N_2. On the contrary, when it is at high concentration, it can be used as active oxygen donor. However, the catalytic decomposition of N_2O typically occurs at high temperatures and cannot be used as a valuable intermediate to produce other fine chemicals [10].

Due to these current problems, the adsorption technique, specifically for gas capture, has gained importance in industry and environmental protection in recent years with the development of a wide variety of adsorbents. The adsorption-desorption process to capture and concentrate N_2O can be used to obtain high purity N_2O which is a useful oxidant to produce fine chemicals such as phenol [10]. This technique has also been identified as an appropriate method for removing diluted contaminants in the air due to its high selectivity, its adsorption capacity, its efficiency and its low operational cost [11]. The development of an efficient and economic technology such as adsorption-desorption could produce feasible processes to control the emissions of N_2O.

1.5. Gas adsorption

Gas separation by adsorption technology is a well-established unit operation for environmental, industrial, biological and pharmaceutical applications [12]. It has shown promising advantages such as low energy consumption, high economic benefit, easy industrialization, and high efficiency [13]. Adsorption is a physicochemical process where molecules of gases (adsorbates) are retained on a solid surface (adsorbent) due to chemical or physical interactions. These types of interactions are defined by the adsorption potential energy which determines the nature of interaction between a molecule and the surface of the adsorbent material [14]. The gas adsorption process is currently

used due to its efficiency for dealing with a large range of gas separations including trapping, impurity removal, gas purification and separation in recycle streams [15].

1.5.1. Types of gas adsorption

There are two types of interactions for gas adsorption: physical and chemical.

1) Physical adsorption (physisorption) occurs when an adsorbate is retained on the surface of the adsorbent, conserving its chemical nature [16]. The attractive force between the adsorbate and the adsorbent surface is relatively weak because the forces that link the compound to the surface come from dipolar interactions like Van der Waals forces or London dispersion forces [17]. A way to measure these type of interactions between adsorbate-adsorbent is through the adsorption energy (E_{ads}), a parameter which indicates the adhesion strength of an adsorbate on the adsorbent surface and determines the interactions effectiveness on the adsorbent surface [18]. This type of interaction is reversible by modifying the conditions that influence the strength of the interaction such as the temperature and the pressure. The E_{ads} is a result of an electron charge redistribution and a mechanical strain energy due to the changes in the atomic configuration of the adsorbate-adsorbent system during the adsorption process [19]. Physical adsorption can be also a multilayer process where not all the adsorbed molecules are in direct contact with the surface layer of the adsorbent [16].

2) Chemical adsorption (chemisorption) is another type of adsorption, much stronger than physical adsorption because the gas molecules react with an active surface (the adsorbent), producing chemical bonds between them [20]. Among the gases that can be removed by chemisorption, can be mentioned the following: ammonia (NH_3), carbon dioxide (CO_2), carbon monoxide (CO), hydrogen (H_2), nitrous oxide (N_2O), oxygen (O_2), nitrogen (N_2), and sulfur dioxide (SO_2) [20]. Therefore, the interaction is more specific because there is a chemical reaction between the adsorbed molecules and the adsorbent surface. This allows an irreversible bonding between them regardless of the weight, the compound concentration, the humidity and the temperature [16]. Chemisorption, unlike physisorption, is a monolayer process in which the adsorbate needs to be in direct contact with the active surface (adsorbent) to produce chemical bonds [20].

1.6. Adsorbents

Adsorbents are solid porous materials with intrinsic properties such as high surface area, large pore volumes and flexible pore size on which molecules will be attached [21]. Pore structure and surface chemistry for any adsorption material is imperative for describing adsorption phenomena [14]. The adsorbents are classified according to their nature or their preparation method. For example, natural adsorbents are composed of charcoal, clays, clay minerals, ores, zeolites, etc [11]. However, there are also synthetic adsorbents based on agricultural and industrial wastes, activated carbon nanotubes, graphene, cellulose, carbonates, zeolites and phosphates [22].

Unlike natural adsorbents, the advantage of the synthetic adsorbents is that they can be used in specific processes because of the modifications of their chemical structures to obtain desirable properties [22]. For example, Metal-Organic Frameworks (MOFs), also known as Porous Coordination Polymers (PCPs), are copolymers of metal ions or clusters and bridging ligands in different topologies [15]. MOFs have various pore systems and architectural structures, relatively flexible frameworks and easily modifiable functional groups. MOFs are used in gas capture processes (CO_2 and other gases) by adsorption, membrane separation and catalysis [23].

1.6.1. ZIF-8

Zeolitic Imidazolate Frameworks (ZIFs) are porous crystalline materials that constitute a subclass of MOFs. The structures of ZIFs are formed of tetrahedral networks that resemble those of aluminosilicate zeolites [24]. Thus, transition metals like zinc (Zn^{2+}) ions replace coordinated tetrahedral atoms and play the role of silicon (Si) bonds and the imidazolate anions form bridges that mimic the role of oxygen in zeolites with metal-imidazole-metal [21]. However, even when ZIFs tend to form zeolite-like topologies with structures similar to those observed in zeolites, ZIFs possess a fusion of the characteristics and the advantages of both MOFs and zeolites. As a result, ZIFs show ultrahigh surface areas, unimodal micropores, high crystallinity, abundant functionalities and exceptional thermal and chemical stability [21]. Also, they have showed a flexible structure which is reflected by the gate-opening effect due to external stimuli on the adsorption behavior of gases such as temperature and pressure conditions and adsorbate presence [25].

Specifically, Zeolitic Imidazolate Framework-8 (ZIF-8) has a sodalite type structure, also called *sod* topology. This means that the metal–imidazolate networks of ZIF-8 have a topology that is

found in natural sodalite zeolites [26]. It is composed of Zn (II) ions clusters linked by 2-methylimidazole (2-mIm, $C_4H_6N_2$) ligands. The bond length between Zn and nitrogen (N) is of 1.987 Å [23]. Also, ZIF-8 exhibits big pore widths of 11.6 Å formed by six Zn atoms and six molecules of 2-mIm and a diminutive aperture of 3.4 Å which forms a small pore constituted by four Zn atoms and four molecules of 2-mIm [27].

Small pores help to improve the separation of small molecules from the larger molecules (e.g. CH_4 from CO_2), while large pore internal cavities allow rapid diffusion of molecules during the adsorption process, otherwise some blockages could be created and inhibit permeation [28]. Besides, ZIF-8 has a thermal stability at T<673 K as zeolites and a hydrophobic behavior which could be an advantage to separate H_2 from a mixture that contains moisture and other larger molecular size gases [24], [29].

1.8 Molecular modeling and computational chemistry

A combined experimental and theoretical approach for understanding gas adsorption is widespread. Molecular modeling and computational chemistry will be used to determine the adsorption capacity of several materials under different adsorption conditions without performing all laboratory tests, saving resources and time. Also, mathematical models have been applied to contribute to several irrefutable scientific questions, so this method of study can generate information that would be essentially impossible to determine experimentally [30].

Advances in computational power, computing infrastructures, new storage hierarchies, and improved algorithms for dealing with more realistic complex multi-scale models supported by modern data science techniques, including machine learning and artificial intelligence, provide new opportunities for rapid progress in gas treatment by adsorption technology [12]. The use of physics-based understanding of nano-porous material adsorption properties combined with data-driven techniques has demonstrated the ability for a rapid and efficient means to increase materials discovery, design and deployment for adsorbent manufacturing [12].

It is necessary and desirable to develop green and energy-efficient technologies to effectively treat gases emissions. The adsorption process using new materials such as ZIFs to capture gases promises to be a feasible, efficient, and fast solution because ZIFs are less expensive and more energy-efficient than other adsorbents. The adsorption technology is far from being completely

developed. However, a better understanding of the physical phenomena of adsorbent is an important way to increase their application and improve their efficiency. Major contribution for innovation in gas separation by adsorption process is related to the study of different and new adsorbents with better separation characteristics and the optimization of the experimental techniques by using a molecular modeling approach.

CHAPTER 2. STATE OF THE ART

2.1. Study of N$_2$O adsorption on different types of adsorbents

Nowadays, the development of sustainable solutions to global pollution problems requires a great deal of scientific research. One example of that is the difficulty to treat atmospheric pollutants due to the very specific interactions between gases and other substances [31]. For GHGs adsorption, it is necessary to study case by case, i.e., a type of adsorbent with a specific GHG. However, this consumes a lot of resources, materials, and workforce to characterize an efficient gas-adsorbent system [32].

Specifically, for N$_2$O and other types of nitrogen oxides, an efficient removal process would be to trap N$_2$O with an absorbent and decompose it after being desorb it into nonpolluting gases: N$_2$ + O$_2$ [33]. However, the current adsorption technology works between medium pressure (3400-8000 kPa) and high pressure (>8000 kPa) [17]. This technology requires a high energy consuming, implying high operating costs too. Based on these obstacles that are presented in gas treatment technology, some materials have been studied to adsorb N$_2$O to later carry out a catalytic decomposition of the gas, combining molecular simulations and experimental methods to accelerate the development of new and better technique based on adsorption-desorption and decomposition.

2.1.1. Silicalite-1

Silicalite-1 is a type of zeolite that has been used to adsorbed N$_2$O gas due to its high-temperature resistance, and its strong hydrophobicity. The adsorption capacity of this material was analyzed experimentally by isotherms obtained varying the temperature from 273 to 398 K and pressures up to 120 kPa [6]. The selective adsorption by zeolites (based on metals) at room temperature is an important study to concentrate gas streams that contains N$_2$O for carrying out catalytic decomposition, selective catalytic reduction and/or selective catalytic oxidation processes. With the increase in temperature, the amount of N$_2$O adsorbed decreases: 2.94 mol/kg (T = 273 K), 2.77 mol/kg (T = 298 K), 2.45 mol/kg (T = 323 K), 1.34 mol/kg (T = 373 K) and 1.01 mol/kg (T = 398 K) [6].

2.1.2. Zeolite Socony Mobil-5 (ZSM-5) substituted with transition-metals

Ion-exchanged zeolites with transition-metals are attractive catalysts for N$_2$O decomposition because of their high catalytic activity, good thermal stabilities, and low costs. Introduction of

transition-metal ions into the porous materials can lead to a remarkable increase of binding strength to N_2O. Several studies have focused on ion-exchanged ZSM-5 zeolites because their special channel system prefers to entrap N_2O and to promote N_2O catalytic decomposition in a complex atmosphere [33]. The ZSM-5 is a zeolite-type material that has been usually modified with some metal ions to improve the adsorption capacity of this material for adsorbing and decomposing N_2O through a catalytic process. For example, the Fe-ZSM-5 has been used to adsorb N_2O prior to its catalysis oxidation [34]. Also, it has been used to study the direct decomposition of N_2O trough a catalytic conversion in the presence of carbon monoxide (CO) and nitric oxide (NO) at different partial reactant pressures [35]. The advantage of this material is that the active iron center allows the direct oxidation of organic molecules like N_2O.

On the one hand, the molecular modeling was applied to study the adsorption process in a cost-effective strategy for analyzing a large extended framework structure. The 5T quantum cluster and 46T ONIOM methods were used to study the interactions of N_2O on the active sites of Fe-ZSM-5. The N_2O adsorption energy calculated by the 5T quantum cluster was -41.2 kJ/mol, while the N_2O adsorption energy calculated by the 46T ONIOM2 was -57.3 kJ/mol. This data was compared to the experimental result which was -67 kJ/mol [34]. For getting similar results, a correction scheme was done combining the mathematical methods B3LYP/6-31G and MP2/6-31G with the universal force field (UFF) method, giving a simulation result of -66.9 kJ/mol which is similar to the experimental result. The results obtained suggest that the ONIOM approach has a good precision and it is a practical model in the study of adsorption using zeolites as adsorbents [34].

On the other hand, the catalytic conversion of N_2O in a temperature range of 473-873 K has been studied in binary (N_2O + CO; N_2O + NO; NO + CO) and ternary (N_2O + NO + CO) systems. The NO accelerates O_2 desorption via adsorbed NO_2-intermediates, while CO acts as a stochiometric reductant, scavenging adsorbed atomic oxygen as CO_2 [35]. At low partial pressures, the catalytic effect of NO as O_2 desorption-accelerator is more effective than the reducing effect of CO. The rate of N_2O removal with CO is superior at high partial CO pressures and low temperatures [35].

Unlike the two adsorption studies mentioned above with Fe-ZSM-5, the ZSM-5 has been also modified with active centers of the mononuclear gallium $[Ga]^+$ and the metal-oxo gallium cation $[Ga=O]^+$ to study the adsorption and decomposition of N_2O. The cation exchange capacity of transition-metals in ZSM-5 participates also in the catalysis of the dissociation of N_2O to oxygen

and nitrogen. For this study, the surroundings of the material were composed of two type of clusters: 3T-ring ($AlSi_2O_4H_8$) and 10T-ring $[AlSi_9O_{16}H_{20}]^-$ [36]. A computational approach was applied using density functional theory (DFT at B3LYP/6-31+G* level) to assess a possible reaction pathway for the catalytic dissociation of N_2O. In the adsorption process, N_2O can be adsorbed via terminal –O atom or terminal –N atom which is an important parameter to considered during the analysis. The activated energies for N_2O dissociation in Ga-ZSM-5 and GaO-ZSM-5 at T = 298 K were 92.9 kJ/mol and 104.2 kJ/mol, respectively, which agree with experimental measurements [36].

Some other metal ions (transition-metal and noble metal cations) can be inserted in ZSM-5 structure; for example, Barium (Ba^{2+}), Calcium (Ca^{2+}), Cesium (Cs^+), Potassium (K^+), Sodium (Na^+) and Magnesium (Mg^{2+}), which can modify the adsorption capacity of ZSM-5, focusing on the adsorption and desorption of N_2O on the main-group ion-exchanged [37]. Density functional theory (DFT) was used to analyze the adsorption behavior of N_2O on ZSM-5 zeolites exchanged with the six main group metal cations mentioned above. The desorption process was conducted experimentally using temperature-programmed desorption (TPD) to determine the temperature maximum of the desorption for each metal [37]. The T_{max} was: 413, 409, 408, 402, 398 and 375 K for Ba^{2+}, Ca^{2+}, Cs^{1+}, K^{1+}, Na^{1+} and Mg^{2+}, respectively. The adsorption capacity based on the adsorption energy (E_{ads}) allows to analyze the interaction forces between the metal cations and the N-end or O-end of N_2O. The best adsorption behavior was found in the Ba-ZSM-5 with the highest desorption temperature at 413.25 K and an adsorption capacity of 43.31 kJ/mol in the N-end and 36.7 kJ/mol in the O-end [37].

Gold (Au) containing zeolite is one of the catalysts that have been studied for catalyzing the N_2O decomposition. Density functional theory (DFT) calculations have been carried out to study the for the initial N–O bond breaking process of N_2O decomposition over Au^+ supported ZSM-5 (Au/ZSM-5) and Au^0 supported ZSM-5 (Au/H-ZSM-5) by using the M06-L method [38]. The adsorption energy for Au/ZSM-5 is -66.57 kJ/mol. For the case of Au/H-ZSM-5, the N_2O is weakly adsorbed on zeolite. The adsorption energy is -23.03 kJ/mol, which is almost three times lower than that derived from the Au/ZSM-5 complex. The big difference between the zeolites is a result of a bigger charge transfer from the gold active species to the N_2O molecule [38]. The supported zeolite

facilitates the charge transfer of the Au species and plays an important role in stabilizing all the species in the reaction coordinate as well as the transition state complexes over the Au system [38].

Six transition-metal cation-exchanged in ZSM-5 have been used: manganese (Mn), iron (Fe), cobalt (Co), zinc (Zn), nickel (Ni) and copper (Cu) [33]. The interaction between transition metal cation-exchanged ZSM-5 and N_2O is important for selecting the correct adsorbents for N_2O and being able to study the catalytic decomposition of N_2O. The adsorption behavior of N_2O on the different ZSM-5 zeolites was investigated to determine the strength of interaction between the metal ions and the gas and to calculate the adsorption enthalpy (ΔH_{ads}) using density functional theory (DFT) [33]. The T_{max} of desorption was determined with the temperature-programmed desorption (TPD) in which T_{max} was: 378, 377, 372, 364, 355 and 353 K for Mn, Fe, Co, Zn, Ni and Cu, respectively. The adsorption and desorption behaviors of N_2O significantly depended on the type of ions, specifically on the electron transfers of cations. Theoretical and experimental results consistently indicate that the adsorption strength of N_2O on transition-metal ions followed this order: Fe>Mn>Co>Zn>Ni>Cu; the associated ΔH_{ads} were: -242.6, -221.7, -203.3, -144.4, -108.8 and -51.6 kJ/mol, respectively [33].

2.1.3. Beta zeolite (BEA) substituted with transition-metals

The Beta zeolite is a type of zeolite used as an adsorbent material that can be modified by substituting the silicon (Si) atoms with different metal ions to improve its adsorption capacity [39]. Transition-metal ion-exchanged zeolites, especially for the Fe-, Co-, and Cu-exchanged zeolites, exhibit unique and fascinating properties which have been widely used for the catalytic decomposition of N_2O [40]. Specifically, copper-containing (Cu^+) zeolites are known as excellent catalysts and give good results for the decomposition of N_2O to nitrogen and oxygen while they are stable under reaction conditions. Cu-Beta zeolites exhibit high and stable activity in NO_x decomposition [39].

Density functional theory (DFT B3LYP/6-31G) has been applied to analyze the adsorption and decomposition of N_2O/NO in the active sites (Al(T1)‑OH‑Si and Al(T9)‑OH‑Si) of a 10T cluster of Cu-BEA. Nitric oxide (NO_x) could be adsorbed on Cu^+ species in two modes: η-O and η-N [39]. The adsorption energies of N_2O varied in the range from -14.80 kJ/mol for Cu-BEA-ONN T1 to -75.96 kJ/mol for Cu-BEA-NNO T9. The adsorption energies of N_2O molecules in η-N mode on Cu-BEA are larger than in η-O mode [39]. The interactions between N_2O and Cu-BEA at site T9

are stronger than at T1 site, and Cu-BEA at sites T1 and T9 have high activities for NO decomposition. The calculated results showed that NO_x could be adsorbed on Cu^+ species in two modes (η-O and η-N) [39].

Apart from Cu-containing zeolites, some other metals like Fe and Co have been also studied as part of BEA zeolites to produce more selective adsorbents for the adsorption and decomposition of N_2O. In this study, quantum chemistry based on density functional theory (DFT B3LYP/6-31G and DFT B3LYP/6-311++G)) at T = 600 K was used to analyze the catalytic activities of these metals with the N_2O. It was found that the activity differences of M-BEA (M = Fe, Co, Cu) were mainly attributed to the different energy barriers for O_2 desorption, which was the rate-determining step for the whole N_2O direct decomposition. The activations energies were: Fe-BEA = 141.41 kJ/mol, Co-BEA = 106.69 kJ/mol and Cu-BEA = 175.30 kJ/mol. In this way, the results revealed the sequence following the trend of Co-BEA>Fe-BEA>Cu-BEA, in which Co-BEA was the material that needed less energy to decompose directly the N_2O due to its two activation energy barriers (N_2O-M-BEA) [40].

2.1.4. Iron (Fe 111) surface

For catalytic processes to convert nitrogen oxides to nitrogen, some cubic structures, crystals of large surface area, or single crystals have been used as adsorbents. Some of these materials have been covered with iron (Fe), being the Fe(111) one of the most used for this purpose. Spin-polarized density functional theory (SP-DFT) was used to study the adsorption and dissociation behaviors of N_2O on the Fe(111) surface of six layers [41]. Because the N_2O can be adsorbed from the –O side or from the –N side, some geometries and adsorption sites were determined as follows: FeN_2O-η^2-[$N_t(1,2)$, $O_t(1)$], FeN_2O-η^2-[$N_t(1)$, $O_t(1)$], FeN_2O-η^2-[$N_t(1,2)$, $N_c(1)$], FeN_2O-η^2-[$N_t(1)$, $N_c(1)$] and FeN_2O-η^1-[$N_t(1)$]; where, N_t, N_c mean the terminal and central N atom and (1, 2) is the atom bridge on 1st and 2nd atomic layer of Fe(111) surface. This adsorption sites were analyzed to know which one is the most energetically favorable in the adsorption process. The adsorption site FeN_2O–η^2-[$N_t(1,2)$, $O_t(1)$] exhibited the greatest adsorption energy with 111.92 kJ/mol on Fe(111) surface [41]. As part of the treatment, the N_2O dissociation, consisting of separating the molecule into $N_2 + O_2$, could be hardly difficult to analyze experimentally in some of the adsorption sites, so the information obtained using DFT calculations could be useful for the design of catalytic surfaces for N_2O dissociation [41]

2.1.5. Nanotubes (NTs)

Aluminum nitride nanotubes (AlNNTs) is a type of nanotubes which have been used in gas sensors, fuel storage, and the reduction of hazardous pollutants from gas streams. However, it has been studied as adsorbent for N_2O dissociation [42]. Density functional theory (DFT) was applied to analyze the energetic, geometric, and electronic properties of the N_2O adsorption process by AlNNTs doped with pristine and silicon. The adsorption energies of N_2O on the pristine and Si-doped AlNNTs were in the range +29.71 to -23.85 kJ/mol and -20.08 to -433.47 kJ/mol, respectively [42]. It was observed that N_2O was weakly adsorbed onto the pristine nanotube and the electronic properties of the pristine nanotube were not influenced by the adsorption process. The N_2O molecule strongly interacted with the Si-doped nanotube, diffusing the oxygen atom of N_2O into the tube wall, and releasing a N_2 molecule [42].

Another type of NTs are carbon nanotubes (CNTs) that show good properties such as large surface, large volume ratio and good porous structure. Substitution doping of transition-metals can induce localized change within the nanotube and modify the chemical and electronic properties. Palladium (Pd) is a metal that has shown strongly influence in the chemical reactivity of inert nanotubes towards the adsorbing gas species [43]. Because of this, Pd-doped single-walled carbon nanotubes (Pd-CNT) have been used to study the adsorption of N_2O by Density functional theory (DFT WB97XD/6-311G) calculations. This study resulted in a chemisorption process because during the N_2O adsorption by –N side (N/Pd-CNT) and –O side (O/Pd-CNT), there was a slightly increase of the energy gap. Both configurations N/Pd-CNT and O/Pd-CNT showed the highest adsorption energies with -78.73 kJ/mol and -87.71 kJ/mol, respectively [43]. The atoms in molecules (AIM) theory and the natural bond orbital (NBO) calculations were performed to get more details about the nature and charge transfers in intermolecular interactions within the adsorption process. As a result, Pd-CNT can facilitate the adsorption of N_2O and this material can be introduced as a novel detectable complex for designing highly sensitive, fast response and highly efficient carbon nanotube-based gas sensor to detect N_2O gas as an air pollutant [43].

2.1.6. Natural zeolites

Erionite (ZAPS), mordenite (ZNT) and clinoptilolite (ZSL) are three natural zeolites that can be used to adsorb N_2O due to the fact that some synthetic zeolites have worked well for the same purpose. The adsorption capacity of these zeolites was studied with N_2O experimentation in a

temperature ranging from 273 to 373 K [44]. The activation energies for adsorbing the N_2O on ZAPS, ZNT and ZSL were: 174.7 kJ/mol, 414.9 kJ/mol and 443.8 kJ/mol, respectively. The adsorbed amount and the adsorption rate decreased when the temperature increases. This behavior suggested that the N_2O adsorption on ZAPS can be more efficiently at ambient temperature (293 K), whereas the adsorption capacity of ZSL could be better at 373 K [44].

2.1.7. Graphene (G)

Graphene is a material that has been used as adsorbent. Because the properties of the graphene are less than the graphene modified with foreign atoms and molecules, the adsorption capacity of the material could be enhanced predominantly by modifying its surface (doped or decorated) with metals such as platinum, cobalt, and indium. Platinum (Pt)-doped graphene sheet, for example, has been studied as a new type of adsorbent to capture N_2O, using density functional theory (DFT B3LYP 6-31G) [45]. All the possible initial configurations were examined to find the most stable configurations of N_2O on PtG, and two different positions were studied: i) P1, N–N–O axis parallel configuration with respect to the surface, and ii) P2, each terminal side of molecule (–N or –O) was placed vertically to the PtG surface. Different adsorption energies were generated between the N_2O and the PtG sheet resulting in -113.6 kJ/mol for P1 and -41.2 kJ/mol for P2 [45].

Graphene-based catalysts are interesting candidates for decreasing CO and N_2O concentrations. One of them is the zinc oxide (ZnO(0001))-doped graphene that has been studied for the catalytic adsorption and decomposition of N_2O through *ab initio* methods in order to explore some important properties such as adsorption energy and activation energy on ZnO-G nanocomposite [46]. Likewise, density functional theory (DFT) was used to analyze the molecular mechanism of the elementary steps of the decomposition of N_2O over the most stable surface (0001) of ZnO, studying different adsorption sites. It resulted in three most stable configurations for the N_2O molecule to be adsorbed: i) horse-like (N–N–O), ii) parallel (N–N–O), and iii) lying-atop-011 (O–N–N), in which the three atoms of the N_2O molecule interacted with the surface. The adsorption energies were 26.05 kJ/mol, 22.19 kJ/mol and 22.19 kJ/mol, respectively. This study revealed that the ZnO(0001)-G composite as a magnetic oxide could be one of the materials able to reduce the effect of the air pollutant gases like N_2O in the environment [46].

To summarize, different types of materials (adsorbents) have been studied to adsorb N_2O under different operating conditions, combining experimental techniques with computational approaches.

However, zeolites and other type of materials have been modified by transition metal ion-exchanged to provide active sites that enhance selective adsorption. Some of these materials have been doped with transition-metals to improve the adsorption capacity for N_2O. Iron, for example, has been one of the most common metal used to modify many adsorbent materials for an ultimate N_2O decomposition process.

As part of the adsorption process, the adsorption energy has been an important parameter to indicate the interaction effectiveness and the adhesion strength of N_2O on the adsorbent surface. Also, the DFT calculation has been the most used molecular modeling method to carry out the simulations of N_2O adsorption [18]. This methodology of experimentation combined with molecular modeling helps to develop new materials not only to adsorb N_2O but also to reduce it into N_2 and O_2. Aside from that, different type of zeolites has been used as adsorbent materials to adsorb and desorb N_2O; however, ZIF-8 has not been used for adsorbing N_2O even when it is considered a potential adsorbent material for GHGs.

2.2. Gases adsorbed on ZIF-8

The ZIF-8 is a porous material with characteristics which permits to be a feasible adsorbent for the retention and the treatment of GHGs [5]. Even though this material has not been used to adsorb N_2O, it has been studied to capture the two most important GHGs: CH_4 and CO_2, due to their high concentration in the atmosphere and their big environmental impact [47], [48]. However, ZIF-8 has also been studied to adsorb some other gases like carbon dioxide (CO), nitrogen (N_2), sulfide hydrogen (H_2S), hydrogen (H_2), alkenes, argon (Ar), oxygen (O_2), etc [49]–[53].

2.2.1. Methane (CH_4)

Methane is a GHG and it is generated by farming, livestock, burning biofuel, and burning fuels like coal, oil, natural gas, etc. In order to reduce this gas in the atmosphere, efficient and cost saving methods are studied worldwide. The use of porous materials like ZIFs has been investigated because of their high capacity and cost-effective gas separation and storage [54]. In the case of ZIF-8, it has been experimentally observed that molecules, such as CH_4 and N_2, which are theoretically too large to pass through the windows of its framework are adsorbed on the material. The impact of the flexible geometry of ZIF-8 to adsorb CH_4 has been evaluated, combining experimental gas

adsorption and quantum mechanics like density functional theory (DFT) and molecular mechanics simulations like dynamic simulations or Grand Canonical Monte Carlo (GCMC) simulations [47].

The CH_4 adsorption on ZIF-8 has been analyzed with adsorption isotherms at different temperatures and pressures. For example, Fairen-Jimenez *et al*. [47] have analyzed the interaction between CH_4 and ZIF-8 at temperatures from 125 to 300 K, illustrating the CH_4 adsorption sites and concluding that the C=C double bond of the imidazolate ligand is the most favorable adsorption site for CH_4 at the center of the 6-ring pore-window. The calculations show the importance of the N atoms of the imidazolate ring and their favorable role in the interaction with CH_4 [47]. Some other studies have also investigated the adsorption of CH_4 but combining the gas in a binary mixture with CO_2, CO or N_2 in order to analyze the selectivity of the ZIF-8 material at 273, 298, 323, and 348 K. They concluded that for gas mixtures, systems with large selectivity are more sensitive to temperature [49].

2.2.2. Carbon dioxide (CO_2)

Carbon dioxide is the primary anthropogenic GHG because of the amount of its release to the atmosphere and its role. The development of a feasible carbon capture processes is a scientific and technological challenge. Currently, several methods have been proposed to sequester CO_2 from the flue gases, such as membrane separation, chemical absorption, and adsorption with solid adsorbents [55]. ZIF-8 is a solid porous material which has been studied to adsorb CO_2. Several studies have been carried out experimentally, and some others by molecular modeling simulations. Hu *et al*. [48] studied, by experimental methods, the adsorption of CO_2 on ZIF-8 at room temperature and pressures around 800 000 kPa which are higher than the conventional adsorption process at 10 000 kPa. They observed that ZIF-8 has significant ability to retain CO_2 on its surface with a strong influence of pressure and an adsorbate-adsorbent interaction [48].

As well as CH_4, CO_2 has been analyzed in a binary mixture with CO and N_2 at different temperatures using experimental measurements and GCMC simulations. This work showed that temperature influenced the capacity of CO_2 in temperature swing adsorption process with the interplay of pressure [49]. Also, CO_2 has been studied in a synthetic natural gas mixture with sulfide hydrogen (H_2S). However, ZIF-8 nanoparticles were synthesized and modified in different forms to use it for acid gases capture [50]. The results of CO_2 and H_2S adsorption showed that the modified ZIF-8 nanoparticles are good materials for natural gas CO_2/H_2S removal. Specially the ED-ZIF-8

nanoparticles, modified with ethylenediamine (ED), that had the highest adsorption energy. It was observed that CO_2 can be inserted into the ZIF-8 framework at high pressures around 800 000 kPa [50]. In this way, pressure has shown to play a regulating role in the insertion and extrusion of CO_2 with respect to the framework, even at room temperature. The strong interaction between CO_2 and ZIF-8 is near the C=C double bond of the imidazolate ligand which shows an important interaction site. The enhanced CO_2 storage capacity of ZIF-8 at high pressure provides new insight into the gas capture and storage applications of ZIFs [50].

The CO_2 adsorption in binary mixture has been also studied. For example, Wang *et al*. [53] analyzed the adsorption of CO_2 mixed with hydrogen (H_2) and the ZIF-8 was modified with silicon nitride (Si_3N_4) hollow fibers as a support. The binary H_2/CO_2 gas separation factor (50 % v/v H_2 and 50 % v/v CO_2 gas mixture) was 11.67 with a flow rate of 3.44×10^{-8} mol/ $m^2 \cdot Pa \cdot s$ for CO_2 and 4.02×10^{-7} mol/ $m^2 \cdot Pa \cdot s$ for H_2 [53]. The H_2 permeance increased in the beginning and keep steady at 8.35×10^{-7} mol/$m^2 \cdot Pa \cdot s$ due to the high storage properties of ZIF-8. On the contrary, CO_2 permeance decreased in the first hour, then maintained at 1.15×10^{-7} mol/$m^2 \cdot Pa \cdot s$ due to the strong CO_2 adsorption in the ZIF-8 [53]. Fischer and Bell [52] also studied the interaction of H_2 and CO_2 on ZIF-8, using Dispersion-corrected density-functional theory (DFT-D) calculations. Four distinct adsorption sites were identified. Two of the sites were associated with the six-ring windows, a third site was located close to one imidazolate moiety, and the fourth site was situated close of two methyl substituents of the methylimidazole linkers [52]. Using DFT-D method, a modification of ZIF-8 was realized to optimize structures of ZIF-8 derivatives (X), with X = hydrogen (–H), nitrous oxide (–NO_2), azanide (–NH_2), aldehyde (–CHO). The average interaction energies obtained over different adsorption sites based on the simulations with the method DFT-D were compared with experimental data. The strongest adsorption interaction with CO_2 was observed in ZIF-8_NO_2 and ZIF-8_CHO in which the increased affinity of the gas in these two derivatives of ZIF-8 was promising for the separation of CO_2/H_2 mixture [52].

2.2.3. Propylene (C_3H_6) and Propane (C_3H_8)

Propylene (C_3H_6) and propane (C_3H_8) are two gases that have been studied to be adsorbed on ZIF-8 with CH_4 and CO_2. Some adsorption isotherms were determined through volumetric measurements (experimental process) under different pressures (7000 and 600 kPa) and temperatures (298.2, 323.2, and 348.2 K) [56]. In order to decrease the pressure drop in adsorbent units, the ZIF-8 was

tested under the form of pellets using three forms (T-form ZIF-8, C-form ZIF-8, and N-form ZIF-8), which were studied and compared to powder ZIF-8. The adsorption capacities of the gases on the ZIF-8 powder and the pellets were as follows: C_3H_6>C_3H_8>CO_2>CH_4. The experimental results revealed that the adsorption capacities of the four gases on the pellets were approximately 10-20 % lower the powder ZIF-8 [56].

2.2.4. Nitrogen (N_2), Argon (Ar) and Oxygen (O_2)

Nitrogen (N_2), Argon (Ar), Oxygen (O_2) are liquefied gases, including CH_4, that have been studied individually on ZIF-8 under wide ranges of pressures: N_2 (P = 0-3 250 000 kPa), Ar (P = 0-1 250 000 kPa), O_2 (P = 0-2 000 000 kPa) and CH_4 (P = 0-1 400 000 kPa) [51]. The study was carried out as an integrated experimental and computational study, using high-pressure crystallography, GCMC simulations and DFT calculations. Six adsorption sites within the ZIF-8 were identified for these gases at high pressure and room temperature [51]. The interaction energy of the adsorption sites was calculated using GCMC simulations and DFT calculations. The combination of these techniques provides a holistic approach to understanding both structural and energetic changes upon adsorption in MOFs [51].

Summarizing, ZIF-8 has been used as an adsorbent, specially, for treating some GHGs like CO_2 or CH_4. However, this material has also been studied for treating a wide range of other gases. The adsorbent ZIF-8 has shown specific characteristics that confer it a good adsorption capacity and make it an attractive adsorbent for GHGs compared to zeolites or other type of ZIFs or MOFs [5]. Besides, the combined technique of experimentation and molecular modeling has allowed progress in the study of the adsorption process on ZIF-8, offering a new way to contribute to the development of scientific knowledge without the need of an experimental methodology only [32].

2.3. Molecular modeling methods applied to the study of gas adsorption simulations

Molecular modeling helps to describe and predict experimental results. It is useful to understand phenomena based on theory with complex mathematical manipulations [32]. One of the advantages of molecular modeling, using it as a prior tool before doing experimental studies, is the lower requirement of working time, saving raw materials, and reducing waste generation. Also, molecular

modeling helps to understand a problem in a better way because some properties of the molecules can be obtained easier by using computational methods than by experimentation [32].

The research about GHGs adsorption like N_2O by molecular modeling would allow to study some characteristics of N_2O due to the application of mathematical methods and computational strategies which would help to predict the behavior of N_2O in the presence of different adsorbents [31]. For example, quantum mechanics and molecular mechanics can be applied to study gas adsorption under certain operating conditions.

2.3.1. Quantum mechanics (QM)

Quantum mechanics (QM), part of molecular modeling techniques, is a fundamental theory in physics that can be applied to chemical and physicochemical problems. It provides a description of the physical properties of a system of particles at atomic and subatomic scale. Thus, QM calculations are performed employing theories of quantum physics, which account the interaction between nuclei and electrons [57]. Schrödinger equation is the basis for nearly all computational chemistry methods like QM and it is defined as follows [32]:

$$\hat{H}\Psi = E\Psi \tag{2.1}$$

where,

$\hat{H}$ is the Hamiltonian operator. It is defined by interaction terms between (i) electron-electron, (ii) electron-nucleus, and (iii) nucleus-nucleus, accounting for all possible energy components and kinetic energy of the electrons;

Ψ is a wave function of electron and nuclear positions which provides a description of the system;

E is the total energy of a system (kinetic energy and potential energy).

Considering the high operation cost and time consumption in some mathematical methods used in QM to solve all the Schrödinger equation, only simple systems comprising a small number of atoms can be studied [57]. Therefore, this technique is very useful to identify the potential adsorption sites in a segment of materials that can be used as adsorbents. Also, these types of calculations allow to study important parameters related to the adsorption like the adsorption energy, isosteric heats of adsorption or the approach adsorption distance to determine some characteristics of the adsorbents and the effectiveness of the interactions between adsorbate and adsorbent [58].

2.3.2. Molecular mechanics (MM)

In molecular modeling, molecular mechanics (MM) is a useful method for modeling very large molecular systems and carry out molecular dynamics or Monte Carlo simulations. It assumes that the relative positions of the nuclei of the atoms forming a structure are a function of operating attractive and repulsive forces [57]. One of the main objectives of MM is to generate the trajectories of the particles by calculating the potential energy for each interval of time in order to have a description of the different types of interactions occurring in a system, being able to calculate specific physicochemical properties [59].

The determination of the evolution of the system in time is done by solving a set of equations of motion for all particles considered in the system. The total potential energy of a system of molecules is expressed as a set of equations that represent different types of attractive and repulsive forces between the atoms in the structure, considering the impact of nuclei and avoiding the explicit treatment of the electrons. These forces are reproduced by a set of parameters called force field (FF) that employs equations of classical physics [57].

A general form of the equation showing components of the total energy (kcal/mol) can be represented as follows [57]:

$$E_{total} = E_{bond} + E_{angle} + E_{dihedral} + E_{vdW} + E_{electrostatic} \qquad (2.2)$$

where,

The total energy (E_{total}) depends on the bond stretching (E_{bond}), the angle bending (E_{angle}), the dihedral torsions ($E_{dihedral}$) parameters, the van der Waals potentials (E_{vdW}) and the electrostatic partial charges ($E_{electrostatic}$).

Molecular mechanical methods are comparatively faster and generate accurate (or nearly accurate) molecular geometries and conformational energies. There are different applications in MM that use high-level mathematical expressions or quantum calculations adapted to experimental values [60].

Types of simulation techniques in molecular mechanics (MM)

In MM, there are two types of techniques to calculate the minimum of interaction energy and predict the number of adsorbed molecules: Molecular dynamics (MD) and Monte Carlo (MC) simulations.

1) Molecular dynamics (MD) is a computer simulation technique and is one of the most common methods for modelling complex systems which are defined by an initial condition and a boundary

condition. Unlike QM, in MD a molecule is described as a series of charged points (atoms) linked by springs (bonds), also known as the ball-and-stick model [57]. By carrying out MD simulations, it is possible to analyze the behavior of a system in which atoms and molecules interact for a fixed period of time, generating a visualization of the trajectory of particles thanks to a vibrational motion and a position-velocity vector [60].

Molecular dynamics involves a set of conditions that define the initial positions and velocities of all particles and the interaction potential that defines the forces among all the particles. In this way, the energy of a system and the forces of atoms for any geometry can be computed [32]. Thus, it is possible to simulate the interaction between ZIF-8 and N_2O molecules due to a mixed integration of Newton's second law of motion and algorithms that determine the atomic trajectories in space and time [60]. Besides, MD plays a key role in structure determination of adsorbent materials like ZIF-8 and it can provide information about the adsorption capacity and the thermodynamic properties of a whole system, e.g., adsorption of N_2O gas on ZIF-8 [31].

2) Monte Carlo (MC) simulations are used to model the probability of different outcomes in a process that cannot easily be predicted due to the intervention of random variables. The objective of a MC simulation is to generate an ensemble of representative configurations under specific thermodynamics conditions for a complex macromolecular system [61]. Applying random perturbations to the system generates these configurations, for example a rotation of dihedral angles or a displacement of atoms. To properly sample the representative space, the perturbations must be sufficiently large, energetically feasible and highly probable. Thus, the performance of the system can be analyzed until obtain results based on Boltzmann factor [61].

The probability of different outcomes in a process reproduced in MC simulations is defined by the Boltzmann distribution, as follows [57]:

$$Boltzmann\ factor = exp\left(-\frac{\Delta E}{kT}\right) \tag{2.3}$$

where,

ΔE (J) is the energy of the system; k is the Boltzmann constant (1.38064852×10^{-23} J/K); and T (K) is the absolute temperature of the system.

If a randomly generated number is smaller than the Boltzmann factor, the configuration is accepted.

Generally, in MD simulations, the canonical ensemble is conventionally used defining the system with a constant number of particles (N) in a given volume (V) and at certain temperature (T). However, for studying the adsorption process in the Grand Canonical Monte Carlo (GCMC) simulation, the grand-canonical ensemble is frequently used. This is a statistical-mechanical method, in which a rigorous molecular-level model of adsorption is solved. In this ensemble, the temperature (T), the volume (V), and the chemical potential (μ) are fixed, and unlike the canonical ensemble NVT, the number of particles is allowed to fluctuate during the simulation [62]. The type of ensemble used depends on the process to be studied.

Summarizing, QM and MM are useful techniques commonly employed to study gas adsorption process. Both types of molecular modeling approaches are complementary to each other. In some studies, a mix of both (QM/MM approach) is used to have a better analysis or prediction of the adsorption process. In the study of the adsorption capacity of ZIF-8 with N_2O gas, the use of MD simulations helps to analyze the adsorption process over time and to have a better approach to experimental results because it considers important variables like temperature and pressure while QM simulations help to study specific molecular interactions that occur between ZIF-8 and N_2O during adsorption process, calculating the energy of the molecular system in equilibrium [63].

There are several molecular modeling software that can be used for QM like CHARMM, SPARTAN, NAMDI, Gaussian, etc., to name just a few of them, and also, there are some others for MD like Tinker, GROMACS, Odyssey, NAMD, etc. which are useful to study and understand some reaction paths and transition structures [31]. In addition to the calculation software that exist for MD simulations, there are other type of software such as VMD that are designed only to visualize dynamic simulations.

2.4. Mathematical methods in quantum mechanics applicable to gas adsorption

The use of mathematical methods is essential for a software simulation based on QM. These mathematical methods perform calculations using the fundamental laws of physics to obtain the structural information of chemical systems. Different approaches used to carry out quantum mechanical calculations include the *ab initio* method, density functional theory (DFT) technique, and semiempirical analysis [31].

2.4.1. *Ab initio* methods

Ab initio is an approximate quantum mechanical calculation that employs a convergent approach that gives high-quality and accurate results. These approximations have a mathematical basis only, using a simpler functional form for a function or finding an approximate solution to a differential equation [32]. *Ab initio* calculations are currently used to study the adsorption process, specially to determine the adsorbate-adsorbent potential interaction which is an important parameter to determine the effectiveness of a material to adsorb a gas [58].

Hartree-Fock (HF) approximation

This method is the most common of the *ab initio* calculations. Hartree-Fock approximation considers coulombian repulsions due to the negative charge of an electron pair. The model generates some information about the interactions but without considering the electron correlation, i.e. how much the movement of one electron is influenced by the presence of other electrons [64].

2.4.2. Density Functional Theory (DFT)

Density Functional Theory (DFT) proposes that the energy of a molecule can be determined from the electronic density rather than its wave function. In this way, DFT provides a favorable performance, considering the cost, and gives reasonably accurate results for medium-sized molecules because it uses approaches that make calculations easier for systems with larger numbers of atoms. Besides, DFT describes the quantum behavior of atoms and molecules and investigates their electronic structure or their nuclear structure [57].

The general equation of DFT can be represented by the Hamiltonian operator (Ĥ) as follows:

$$H = T + V_{ee} + \sum_{i=1}^{N} V_{ext}(r_i) \qquad (2.4)$$

where,

T is the kinetic operator; V_{ee} is the electron-electron interaction operator; N is the number of electrons; and $V_{ext}(r_i)$ is the external potential where the electrons are moving.

Using DFT, the properties of a multiple electron system can be determined approximately. This theory is among the most popular and versatile methods available in condensed-matter physics, computational physics and computational chemistry [31]. Many molecular attributes like vibrational frequencies, atomization energies, ionization energies, electric and magnetic properties,

reaction paths, etc. are computable using DFT technique [57]. Besides, the functional B3LYP is the most used among its functional hybrids. Specially, DFT B3LYP-D3 6-31G*[1] is useful because of its time efficiency for making calculations, its ability to calculate reaction energies between molecules and its ability to determine the equilibrium energy and transition-state structure for organic molecules, incorporating transition-metals [64].

2.4.3. Semi-Empirical methods

Semi-Empirical methods have a structure similar to the Hartree-Fock approximations because they have a Hamiltonian operator and a wave function. They use empirical parameters that allow to include electron correlation effects into the methods and employ assumptions, generalizations or approximations in order to simplify complex calculations for solving the Schrödinger wave equation [64].

Normally, for obtaining the geometry and the energy as heat of formation, it is necessary to use some experimental data or data obtained from *ab initio* calculations. An advantage is that semi-empirical calculations are faster than *ab initio* calculations and they are very efficient, being applied to large systems [57]. However, one disadvantage is that the reliability of the results depends on the fact that the molecules studied must have some similarity with the ones that were used to obtain the fitted parameters of the method [32].

Semi-empirical calculations have been successfully applied in organic and inorganic chemistry. Some of the most popular semi-empirical methods are the following:

Austin Model 1 (AM1)

This method is popular for modeling organic compounds. Generally, AM1 gives a good prediction of the heats of formation of these compounds with a better level of prediction than Complete Neglect of Differential Overlap (CNDO) method. Austin Model 1 is an improved version of CNDO by reducing the repulsion of atoms at close distances, mimicking the van der Waals interactions as a nonphysical attraction force. This method can give accurate results for organic molecules depending on the nature of the system and the information desired [32].

---

[1] B3LYP-D3 represents the hybrid functional, while 6-31G* represents the Gaussian base functions to describe the atomic orbitals.

Parametric Method 3 (PM3)

This method is one of the most popular for studying organic molecules and it uses nearly the same equations than the AM1 method but with an improved set of parameters. It is parameterized in reproducing a large number of molecular properties. Hydrogen bonds are well assessed in PM3 method due to its specific parameterization protocol and nuclear repulsion treatment [57]. Besides, it is more accurate than AM1 for calculating bond lengths and heats of formation of organic compounds, and for studying hypervalent molecules. The recent extended versions allow the inclusion of transition metals [64].

Parametric Method 6 (PM6)

The recently developed semiempirical method PM6 can be considered an improve version of other semiempirical methods, such as AM1, and PM3. The recently developed semiempirical method PM6 has been shown to reproduce with good accuracy the heats of formation and geometries of small molecules, simple organic and inorganic crystals. Also, it allows the geometries of such large systems to be optimized rapidly [65]. Due to this, Semi-Empirical Method PM6 has been used more frequently than other methods like AM1 or PM3 because it has shown a better computational precision to give more real and closer results to those obtained experimentally [66].

To summarize, mathematical methods are the basis to carry out QM calculations. Many mathematical methods have been developed and applied to study the gas adsorption process. For example, Semi-Empirical Method and DFT which help to analyze the adsorption process using molecular modeling and computational chemistry. *Ab initio*, DFT, and semiempirical method are the three most common approaches to study physicochemical process like adsorption, and among these mathematical methods, PM6 and DFT B3LYP-D3 6-31G* has shown to have a good computational precision and time efficiency for doing calculations.

2.5. Molecular mechanics strategies employed to simulate gas adsorption process

2.5.1. Molecular mechanics force fields (FFs)

A force field (FF) is a mathematical model, used in molecular mechanics and composed by a set of analytic terms aimed to replace the complicated electronic interactions, and to estimate the forces acting on the atoms within molecules and the forces between one molecule and another. These

analytic terms consist of a set of potentials and parameters used to calculate the potential energy of a system of atoms. The potentials and parameters of a FF may be derived from experiments in physics and chemistry (e.g. X-ray diffraction method), from calculations in quantum mechanics, or from both [67].

There are two types of terms considered in the total energy equation to calculate the potential energy used in a FF. They provide a reasonable description of underlying interactions. The first type is the bonded terms which are related to the interactions of atoms linked by covalent bonds. The second type is the nonbonded terms, assigned for describing noncovalent bonds, such the long-range electrostatic and van der Waals (vdW) forces [59].

A general expression of the total energy in a FF can be written as follows [68]:

$$E_{total} = E_{bonded} + E_{nonbonded} \qquad (2.5)$$

The bonded terms represent the intramolecular forces necessary to join atoms together within a molecule and they depend on the bond stretching, angle bending and dihedral torsions parameters [69]:

$$E_{bonded} = E_{bond} + E_{angle} + E_{dihedral} + E_o \qquad (2.6)$$

Depending on the type of molecule, the parameter related to the out-of-plane bending (E_o) coordinate can be considered in the bonded terms of the FF. It calculates the forces for trigonal centers which consist in four atoms with three valence bonds formed to one center atom [67].

The nonbonded terms represent the intermolecular forces that exist between molecules because of their interaction and they depend on the electrostatic partial charges and the van der Waals potentials [69]:

$$E_{nonbonded} = E_{vdW} + E_{electrostatic} \qquad (2.7)$$

The FF energy expressions require many parameters to define each of the terms; for example, the stretching (k_b) and bending (k_a) constants, the equilibrium bond lengths (r_0), the angles (θ_0 and ϕ_0), the torsional ($k_{dihedral}$) constant, and the non-bonded parameters: distance between two atoms (σ), strength interaction between two atoms (ε) and partial atomic charges (q). These parameters can be assigned separately to reflect the different chemical environment of each atom in the system [67]. The equations related to the bonded and non-bonded terms are found in Appendix A.

Besides considering a set of potentials and parameters in a FF, the definition of atom types is required. The atom types represent the atoms that share the same expected bonding and interaction properties, and they are defined by a unique number in the FF. Correctly defining the atom types, it simplifies the application of a FF in MD simulations [59].

It exists different types of FFs that have been developed specifically for reproducing certain families of structures. However, it is possible to use the mathematical terms of an existing FF and adapt all the parameters for a specific process e.g., gas adsorption process [70]. Some of the most common FFs applied in gas adsorption are the following:

Universal Force Field (UFF)

The UFF has registered many types of atoms and includes all the elements of the periodic table. All atoms have the same chemical and physical characteristics and they are represented only by the chemical symbol, the geometry (linear, trigonal, tetrahedral, etc.) and the oxidation state [32]. This force field is the most used for systems containing inorganic elements. It was designed to use four valence terms, but any electrostatic term. Besides, it has been used to study gas adsorption on MOFs and some studies have demonstrated the accuracy of results to be significantly better without charges [71].

Chemistry at Harvard Macromolecular Mechanics (CHARMM)

This force field was devised for proteins and nucleic acids, and it has been applied to a range of biomolecules, molecular dynamics, crystal packing, vibrational analysis, and quantum mechanics/molecular mechanics studies. Besides, CHARMM is a force field that uses five valence terms, one of which is an electronic term [32].

DREIDING

DREIDING is a generic force field developed to predict structures and dynamics of organic, biological, and main group inorganic molecules. DREIDING has been most widely used for large biomolecular systems, and due to its capacity, the application of this force field has been extrapolated to model some materials like MOFs for studying the adsorption process of some GHGs like CO_2 [32], [71].

Assisted Model Building with Energy Refinement (AMBER)

The AMBER force field was primarily developed for protein and nucleic acid systems like biomolecules. AMBER uses only five bonding and non-bonding terms with a sophisticated

electrostatic treatment. This force field has shown good results for protein and nucleic acids but also it has shown a good description of the organic linkers, being used to study the adsorption process on porous materials [32], [72].

Molecular Mechanics 3 (MM3)

The MM3 force field was originally developed for hydrocarbons, but it has been extended to many important classes of organic compounds. It accounts the structures and energies, including heats of formation, conformational energies, and rotational barriers of a wide variety of hydrocarbons [68]. This force field has shown good accuracy in modeling organic molecules and it has been studied as the basis to create a transferable force field in which its parameters can be applied in molecular modeling of MOFs, which consist of both organic and inorganic components [69].

2.5.2. Periodic boundary conditions and electrostatic cut-offs

Molecular mechanics is mostly used to model the properties of very large systems, and it exists some artifacts that simplifies the analysis of these systems. The first artifact is the electrostatic cut-off used to minimize the computer time needed to evaluate a very large system [73]. Applying a cut-off distance (limited from the central atom to the half of the simulation 3D box length) is reasonable for very large thresholds where the interaction is very small. Thus, coulombic interactions (repulsion - attraction) will be roughly neutral. This means that the repulsion or the attraction to charges can be cancel out [74]. However, use solely the technique of the cut-offs are not enough to build large enough models that represent the correct behavior of a system in a meaningful way.

The second artifact is the periodic boundary conditions that represent a complementary technique for the cut-offs. It allows very extended systems to be modelled without needing punitively large numbers of atoms to be considered [74]. Applying periodic boundary conditions, it is possible to study a large molecular system that can be assumed infinite in size but represented as a symmetric unit cell. This unit cell is delimited by the simplest cubic arrangement in the 3 dimensions (coordinates x, y, z) with a specific number of atoms. However, this unit cell can accurately describe the phenomenon of interest and represents the behavior and the characteristics of the entire system [75].

In summary, the force fields, the periodic boundary conditions, and the electrostatic cut-offs are considered as three important strategies used in molecular mechanics to simplify the study of large molecular systems e.g., MOFs, and complex processes like adsorption. Choosing the appropriate force field, depending on the type of molecule and process, is essential to make reliable predictions about the materials' performance. So, the set of equations and parameters (force fields) describing the physical and the chemical interactions between the molecules can be considered as the main and the most important input in molecular simulations. Even if a specific force field for studying MOFs' performance does not exist, the existing force fields can be applied in MD to analyze the adsorption process using different MOFs as adsorbents. Thus, the generality of these force fields has allowed to extend the application to different studies that were not considered from the beginning in the design of the force field.

Summarizing, N_2O is a harmful gas for the environment. Some studies have been realized to decompose N_2O into N_2 and O_2 for reusing these gases in other processes. The main purpose of these studies is to apply a catalytic decomposition of N_2O in which the adsorption technique is part of a previous step for carrying out this type of process. The materials used to adsorb the N_2O are zeolite type and nanotubes and they have been specially modified with metal ions-exchange to improve the selectivity adsorption of N_2O. The ZIF-8, e.g., is a porous material with good adsorption characteristics that has not been deeply studied to adsorb N_2O but other GHGs like CO_2 and CH_4. The study of N_2O on ZIF-8 is an interesting research topic due to the fact that ZIF-8 has already demonstrated to be a potential adsorbent for CO_2, which is a molecule very similar to N_2O because they share many structural and physical similarities including molecular size and quadrupole moment.

Molecular modeling methods have been applied to study the gas adsorption process. They help to optimize some adsorption parameters that can be difficult to obtain by experimental approaches. The study of new combinations of materials and gases for adsorption techniques under non-studied operating conditions has been a popular application in molecular modeling. Thanks to the different types of molecular modeling (MM and MD), it is possible to deepen in the study of gas adsorption, changing the most important adsorption parameters like temperature and pressure. This can help to predict the efficiency of the process, the behavior of the gases on the adsorbent materials' surface, and the performance of the material, saving time and resources. The combination of experimental

and simulation methods seems to provide significant advantages in the research of new materials for gas adsorption processes, offering a new way to contribute to the development of scientific knowledge and to act against the current environmental problems caused by GHGs emissions.

CHAPTER 3. PROBLEMATIC, RESEARCH QUESTION AND OBJECTIVES

3.1. Problematic

Nitrous oxide is one of the main GHGs that constitutes a global environmental problem due to its role in the ozone layer depletion in the stratosphere. Some gas treatment technologies have been developed for trapping N_2O in order to treat it and return it to the atmosphere as N_2 and O_2 [76]. The adsorption process seeks to be a sustainable solution to one of the world's greatest problems in order to close the N_2O life cycle. However, this kind of process to control gas emissions uses materials like activated carbon or polymers such as polystyrene, resin, styrene–divinylbenzene, etc. that operate at medium (3400-8000 kPa) and high (>8000 kPa) pressures with a high energy-consuming. One of the reasons is because activated carbon and polymers present a more efficient adsorption at high pressure [17].

The problem with this physicochemical adsorption technique is that N_2O emissions are generally emitted under atmospheric conditions. Thus, the capture of N_2O requires to increase the pressure of a huge volume of polluted air to mitigate the impacts that N_2O has on the environment, implying a high-cost performance [76]. Likewise, the technology related to the adsorption process is far from being mature and the opportunities to apply it at an industrial scale and improve its efficiency are high [12]. Therefore, a major contribution for innovation in gas treatment based on adsorption technology requires a better understanding of physicochemical phenomena and engineering research for technological progress in materials to discover new adsorbents with better separation characteristics by the aid of multi-objective and multi-domain numerical approaches [12].

3.2. Research question

Nowadays, one of the big challenges about air treatment methods is the production of highly specific adsorbents able to capture N_2O under atmospheric pressure. Based on previous studies about GHGs capture processes, ZIF-8, a porous crystalline material, has demonstrated a high adsorption capacity for CO_2 and CH_4 [47], [48]. The fact that ZIF-8 has two pore sizes and some specific properties like flexible structure, due to the gate-opening effect, and hydrophobic behavior allow the study of ZIF-8 as a potential adsorbent to capture N_2O, the third most important GHG after CO_2 and CH_4. This could be possible due to the similarity that the molecular structure of N_2O has with the molecular

structure of CO_2. In this way, in order to study the adsorption process of N_2O on ZIF-8, two mainly questions have arisen: 1) which factors affect the adsorption process between the N_2O and the ZIF-8?, and 2) which is the effect of these factors on the adsorption capacity of ZIF-8 to capture the N_2O gas?

Unlike experimental studies of adsorption process, molecular modeling and computational chemistry are helpful tools that could be used to identify these important factors and to determine their effect on the adsorption process (N_2O and ZIF-8). This study, based on computational approaches, will also allow to visualize and understand how much this strategy of analysis helps to reduce time and resources for an adsorbate-adsorbent system that has not been studied yet, such as the gas N_2O (adsorbate) and the adsorbent material (ZIF-8), before carrying out experimental adsorption studies.

3.3. General objective

The objective of this research is to develop a method for calculating the N_2O adsorption capacity of ZIF-8 using molecular modeling and computational chemistry.

3.3.1. Specific objectives

The following specific objectives are divided in two groups: the molecular simulation to calculate the adsorption capacity of an adsorbent material, and the experimental determination of the adsorption capacity.

Molecular simulation to calculate the adsorption capacity of an adsorbent material:

- For quantum mechanics (QM), the objectives are:
    - To design 3D physical models of the structures of ZIF-8, CO_2, CH_4 and N_2O using a molecular modeling interface,
    - To simulate the molecular interactions between the two interaction configurations of N_2O (–ONN and –NNO) and ZIF-8 in three adsorption sites localized in both pores,
    - To calculate the adsorption energy and the approach distance based on the molecular interactions of ZIF-8 and N_2O for determining the most stable interactions.
- Using molecular dynamics (MD), the objectives are:
    - To design 3D physical models of the structures of ZIF-8, CO_2, CH_4 and N_2O using a molecular modeling interface,

- To simulate, the dynamic adsorption process between 1) N_2O and ZIF-8, 2) CO_2 and ZIF-8 and 3) CH_4 and ZIF-8, under different gas concentrations, to obtain the total pressure of the system and the number of molecules adsorbed for each gas,
- To calculate the excess uptake of N_2O, CO_2 and CH_4 (separately) for building the adsorption isotherms and analyze the adsorption capacity of ZIF-8 with N_2O,
- To obtain the radial distribution functions (RDFs) in order to calculate the adsorption energy of each of the three gases (N_2O, CO_4 and CH_4) on ZIF-8.

Experimental determination of the adsorption capacity:

- To produce the ZIF-8 powder by a solvothermal synthesis,

- To characterize the ZIF-8 powder,

- To analyze the adsorption capacity of ZIF-8 with CO_2 at atmospheric pressure and ambient temperature, using the thermogravimetric adsorption-desorption technique,

- To validate the adsorption capacity results obtained in the laboratory with experimental data reported in the literature,

- To develop an analytical protocol that could be applied to other adsorption systems with different adsorbates and adsorbents.

CHAPTER 4. HYPOTHESES

4.1. Proposed hypotheses

According to the exposed problematic and the specific objectives, the hypotheses of this research are divided and presented as follows:

Adsorbent model

- Zeolitic Imidazolate Framework-8 (ZIF-8) can be used as good adsorbent material to adsorb N_2O due to some specific characteristics, such as its flexible structure due to the gate-opening effect that allows the cavities of its porous structure to enlarge and be able to retain large molecules like CO_2 or N_2O. Also, its hydrophobicity would allow to selectively attract, select, and retain N_2O molecules in a mixture of gases.

- Zeolitic Imidazolate Framework-8 might be able to work efficiently, as gas adsorbent, under atmospheric pressure because ZIF-8 has high adsorption capacity at different operating conditions, including atmospheric pressure and ambient temperature.

- Zeolitic Imidazolate Framework-8 might be a good adsorbent for N_2O because this porous material has been extensively and successfully used to adsorb other GHGs like CO_2 that has similar characteristics to N_2O.

Computational approaches for studying N_2O adsorption on ZIF-8

- The application of molecular modeling and computational chemistry will allow to study the adsorption process at a molecular level and to predict the molecular interactions between the adsorbate (N_2O) and the adsorbent (ZIF-8). After developing the 3D models for the system, the time and resources needed for studying the N_2O adsorption will be smaller than doing experimental studies at the laboratory.

- The precision and the performance of different computational approaches based on quantum mechanics calculations and molecular mechanics simulations will produce simulated results comparable with experimental results.

- The combination of two mathematical methods (Semi-Empirical Method (PM6) and Density Functional Theory (DFT B3LYP-D3 6-31G*)) will optimize the time of computer calculations for obtaining the adsorption energy and determine the equilibrium (molecular stability) of the system.

- The adsorption energy (calculated using the mathematical methods) will determine the theoretical adsorption capacity of ZIF-8 to capture N_2O.

- Molecular mechanics, specifically molecular dynamics, will be useful to study the adsorption process in a large molecular system like a large fragment of ZIF-8, being able to interact with several gas molecules.

- The supplementary study of the adsorption capacity of ZIF-8 with highly know and studied GHGs such as CO_2 or CH_4 will be useful to create a reproducible and transferable methodology for the main study of N_2O adsorption on ZIF-8 using molecular dynamics.

- Molecular dynamics will allow to study the individual adsorption process of CO_2, CH_4 and N_2O on the surface of ZIF-8 over time to build a theoretical adsorption isotherm in a wide range of gas pressure, while considering constant the number of gas molecules (gas concentration, N), the volume (V), and the temperature (T), i.e. a NVT system.

Experimental determination of gas adsorption

- The thermogravimetric balance could be used to develop an experimental method to determine the gas adsorption process.

- A general method can be developed, and it could be applied to different gas-adsorbent systems.

CHAPTER 5. METHODOLOGY AND SCHEDULE

5.1. Methodology

5.1.1. Simulation: Quantum mechanics (QM)

Design of the 3D physical models for QM simulations

A molecular modeling simulator will be used to create the 3D molecular structures of the N_2O molecule and the small and the big pore of ZIF-8. The simulator interface allows to join every atom that constitutes the adsorbate (N_2O) and the adsorbent (ZIF-8) to build both molecules. For the N_2O molecule, two nitrogen atoms (triple bond) and one oxygen atom (simple bond) will be linked: N≡N−O (See Appendix B.1). For the small pore of ZIF-8, four 2-mIm molecules ($CH_3C_3H_2N_2H$) and four zinc atoms (Zn (II)) must be linked, and for the big pore of ZIF-8, six 2-mIm molecules ($CH_3C_3H_2N_2H$) and six zinc atoms (Zn (II)) must be linked (See Appendix B.2).

Quantum mechanics simulations

Quantum mechanical simulations will be carried out using one N_2O molecule and a small and a big pore of ZIF-8. These simulations will be performed in three adsorption sites located in the ZIF-8: 1) Center, 2) Side, and 3) Methylcenter. These adsorption sites are the places where the N_2O molecule will interact from its oxygen atom (–ONN) or from its terminal nitrogen atom (–NNO) with the surface of the small and the big pore of ZIF-8, as shown in Appendix C.1 and C.2.

Two mathematical methods will be used to do the calculations for the molecular simulations: 1) Semi-Empirical Method PM6, and 2) Density Functional Theory DFT B3LYP-D3 6-31G*. The combination of these mathematical methods will help to optimize the time of the calculations.

A simulation tool called *define ligand point* will be used to fix the ligand point that helps to simulate a physical interaction i.e., the adsorption process, and not a chemical reaction, between the N_2O molecule and the adsorption sites of the ZIF-8 (See Appendix D.1). This tool will also help to calculate the approach distance due to the attractive forces between the atoms –N or –O (corresponded to the N_2O molecule) and the adsorption sites of the small and the big pore of the ZIF-8.

Three symmetry constraints will be used to carry out the simulations: 1) *Frozen atoms* to avoid deformation in the geometry of both pores of ZIF-8 (Appendix D.2), 2) *Constraint angle* to avoid

angle modification in the molecular structure of both pores of ZIF-8 (Appendix D.3), and 3) *Constraint distance* to avoid the resize of bond lengths between atoms (Appendix D.3).

Adsorption energy and approach distance

The adsorption energies will be calculated from the following equation for the three adsorption sites in both pores of ZIF-8 [37]:

$$E_{ads} = E_{ZIF-8/N_2O} - (E_{ZIF-8} + E_{N_2O})$$

where,

E_{ads} is the total energy of the adsorbate-adsorbent system (kJ/mol);

E_{ZIF-8/N_2O} represents the non-bonded energy of the interaction between the adsorbent (ZIF-8) and the adsorbate (N_2O) and considers the attraction or repulsion forces between not connected atomic centers and corresponds to van der Waals and Coulombic interactions;

E_{ZIF-8} and E_{N_2O} (separately) represents the strain energy, i.e., the energy stored in molecules due to their formation to rearrange themselves after being subjected to an external force.

Approach distances will be obtained and measured after geometry optimization of every simulation using the *define ligand point* tool (See Appendix D.2).

5.1.2. Simulation: Molecular dynamics (MD)

Design of the 3D physical models for MD simulations

A molecular modeling simulator will be used to create the 3D molecular structures of the N_2O, CO_2 and CH_4 molecules and a fragment of ZIF-8. By linking several big pores, a segment of ZIF-8 will be formed as it is shown in Appendix B.3. The aperture formed by the big pores will allow to form the small pores in the structure.

The Molecular Mechanics 3 (MM3) force field, adapted for MOFs, will be used to allow the program (software for MD simulations) generates and visualizes the initial structures of N_2O, CO_2, CH_4 and ZIF-8 in its interface. The MM3-MOF force field will allow to establish all the parameters that correspond to the intramolecular and intermolecular forces of the adsorbent ZIF-8 (Appendix F.1 and F.2) and the gas molecules (N_2O, CO_2, CH_4), listed in Appendix F.3, F.4 and F.5, respectively. Different atom types will be applied to represent every atom of the gas molecules and the ZIF-8 according to its binding and interaction properties.

Two artifacts will be applied in the molecular structure of ZIF-8 to represent the correct behavior of a complex and very large molecular system and simplify its analysis: 1) Periodic boundary conditions to determine the simplest cubic arrangement (simulation box), in 3 dimensions (coordinates x, y, z), of an infinitive molecular system (adsorbate-adsorbent), and 2) Electrostatic cut-off to determine the coulombic interactions (repulsion - attraction) on the end-atoms of the structure of ZIF-8.

Molecular dynamics simulations

Molecular dynamics simulations will be caried out in three simulation boxes containing several molecules of each gas (N_2O, CO_2 and CH_4) and a segment of ZIF-8. Every gas will be studied individually with the ZIF-8. The molecular structures of the three systems (N_2O and ZIF-8, CO_2 and ZIF-8, CH_4 and ZIF-8) will be minimized as a previous step to dynamic simulations with a convergence criterion of 0.4-0.5.

All the dynamic simulations will be performed under the canonical ensemble NVT, considering the following parameters: 1) N as a variable amount of substance (gas), i.e., different number of N_2O molecules interacting on the surface of the ZIF-8 segment, 2) V as the volume, i.e., the cubic cell defined by the periodic boundary conditions, and 3) T as the temperature, i.e., the operating temperature of every simulation. The number of gas molecules will vary in every dynamic simulation going from 50 to 1000 molecules while the volume and the temperature remain constant.

These dynamics simulations will be carried out in two phases: 1) Equilibration phase where the total pressure of the system does not vary any more over time, and 2) Production phase where, firstly, the number of gas molecules adsorbed will be identified and secondly, the total pressure of the system will be measured. These two phases will be repeated in every dynamic simulation.

One timestep of 1 ns[2] (1 000 000 steps) will be used to analyze the equilibrium of the three systems: 1 ns (1 000 000 steps) or 2 ns (2 000 000 steps). One timestep of 1 ns (1 000 000 steps) will be used to identify the number of N_2O molecules adsorbed, and 0.3 ns (300 000 steps) will be used to measure the total pressure of the system.

---

[2] 1 ns equals 1 000 000 steps in molecular dynamics. The number of steps is used to program the time of the dynamic simulation.

One symmetry constraint will be used to carry out the full equilibration phase and one part of the production phase (identification of the number of adsorbed molecules): 1) *Restrain position* to avoid deformation in the geometry of the ZIF-8 segment.

Adsorption capacity of ZIF-8

After carrying out all the dynamic simulations, the adsorption capacity of ZIF-8 for each gas (N_2O, CO_2 and CH_4) will be determined by three adsorption isotherms corresponding to each gas which depend on the excess uptake and the total pressure of the system.

The excess uptake will be calculated after the production phase from the following equation [17]:

$$Excess\ uptake = \frac{\dfrac{N_g \cdot m_g}{N_A} - \dfrac{\rho_g \cdot V_{free} \cdot M_{ZIF-8}}{N_A}}{\dfrac{M_{ZIF-8}}{N_A}} \ x\ 1000$$

where,

Excess uptake (mg/g) is the computational calculation of the adsorption capacity of ZIF-8 according to the number of gas molecules adsorbed, the total pressure of the gas-adsorbent system (N_2O and ZIF-8, CO_2 and ZIF-8, CH_4 and ZIF-8) and the size of the ZIF-8 segment;

N_g (g/mol) is the number of gas molecules adsorbed on the ZIF-8;

m_g (g/mol) is the molecular weight of the gas;

ρ_g (g/cm^3) is the density of the gas according to the total pressure of the system;

V_{free} (cm^3/g) is the available volume in the ZIF-8 segment to adsorb the gas molecules;

M_{ZIF-8} (g/mol) is the molecular weight of the ZIF-8 segment;

N_A (1/mol) is the Avogadro's number ($6.0221x10^{23}$).

The adsorption isotherm curves for each gas (N_2O, CO_2 and CH_4) will be created as a function of the total pressure (atm) and the excess uptake (mg gas/g ZIF-8), both obtained in the production phase. The adsorption isotherms of CO_2 and CH_4 will be compared with literature. The comparison of these two gases will be backed up with a statistical analysis based on an ANOVA test.

Adsorption energy

The total adsorption energy (E_{adsT}) for each system, also defined as intermolecular energy, will be calculated, at the end of each simulation, directly by the software of MD simulations. This calculation will depend on the Radial Distribution Function (RDF) which: 1) defines the maximum

adsorption distance of the gas molecules in the first layer of adsorption on the ZIF-8, and 2) determines the cut-offs for adsorption (electrostatic charge and Van der Waals) necessary to measure adequately the E_{adsT}. The RDF will be calculated directly by a MD software.

For each gas (N_2O, CO_2 and CH_4), the adsorption energy per gas molecule (E_{ads}) will be calculated dividing the E_{adsT} by the number of the gas molecules adsorbed, previously identified. An average of all the E_{ads} will be determined for each gas.

5.1.3. Experimental

Synthesis of ZIF-8

ZIF-8 will be obtained by solvothermal synthesis, described in detail in Appendix E.1.

Characterization of ZIF-8

The physical and chemical characterization of ZIF-8 will be carried out as follows:

- The thermal stability of ZIF-8 will be measured by a thermogravimetric analysis (TGA);
- The crystallinity of the ZIF-8 structure will be analyzed by an X-ray diffraction pattern (XRD);
- The type of groups and ligands that constitute the ZIF-8 structure will be determined by a Fourier Transform Infrared spectroscopy (FTIR);
- The particle size distribution of ZIF-8 will be determined by a nanoparticle tracking analysis (NTA-Nanosight);
- The effect of the pH on the electronic charge of ZIF-8 will be evaluated by a zeta potential analysis (Zetasizer).

Gas adsorption by thermogravimetric analysis

The experimental adsorption determination will be carried out using a thermogravimetric balance (TGA). The CO_2 will be used for this study and a small sample of ZIF-8. Each determination will be performed by means of an adsorption-desorption cycle which will have five phases: 1) Stabilization phase in which the initial temperature (298 K; 25 °C) will be set up for a few minutes, 2) Pretreatment phase in which the moisture and any pre-adsorbed gases will be removed at 573 K (300 °C) for a period of 1.5 h, 3) Cool down phase in which the adsorption temperature (298 K; 25 °C) will be set up for half an hour, 4) Adsorption phase in which CO_2 will be adsorbed on ZIF-8 at the adsorption temperature (298 K; 25 °C) and atmospheric pressure (101.3 kPa) for a

total of 3 h, and 5) Desorption phase in which the ZIF-8 will be regenerated by removing the adsorbed CO_2 at 573 K (300 °C) for a period of 1.5 h. The CO_2 flow rates will be varied from 50 to 300 ml/min to determine the saturation flow rate under the temperature and pressure fixed for adsorption phase

Adsorption capacity of ZIF-8

After finishing each adsorption-desorption cycle, the adsorption capacity of ZIF-8 will be determined by the gas uptake, calculated from the following equation [77]:

$$Gas\ uptake = \frac{w_t - w_{t=0}}{m_g \cdot w_{t=0}} x\ 1000$$

where,

$Gas\ uptake$ (mmol/g) is the amount of gas adsorbed on ZIF-8;

w_t (mg) is the equilibrium weight of ZIF-8 after adsorption;

$w_{t=0}$ (mg) is the initial weight of ZIF-8 before adsorption;

m_g (mg/mol) is the molecular weight of the gas.

A CO_2 adsorption curve at constant temperature will be created using the gas uptake (mmol gas/g ZIF-8) calculated with the corresponding CO_2 flow rate (ml/min).

5.2. Schedule

Table 5.1 Schedule of master's research project activities.

Activities	Sessions					
	Autumn 19	Winter 20	Summer 20	Autumn 20	Winter 21	Summer 21
Literature review about N₂O and molecular simulations						
DPR						
Student symposium of the Chemical Engineering and Biotechnology Engineering Department (Faculty of Engineering, Sherbrooke)						
QCAM Student Symposium (Montreal)						

Task								
International Conference on Catalysis and Chemical Engineering (Los Angeles, CA)		▓						
Paper 1 writing			▓	▓				
Master's thesis writing					▓	▓	▓	▓
88ᵉ Congrès de l'Acfas (Sherbrooke)			▓					
Paper 2 writing						▓	▓	▓
Simulation	▓	▓	▓	▓				
Design of 3D physical models	▓							
Molecular mechanics simulations	▓	▓						
Adsorption energy and approach distance	▓	▓						
Molecular dynamics simulations			▓	▓	▓	▓		
Adsorption capacity of ZIF-8				▓	▓	▓		
Experimental				▓	▓	▓	▓	▓
Solvothermal synthesis ZIF-8							▓	
Characterization ZIF-8								▓
Thermogravimetric adsorption-desorption analysis								▓
Experimental validation and protocol development								▓

FOREWORD: CHAPTER 6

Authors and affiliation:
- Karen Villegas Domínguez: Master student, Department of chemical and biotechnological engineering, Faculty of engineering, Université de Sherbrooke.

- Beatriz Delgado: Research assistant, Centre National en Électrochimie et en Technologies Environnementales (CNETE).

- Alain Wilkin: Professor, Cégep de Shawinigan.

- Satinder Kaur Brar: Professor, York University.

- Michèle Heitz: Professor, Department of chemical and biotechnological engineering, Faculty of engineering, Université de Sherbrooke.

- Antonio Avalos Ramirez: Researcher, Centre National en Électrochimie et en Technologies Environnementales (CNETE).

Title/Titre:
- Study of adsorption interactions between nitrous oxide and Zeolitic Imidazolate Framework-8 (ZIF-8) by molecular modeling.

- Étude des interactions d'adsorption entre l'oxyde nitreux et le *Zeolitic Imidazolate Framework-8* (ZIF-8) par modélisation moléculaire.

Contribution to the document:
This article is the first part and the basis of the complete study of this thesis. The adsorption process has been applied in the laboratory to capture and treat some gases like GHGs. However, the molecular modeling and the computational chemistry, focused on molecular quantum mechanics simulations, open a new way to study this process and give the opportunity to save some resources such as time, money, and human resources. Also, this technique allows to deepen the analysis of the molecular behavior between the adsorbent and the adsorbate, especially when it has not been deeply studied in the laboratory. For example, ZIF-8 has been used to adsorb successfully GHGs like CO_2 and CH_4. Nevertheless, this material has not been used to capture N_2O. Thus, this study contributes to the progress of new adsorbate-adsorbent combinations and allows to develop the basis

for future studies (molecular dynamics simulations) in which the analysis of the adsorption process between N_2O and ZIF-8 is done through the time, varying the operating conditions (temperature and pressure).

Abstract/Résumé:

- Nitrous oxide (N_2O) is a greenhouse gas (GHG) mainly issued from agriculture and waste management activities. Since N_2O has a global warming potential 298 times higher than CO_2 and an annual emission equivalent to 5.1 % v/v of total GHG emissions, the control of its emissions becomes essential. One of the main challenges to control N_2O emissions is to capture them under the main sources' conditions, i.e. atmospheric pressure, and ambient temperature. The available technologies to control N_2O emissions operate presently at medium/high pressure, being high energy consuming. The development of new and specific adsorbents for capturing N_2O is important. Molecular modeling is a helpful tool to develop engineered adsorbents, generating virtual molecular interactions as a prior adsorbate-adsorbent system before experimental studies. Zeolitic Imidazolate Framework-8 (ZIF-8) has been selected in this study as an adsorbent because of its easy and reproducible synthesis, thermal stability, flexible structure, hydrophobicity, and high adsorption capacity of gases, including GHGs. In the present study, the interactions between N_2O and ZIF-8 were studied by molecular modeling methods, PM6 and DFT. Optimized geometries of N_2O and ZIF-8, adsorption energy and ligand point length parameters were analyzed as part of a physical adsorption process. Three adsorption sites were identified on the four-membered and six-membered windows of ZIF-8. The two possible N_2O interaction configurations (–ONN and –NNO) were simulated and compared in order to determine the most probable behavior of N_2O. The study showed that the –ONN configuration produces more stable interactions with ZIF-8 than –NNO configuration. The six-membered window of ZIF-8 seems to be the pore where the most stable interactions occur based on the adsorption energy and the approach distance. The present study was concentrated on the interactions of one N_2O molecule and a fragment of the ZIF-8, and it will be the basis for molecular dynamics simulations of adsorption with a control volume, containing several N_2O molecules and a representative surface of ZIF-8 under different pressures and temperatures.

- L'oxyde nitreux (N_2O) est un gaz à effet de serre (GES), principalement, issu des activités agricoles et de la gestion des déchets. Le N_2O a un potentiel de réchauffement planétaire 298 fois plus élevé que celui du CO_2 et une émission annuelle équivalente à 5,1 % v/v des émissions totales de GES, ce qui rend important le contrôle de ses émissions. L'un des principaux défis pour le contrôle des émissions de N_2O est de les capturer sous les conditions de ses principales sources, c'est-à-dire, à pression et à température ambiantes. Les technologies disponibles pour contrôler les émissions de N_2O fonctionnent actuellement à moyenne/haute pression, et par conséquent elles sont énergivores. Le développement de nouveaux adsorbants, spécifiques pour capturer le N_2O, est important. La modélisation moléculaire est un outil pratique pour développer des adsorbants, en générant des interactions moléculaires virtuelles en tant que système adsorbat-adsorbant préalable, avant de réaliser des études expérimentales. Le *Zeolitic Imidazolate Framework-8* (ZIF-8) a été sélectionné dans cette étude comme adsorbant en raison de sa synthèse facile et reproductible, de sa stabilité thermique, de sa structure flexible, de son hydrophobicité et de sa capacité d'adsorption élevée des gaz, y compris les GES. Dans la présente étude, les

interactions entre le N_2O et le ZIF-8 ont été étudiées par les méthodes de modélisation moléculaire, PM6 et DFT. Les géométries optimisées du N_2O et du ZIF-8, l'énergie d'adsorption et les paramètres de longueur du point de ligand ont été analysés dans le cadre d'un procédé d'adsorption physique. Trois sites d'adsorption ont été identifiés sur les pores de quatre et six membres du ZIF-8. Les deux configurations d'interaction possibles du N_2O (–ONN et –NNO) ont été simulées et comparées afin de déterminer le comportement le plus probable du N_2O. L'étude a montré que la configuration –ONN produit des interactions plus stables sur le ZIF-8 qu'avec la configuration –NNO. Le pore de six membres du ZIF-8 semble être le pore où les interactions les plus stables se produisent en fonction de l'énergie d'adsorption et de la distance d'approche. La présente étude s'est concentrée sur les interactions d'une molécule de N_2O et d'un fragment du ZIF-8, et elle servira de base à des simulations par dynamique moléculaire sur l'adsorption avec un volume de contrôle, contenant plusieurs molécules de N_2O et une surface représentative du ZIF-8 sous différentes pressions et températures.

Note: Following the corrections requested by the members of the jury, the content of this article differs from the one that was accepted.

CHAPTER 6. ADSORPTION INTERACTIONS BETWEEN N₂O AND ZIF-8: MOLECULAR QUANTUM MECHANICS SIMULATIONS

6.1. Introduction

Nitrous oxide (N_2O) is one of the three main greenhouse gases (GHGs), after carbon dioxide (CO_2) and methane (CH_4). The N_2O remains in the atmosphere for 116 years and it has a global warming potential (GWP) 298 times higher than CO_2 (GHG of reference) [8]. From 1750 to 2018, the concentration of N_2O in the atmosphere increased by 23 % (270 to 331.1 ppbv) [78]. The main sources of N_2O emissions are nitrogen-based fertilizers, livestock, adipic acid and nitric acid production, fossil fuel combustion and waste management [9]. Climate change and global warming are some of the most important environmental problems to which contribute the N_2O emissions. In addition, N_2O has shown a great impact on the ozone layer depletion by being considered as the single most important ozone destroying compound [79].

There are some technologies based on biological, chemical, and physicochemical principles to control GHG emissions. These technologies will capture, concentrate and/or degrade the gas; for example, the adsorption-desorption treatment systems [46], [80]. Specially, gas capture process by adsorption has gained popularity in industry and environmental protection thanks to the development of a wide variety of adsorbents and the environmental policies. The adsorption process where gas molecules assemble in the channels of porous materials is mainly carried out by a typical physical adsorption mechanism, also called physisorption. Van der Waals and Coulombic interactions are the main attractive forces between the adsorbate and the adsorbent for physisorption [17]. This technology has been identified as an appropriate method for removing diluted contaminants in air due to its high selectivity, its efficiency and its low operational cost [11].

Zeolitic Imidazolate Frameworks (ZIFs) are porous crystalline materials that constitute a subclass of Metal-Organic Frameworks (MOFs) with similar topologies to traditional zeolites [24]. The ZIFs have been studied as adsorbents under different operating conditions. Among them, the Zeolitic Imidazolate Framework-8 (ZIF-8) has gained importance because of its molecular structure (sodalite topology; less complex than the other ZIFs or MOFs) and its easier and reproducible synthesis [24]. The specific characteristics of ZIF-8 confer to this material a high adsorption

capacity for a wide range of gases; for example, GHGs like CO_2 or CH_4 [47], [48], and other gases like hydrogen (H_2) and argon (Ar) [51], [52]. ZIF-8 behaves as a composite material because of its organometallic structure which gives 1) thermal stability, at temperatures < 673 K, as zeolites, 2) flexible structure and large cavity, as the MOFs, which allows ZIF-8 to capture molecules larger than 3.4 Å without having a material deformation, and 3) hydrophobicity which could be an advantage for non-polar gases separation that contain moisture [24], [29], [81].

Molecular modeling has been used as a tool to design new materials for gas adsorption and reactional processes [32]. It has showed the potential to give a better understanding of molecular interactions before doing experimental studies because it can describe and predict the behavior of molecular interactions. This allows to save money, resources and time [32]. Also, molecular modeling helps to understand better an adsorbate-adsorbent system because there are some properties of complex molecules that can be predicted computationally, and simplifies the development of analytical methods [32]. Besides, the methods used for molecular modeling play an important role with regard to obtain accurate structural parameters and mechanical properties as well as the optimization of atomic positions [82].

Recently, the Semi-Empirical Method PM6 has been used in simulation studies because of its better efficiency compared to others Semi-Empirical Models (e.g., AM1 or PM3). It produces also a high computational precision, giving results very close to those obtained by experimentation [66]. In the same way, Density Functional Theory (DFT) has been used to describe the quantum behavior of atoms and molecules. Specially, DFT B3LYP-D3 6-31G* is useful because of its efficiency to make calculations in less time, its ability to calculate reaction enthalpies and to determine the equilibrium and transition-state structure of organic molecules and other molecules incorporating transition-metals [31].

The study of adsorption process involves the consideration of certain parameters, especially the adsorption energy that indicates the interaction effectiveness on the surface of the adsorbent and the adhesion strength of the adsorbate on the adsorbent surface [18]. Previous studies have analyzed the adsorption energy of N_2O with different types of adsorbents as shown in Table 6.1, taking into consideration the N_2O adsorption configuration (–ONN or –NNO). DFT is one of the most used molecular modeling methods to carry out simulations of gas adsorption.

Table 6.1 Adsorption energy of N_2O on various adsorbent materials using different molecular modeling methods.

Adsorbent	Adsorption configuration	Adsorption energy (kJ/mol)	Molecular modeling method	References
ZnO (0001)-doped graphene	–ONN –NNO	-22.2 -26.1	DFT-D2 GAUSSIAN 6-31G	Gholizadeh *et al.* [46]
Pt-decorated graphene	–ONN –NNO	-113.6 -41.2	DFT B3LYP/6-31G	Shokuhi Rad *et al.* [45]
Si-doped graphene	–ONN –NNO	-17.3 -12.1	*Ab initio* DFT-D2	Gholizadeha and Yu [83]
Se-doped graphene	–ONN –NNO	-20.9 -15.1	*Ab initio* DFT-D2	Gholizadeha and Yu [83]
Cu-BEA zeolite	–ONN –NNO	-14.8 -39.7	DFT B3LYP/6-31G	Wang *et al.* [39]
ZSM-5-K^+	–ONN –NNO	-43.4 -47.4	DFT	Zhang *et al.* [37]
Ga=O-ZSM-5	–ONN –NNO	-28.8 -37.6	DFT B3LYP/6-31+G	Solkan *et al.* [36]
ZIF-8	–ONN –NNO	-43.9 -35.9	PM6 + DFT B3LYP-D3 6-31G*	Present study

In the present study, the objective was to simulate the molecular interactions between N_2O and ZIF-8 as a physical adsorption process using a sequence of simulation methods to simplify and reduce the time of calculations. Geometry optimization, approach distance and adsorption energy were considered as adsorption parameters to determine the stability of these interactions. The study of the interactions between one molecule of N_2O and a fragment of the ZIF-8 was performed and will be complemented by further calculations using molecular dynamics which considers pressure, volume, temperature, and number of particles adsorbed. The contribution of the present study was to develop a simple and fast modeling method with the aim of being applied in future works to select materials that have higher adsorption potentials for N_2O.

6.2 Materials and methodology

6.2.1 Adsorbent: ZIF-8

The ZIF-8 was used as an adsorbent. It has a structure based on zinc (Zn (II)) and 2-methylimidazole (2-mIm, $C_4H_6N_2$) with two windows (4 and 6 membered pores) and a bond length between zinc (Zn) and nitrogen (N) of 1.987 Å [23]. The small pore (four-membered) has four zinc atoms and four molecules of 2-mIm. It has a pore size of 3.4 Å in diameter. In contrast, the big pore (six-membered), has six zinc atoms and six molecules of 2-mIm, and a pore size of 11.6 Å (in diameter) [27].

6.2.2 Computational details

The calculations using the modeling methods PM6 and DFT B3LYP-D3 6-31G* were carried out using a molecular modeling simulator interface for quantum mechanics calculations: Spartan'18 (V1.3.0) from Wavefunction, Inc. Information about molecular structures were obtained applying computational chemistry methods and creating static scenarios of interactions.

Specifically, for this project, ligand points were used to simulate physical adsorption.

As a first step, the method PM6 was used to create equilibrium structures of the molecules N_2O and the ZIF-8 cluster in order to optimize the structural parameters. Subsequently, the DFT method was used to calculate the energy of the bond at B3LYP-D3 6-31G* level with the functional B3LYP which is one of the most used among the functional hybrids. The combination of PM6 and DFT B3LYP-D3 6-31G* helped to decrease the calculation time. The approach of using only a cluster of the ZIF-8, which is a repetitive structural unit of the ZIF-8 framework, helps to save computation time and to get consistent results with those obtained by full periodic calculations. This is possible when the cluster is formed by all the atoms involved in the interaction between the N_2O molecule and the ZIF-8 framework. In fact, the use of a cluster model for the ZIF-8 framework is similar to the approach applied by Qiu *et al.* [84] and Fellah and Onal [85]. Small clusters, but sufficiently large for the region of central interest, can be constructed to behave as though they were embedded in the bulk solid due to the simplicity and the ease of viewing the arrangement of adsorbate-adsorbent interactions.

6.3 Theory/Calculation

All simulations were performed using fixed positions for zinc atoms of the ZIF-8 to ensure that the initial opening size of its four- and six-membered windows did not distort during the geometry optimization using the method PM6. Some of these simulations (six-membered window simulations) were performed with symmetry constraints: *constraint distance* and *constraint angle*. These symmetry constraints avoid extreme geometry deformations during the simulation sequences to find equilibrium geometries. These constraints were applied: 1) between the bond of the nitrogen atom of the 2-mIm molecule, 2) between the bond of the methyl of the 2-mIm molecule, 3) between the bond of zinc atom and 2-mIm molecules, and 4) between the bond of the N_2O molecule, either for the bond of oxygen-nitrogen (O-NN) or for the bond of nitrogen-nitrogen (N-NO).

For carrying out the molecular simulations of N_2O adsorption on ZIF-8, three interactions sites called as follows were analyzed: 1) Center, in this case, the N_2O molecule interacted with the center of both pores (four- and six-membered windows) of ZIF-8, 2) Side, in this case, the N_2O molecule interacted with the corner of both windows of ZIF-8, close to the zinc atom, and 3) Methylcenter, in this case, the N_2O molecule interacted with the center of the 2-mIm molecule in four- and six-membered windows of ZIF-8. These sites were selected according to studies performed by Fischer and Bell [52] and Hobday *et al*. [51].

The N_2O has the molecular structure: $N{\equiv}N^+{-}O^-$ and a length of 2.5 Å. According to this molecular structure, N_2O can interact with the ZIF-8 with one of the two ends: the oxygen atom (–ONN) and the nitrogen atom (–NNO) [37], [36], [39], [41], [46], [33].

The adsorption energies were calculated according to the following equation [37]:

$$E_{ads} = E_{ZIF-8/N_2O} - (E_{ZIF-8} + E_{N_2O}) \qquad (6.1)$$

where,

E_{ads} is the energy of the adsorption system (kJ/mol);

E_{ZIF-8/N_2O} is the non-bonded energy of the interaction between the adsorbent (ZIF-8) and the adsorbate (N_2O). It considers the attraction or repulsion forces between non connected atomic centers, corresponding to van der Waals and Coulombic interactions;

E_{ZIF-8} and E_{N_2O} (separately) represents the strain energy that is the energy stored in molecules due to their capacity to rearrange themselves after being subjected to an external force that cause a deformation.

6.4 Results and discussion

6.4.1 Geometry optimization of ZIF-8

The molecular structure of ZIF-8 was constructed using the method PM6. Calculations were performed to find the equilibrium geometry. This geometry was used to calculate the bond adsorption energy with the method DFT B3LYP-D3 6-31G*. Fig. 6.1 (a) shows the molecular structure of one unit cell of ZIF-8 from two different angles: the four-membered and six-membered windows of ZIF-8. The geometry of solid surfaces is a challenge in computational modeling because of the large number of atoms required, the complex interactions involved and the electronic interactions that are much different than an isolated section [86]. A link breakage in the molecular structure of ZIF-8 was employed in this study in order to do the simulations of a 3D fragment of the solid. The addition of hydrogen atoms to the fragment of the ZIF-8 is used to respect electroneutrality and valence states of the atoms for the broken bounds. As it is illustrated in Fig. 6.1 (b), the molecular structure of ZIF-8 has two types of windows: a four-membered ring and a six-membered ring.
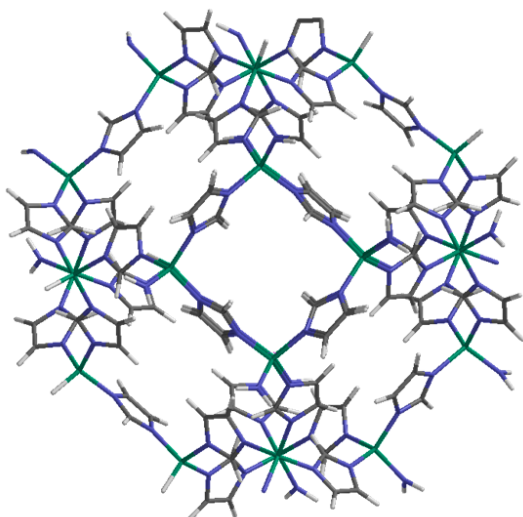
a)   b)
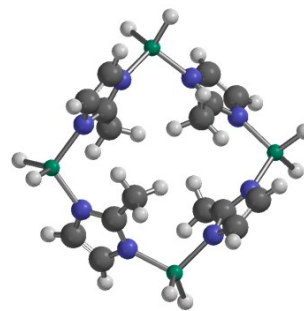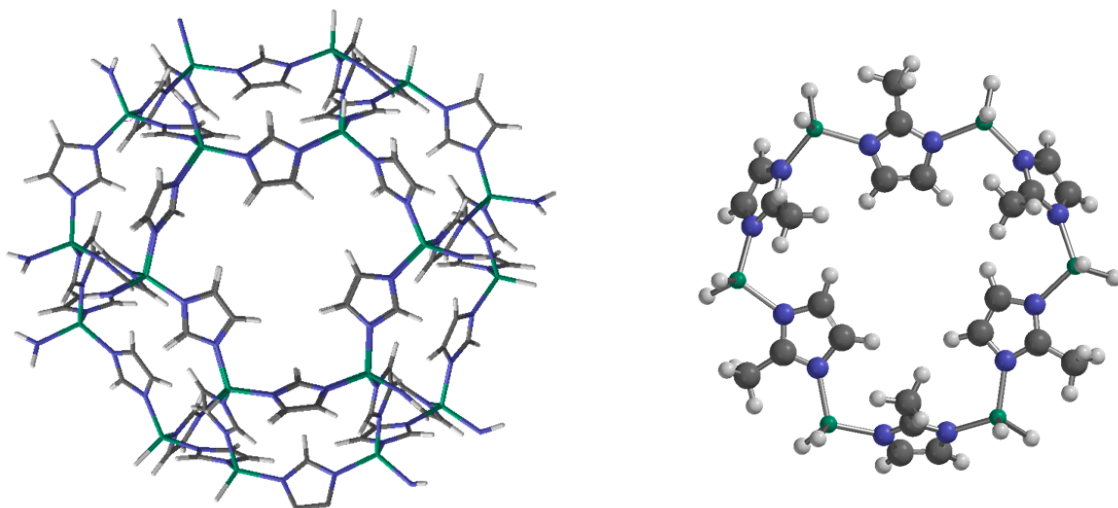
Figure 6.1 (a) Optimized geometry of one unit cell of ZIF-8 showing both windows of ZIF-8. (b) A closer view of the four-membered (top) and six-membered (bottom) windows of ZIF-8. Blue represents nitrogen; Gray represents carbon; White represents hydrogen; Green represents zinc.

The molecular interactions between the molecule of N_2O and the unit of ZIF-8 can occur in different sites of ZIF-8 structure. For this study, the three sites for these interactions were the following: Center, Side and Methylcenter, for both windows (small and big), as shown in Fig. 6.2. The interactions sites are indicated for 2D frontal views of each window of the optimized structure of ZIF-8. Similar interactions sites were reported by using Density Functional Theory (DFT) for the molecular modeling.
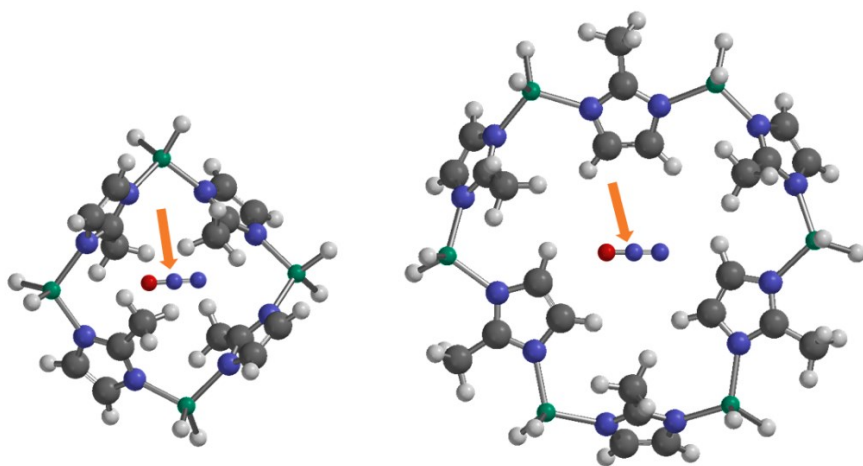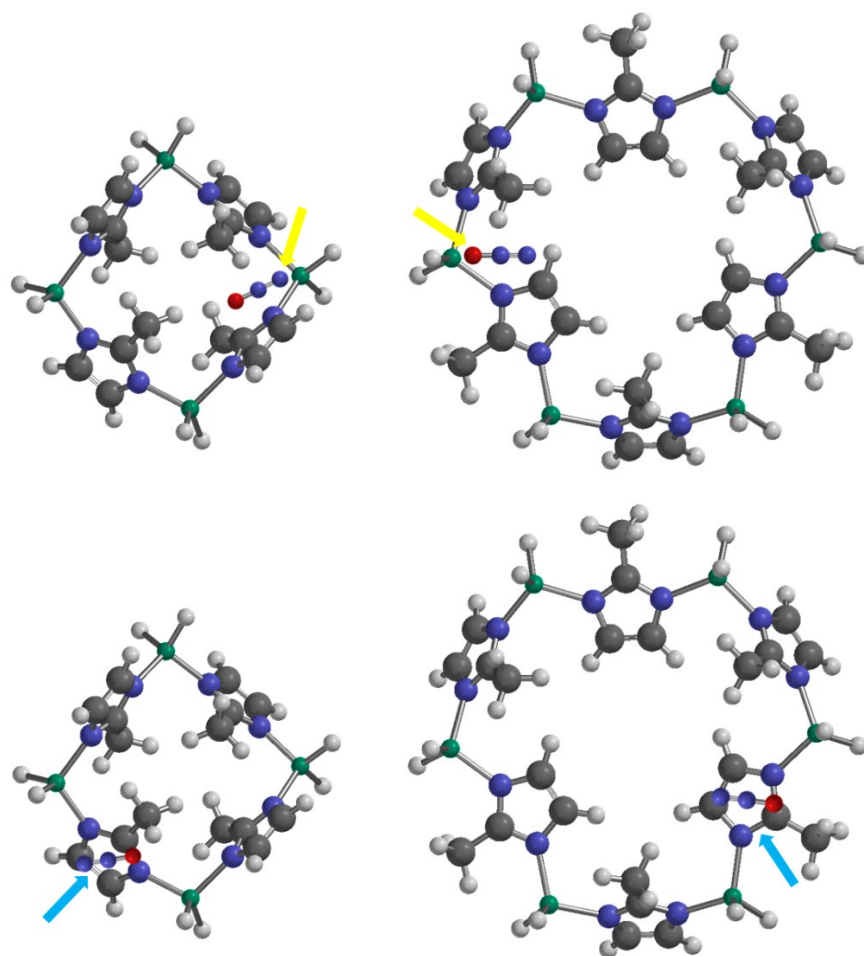
Figure 6.2 Adsorption sites in the four-membered (left) and the six-membered (right) windows. Blue represents nitrogen; Gray represents carbon; Red represents oxygen; White represents hydrogen; Green represents zinc.

Fischer and Bell studied four interaction scenarios [52], placing the hydrogen (H_2) molecule: 1) above the center of the 2-mIm, in both windows, 2) in the center of the six-membered window, 3) above or below the center of the big pore, and 4) on the sides of both pores (small and big), closer to the methyl or C=C bond and above them. Hobday $et\ al$. studied five interaction sites [51], placing the argon (Ar) molecule: 1) in the center of the big pore, 2) above the center of the 2-mIm, in the big pore, 3) above the center of the 2-mIm, in the small pore 4) above or below the center of the small pore, and 5) above the center of the big pore.

6.4.2 Ligand point to perform the simulation of molecular interactions between N_2O and ZIF-8

The molecular interactions between N_2O and ZIF-8 were considered as a physical adsorption process. The ligand points help to visualize the molecular interactions of the adsorption process without affecting the results of calculations which consider only electrons and nuclei [86]. Ligand points also help to maintain the N_2O molecule in the vicinity of the local minimum which attracts the molecule to the surface of the adsorbent. The use of ligand points mainly created interactions resembling van der Waals interactions. The existence of van der Waals forces, for example, can be generated by interactions with conjugated aromatic rings like 2-mIm [17]. The distance between the N_2O molecule and the ZIF-8 surface along with the adsorption energy were used as an indicator of the interaction stability.

6.4.3 Interactions of N_2O and four-membered window of ZIF-8

Based on molecular simulations, the adsorption energy, and the approach distance between N_2O and ZIF-8 varied according to the interactions of N_2O in each site of ZIF-8. A graphic visualization of these interactions on the four-membered window is shown in Fig. 6.3. Different orientations are presented on N_2O molecules depending on the interaction sites and the adsorption configuration of N_2O. These orientations with a certain inclination are due to the repulsions between N_2O and the closest neighbor atoms [86].

a)

b)

c)
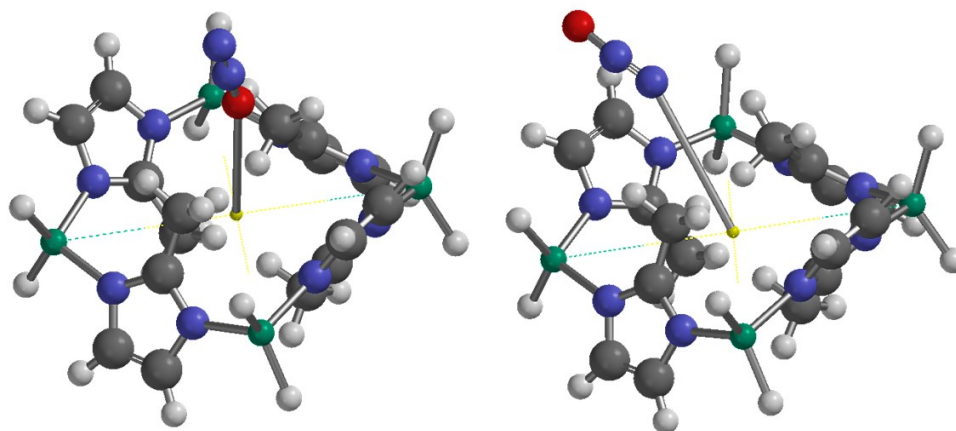
Figure 6.3 Molecular interactions between N_2O and ZIF-8 in the four-membered window: a) center, b) side and c) methylcenter in –ONN (right) and –NNO (left) configurations of N_2O. Blue represents nitrogen; Gray represents carbon; Red represents oxygen; White represents hydrogen; Green represents zinc.

The N_2O molecule in the center and side sites shows a similar behavior according to the approach distances illustrated in Fig. 6.3 (a) and (b). Regarding to the methylcenter site, shown in Fig. 6.3 (c), the N_2O molecule do not interact directly in the center of the 2-methylimidazole molecule but above of it which could be considered like the latest site where the N_2O will be positioned. Besides, since N_2O molecules are closer to the imidazole ligands, which are flexible, the movements of N_2O molecules are additionally induced by them and the position of N_2O molecules around the cage windows, increases the chance of a cage-to-cage migration [54].

Table 6.2 shows the adsorption energy and the distance for the three interactions sites in the small pore. The distances were measured from the ligand point in the structure of ZIF-8 to the first atom of N_2O bound to it, either oxygen end (–ONN) or nitrogen end (–NNO). The highest adsorption energy for the small pore was -35.6 kJ/mol, corresponding to the center site. The corresponding

distance of this interaction was 4.1 Å, in which the N_2O molecule was bonded by the nitrogen end (–NNO). Conversely, the smallest adsorption energy was -8.3 kJ/mol with a distance of 3.4 Å in the same site (center), but the N_2O molecule was adsorbed from the oxygen end (–ONN).

Table 6.2 Adsorption energy and approach distances of the four-membered window from –ONN and –NNO configuration of N_2O.

| | Four-membered window | | | | |
| Interaction site | (–ONN) | | Interaction site | (–NNO) | |
	Approach distance (Å)	Adsorption energy (kJ/mol)		Approach distance (Å)	Adsorption energy (kJ/mol)
Center	3.4	-8.3	Center	4.1	-35.6
Side	3.8	-32.7	Side	3.9	-31.1
Methylcenter	4.1	-29.2	Methylcenter	7.3	-14.4

According to Table 6.2, the interaction from the oxygen end (–ONN) shows shorter distances than the nitrogen end (–NNO), but the adsorption energy of the side and methylcenter sites in the nitrogen end (–NNO) was higher than for oxygen end (–ONN). The side site does not show a big difference between the oxygen (–ONN) and the nitrogen (–NNO) configurations in the distances, 3.8 and 3.9 Å, and the adsorption energy of -32.7 and -31.1 kJ/mol, respectively. The interaction of the nitrogen configuration (–NNO) showed the largest distance (7.3 Å) for the methylcenter site and an adsorption energy of -14.4 kJ/mol which was relatively small compared to the results obtained in the other adsorption sites (center and side).

Unlike the –NNO configuration, when N_2O was bonded by the oxygen atom (–ONN) in the methylcenter site, the adsorption energy was higher (-29.2 kJ/mol), and the approach distance was shorter (4.1 Å). The larger distance for the nitrogen end (–NNO) can be explained by the lack of N_2O molecules where the only N_2O molecule in that site can migrate elsewhere easier [86]. For the small pore, the N_2O molecule was near the side site, where is located the Zn atom. It could attract N_2O stronger, especially by the configuration of oxygen end (–ONN).

6.4.4 Interactions of N_2O and six-membered window of ZIF-8

For the six-membered window, molecular interactions, between N_2O and ZIF-8, showed some differences compared to the interactions in the four-membered window. One was the approach

distance between the N₂O molecule and the adsorption site of ZIF-8. Another difference was the orientation of N₂O molecule in both configurations (–ONN and –NNO), showing an inclined position that allows N₂O molecule to interact more with the 2-methylimidazole molecule than with zinc atoms (Fig. 6.4).
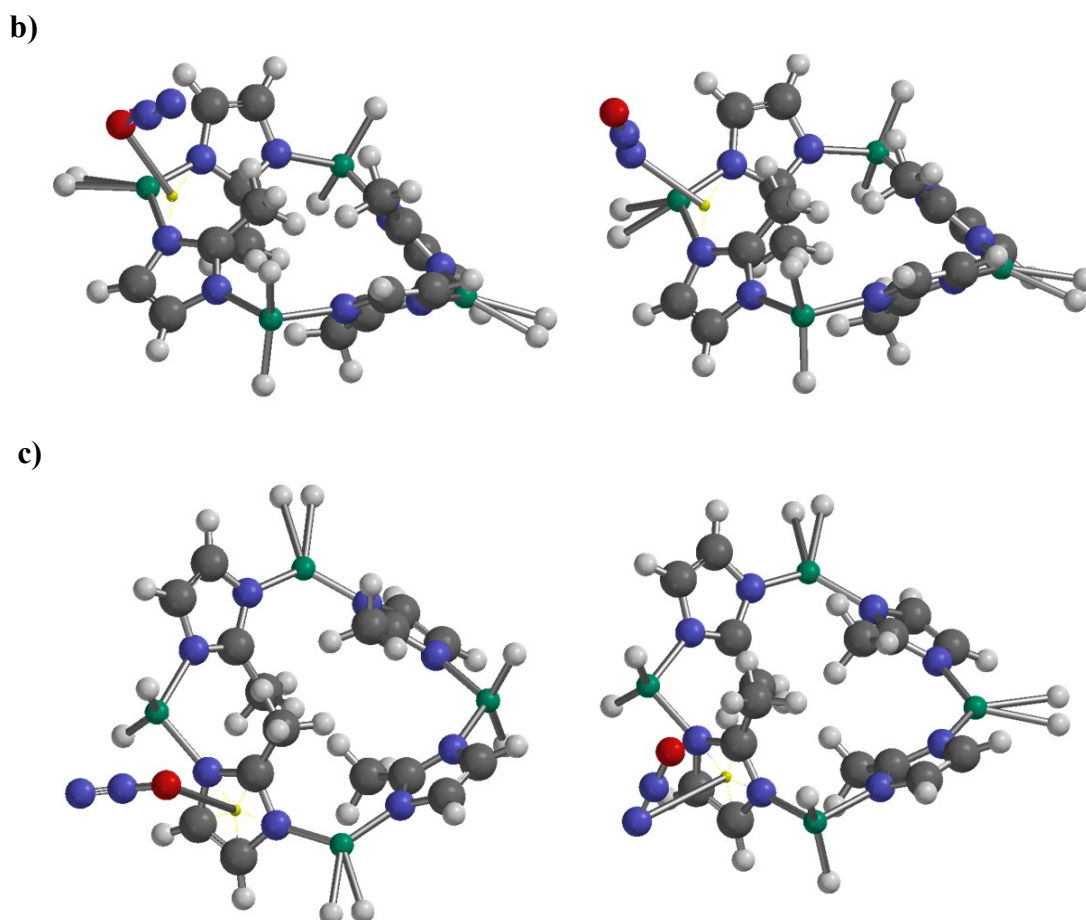
a)
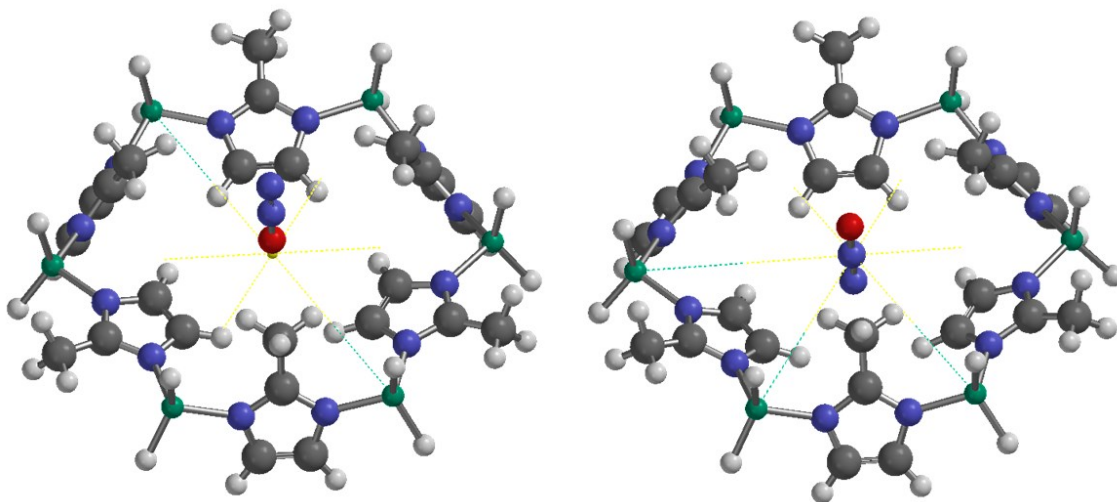
b)
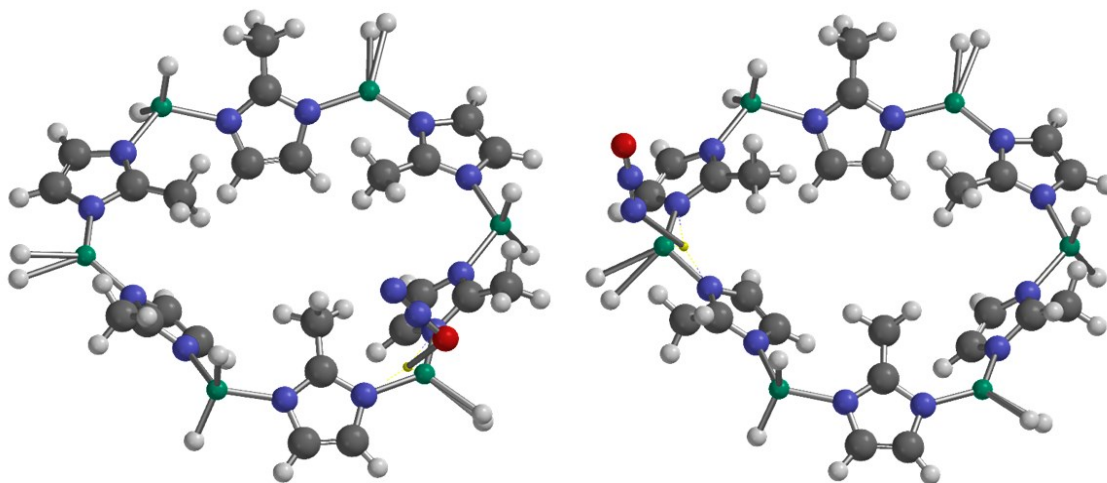
c)
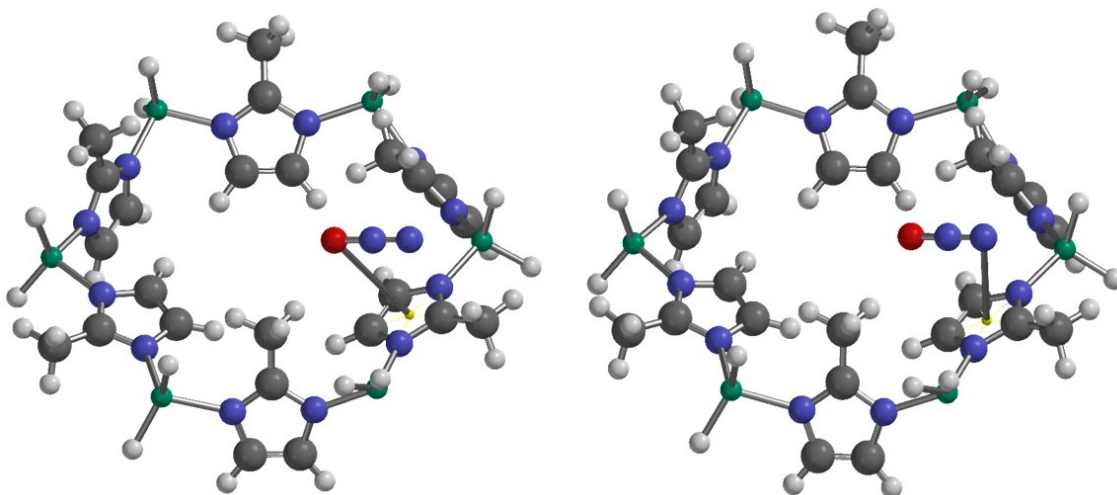
Figure 6.4 Molecular interactions between N_2O and ZIF-8 in the six-membered window: a) center, b) side and c) methylcenter in –ONN (right) and –NNO (left) configurations of N_2O. Blue represents nitrogen; Gray represents carbon; Red represents oxygen; White represents hydrogen; Green represents zinc.

The approach distance was close to zero for the center site, being 0.6 Å for the oxygen end (–ONN) and 0.1 Å for the nitrogen end (–NNO). This means that the N_2O molecule entered in the ZIF-8 cavity, as it is illustrated in Fig. 6.4 (a). With respect to the adsorption energy, it was generally higher for the six-membered window than for the four-membered window. For example, for the center site, the adsorption energy was -35.9 kJ/mol for –ONN end and -43.9 kJ/mol for –NNO end (Table 6.3). This specific behavior for the six-membered window may be explained because of its opening size of 11.6 Å, which is larger than the four-membered window. The repulsion interactions are weaker and allow the N_2O molecule to enter vertically orientated.

Table 6.3 Adsorption energy and approach distances of the six-membered window from –ONN and –NNO configuration of N_2O.

| | Six-membered window | | | | | |
| | **(–ONN)** | | | **(–NNO)** | | |
Interaction site	**Approach distance (Å)**	**Adsorption energy (kJ/mol)**	**Interaction site**	**Approach distance (Å)**	**Adsorption energy (kJ/mol)**
Center	0.6	-35.9	Center	0.1	-43.9
Side	3.4	-35.2	Side	5.6	-61.8
Methylcenter	3.6	-34.6	Methylcenter	3.7	-34.5

Whereas the largest approach distance in the big pore was 5.6 Å, corresponding to the side site and the nitrogen end (–NNO), this scenario corresponded to the highest adsorption energy of -61.8 kJ/mol and it can be considered as the most stable adsorption site even if the approach distance is larger for the other sites of the big pore. This large distance, shown above in Fig. 6.4 (b), could be explained by the increase of vibrational frequencies between nearby molecules that have an identical internal vibration frequency, creating a competition among the electrons [87]. Also, this behavior in the side site can be explained due to strong bonds between zinc atoms and 2-mIm that cause a reduction in Lewis acidity of the zinc sites, decreasing the affinity towards N_2O [87]. For both adsorption configurations of N_2O (–ONN and –NNO), the N_2O molecule had a different orientation with an inclined position that allowed it to interact more with the 2-mIm molecule than with zinc atoms.

In the methylcenter site, N_2O had a horizontal position that allowed the interaction with the whole 2-mIm molecule, shown in Fig. 6.4 (c). This probably occurs because of an edge effect that can be encountered when attempting to simulate a surface fragment with a small number of atoms [86]. The approach distance in this site, methylcenter, was smaller than the distance obtained in the four-membered window. However, the difference of the distance between oxygen end and nitrogen end was 1 Å, being 3.6 Å for –ONN and 3.7 Å for –NNO. Also, the adsorption energy for methylcenter of the six-membered window was similar for both adsorption configurations, -34.6 kJ/mol for –ONN and -34.5 kJ/mol for –NNO. Thus, the molecular interactions in methylcenter site were almost similar for both configurations.

From a general point of view, approach distances, in the six-membered window for both configurations (–ONN and –NNO) of N_2O, were shorter than the distances for the four-membered window. Likewise, adsorption energies were also higher for the six-membered window, for both configurations of N_2O, than for the four-membered window. The adsorption energies obtained in this study varied from -20 to -40 kJ/mol, which are similar to the results reported in other studies about the N_2O adsorption using other adsorbents (Table 6.1). The interactions analyzed in the present study showed that the bond in the six-membered window is more stable than in the four-membered window and the molecules will be retained more strongly in this section of the adsorbent surface.

Generally, molecules with a horizontal orientation show the farthest distances of the surface and this behavior could be attributed to the fact that the adsorbate-adsorbent system looks for a global interaction stability [86]. The space available, between one molecule and another, opens the way to form a second interaction layer since N_2O interacts for the first time with ZIF-8 until its adsorption saturation. Specifically, the van der Waals interactions in the six-membered window of ZIF-8 may lead to multilayer interactions [17]. Also, the oxygen atom configuration (–ONN) of N_2O shows a strong interaction with the molecules of the ZIF-8 structure.

The results show that the molecular modeling can be useful to predict how N_2O molecules will be adsorbed on the ZIF-8 surface, i.e. the highest adsorption energy and the shortest distance representing the most stable interaction which can be classified as a low coverage in the adsorption process. However, the smallest adsorption energy and the largest distance could be considered as a high coverage with multiple layers of interaction.

6.5 Conclusion

The adsorption of N_2O (adsorbate) on ZIF-8 (adsorbent) was studied in order to analyze their molecular interactions using molecular modeling methods (PM6 and DFT B3LYP-D3 6-31G*) in sequence. Geometry optimization, adsorption energy and ligand point length were considered as the main parameters for physical adsorption between N_2O and ZIF-8, carrying out an adsorption simulation analysis where van der Waals forces were dominant.

Molecular simulations indicated that the shortest distance, 0.1 Å, occurred in the center site of the six-membered window with a nitrogen configuration (–NNO) of N_2O, corresponding to an adsorption energy of -43.9 kJ/mol. The oxygen configuration (–ONN) of N_2O seemed to have a stronger interaction with the surface of ZIF-8, especially for the six-membered window where the longest distance and the adsorption energy were 3.6 Å and -34.6 kJ/mol, respectively. Thus, it was predicted that N_2O molecule is going to find the interaction stability firstly in the six-membered window, and then in the four-membered window until ZIF-8 saturation.

In the present study, a simple modeling method was developed with the aim of selecting, easily, adsorbent materials for controlling N_2O emissions by adsorption processes. For future works, this methodology could be extrapolated to other greenhouse gases that are also emitted at ambient conditions.

FOREWORD: CHAPTER 7

Authors and affiliation:
- Karen Villegas Domínguez: Master student, Department of chemical and biotechnological engineering, Faculty of engineering, Université de Sherbrooke.

- Beatriz Delgado: Research assistant, Centre National en Électrochimie et en Technologies Environnementales (CNETE).

- Alain Wilkin: Professor, Cégep de Shawinigan.

- Satinder Kaur Brar: Professor, York University.

- Michèle Heitz: Professor, Department of chemical and biotechnological engineering, Faculty of engineering, Université de Sherbrooke.

- Antonio Avalos Ramirez: Researcher, Centre National en Électrochimie et en Technologies Environnementales (CNETE).

Submission date: September 13th, 2021

Review: Chemical Engineering Journal Advances.

Title/Titre:
- Molecular dynamics simulations of carbon dioxide, methane, and nitrous oxide adsorption on Zeolitic Imidazolate Framework-8 (ZIF-8).

- Simulations de dynamique moléculaire de l'adsorption du dioxyde de carbone, du méthane et de l'oxyde nitreux sur du *Zeolitic Imidazolate Framework-8* (ZIF-8).

Contribution to the document:
This article constitutes the second part of the complete study of this thesis. It applies another useful molecular modeling approach, different to the one used in the first part, in which the interaction between adsorbate-adsorbent is analyzed through the time with a visualization of the evolution of the system. Molecular dynamics simulations allow to study physicochemical process like adsorption by modeling complex molecular systems. This is a practical way to analyze the adsorption capacity of a material that has not been deeply studied with a specific gas, and to study the thermodynamic properties of the adsorbate-adsorbent system. As it has been mentioned in previous chapters, the adsorption of N_2O has not been concretely studied with ZIF-8. Therefore, this study contributes to the expansion of the use of adsorbent materials such as ZIFs with GHGs other than CO_2 and CH_4 and delves into the study of N_2O, which is considered a highly harmful gas for the environment. Besides, this study represents a preliminary step to experimentation in order to analyze the interaction behavior between the adsorbate-adsorbent under different operating conditions of

temperature and pressure and determine if ZIF-8 can adsorb N_2O and which are the best conditions for doing it.

Abstract/Résumé:

- Carbon dioxide (CO_2), methane (CH_4) and nitrous oxide (N_2O) are the three major greenhouse gases (GHGs). Mostly emitted in the atmosphere by human activities, these gases cause global warming and climate change. Among them, N_2O is of special interest because it is a main cause of ozone layer depletion. Despite its significant environmental impact, it is less studied than CO_2 and CH_4.

  In recent years, the adsorption technique has been implemented to control GHGs emissions. Zeolitic Imidazolate Framework-8 (ZIF-8), a subcategory of Metal-Organic Frameworks (MOFs), has been selected as a potential material to adsorb GHGs due to its high porosity and large surface area, and its capacity to adsorb other gases.

  In the present study, the adsorption of CO_2, CH_4 and N_2O on ZIF-8 was studied by molecular dynamics (MD) simulations using the MM3 force field, adapted for MOFs structures. MD simulations of the three gases was performed individually in a representative segment of ZIF-8. The comparison of CO_2 and CH_4 adsorption calculated by MD against data reported in the literature allowed to validate the methodology developed in this work and showed that MD accurately produces physicochemical processes. The adsorption capacity of ZIF-8 was analyzed for each gas at 298 K and different pressures. The average adsorption energy was also calculated for each gas. Results indicated that each gas adsorbs to ZIF-8 with different strength, in the following order: $CO_2 > N_2O > CH_4$. This study contributes to the control of N_2O emissions through an efficient computational study of the adsorption process. The use of MD allows to better understand the interactions and behavior between GHGs and ZIF-8, in particular N_2O, before carrying out experimental tests.

- Le dioxyde de carbone (CO_2), le méthane (CH_4) et l'oxyde nitreux (N_2O) sont les trois gaz à effet de serre (GES) les plus importants. Principalement émis dans l'atmosphère par des activités humaines, ces gaz sont responsables du réchauffement de la planète et des changements climatiques. Parmi eux, le N_2O présente un intérêt particulier car il cause, principalement, l'appauvrissement de la couche d'ozone. Malgré son important impact environnemental, il est moins étudié que le CO_2 et le CH_4. Ces dernières années, la technique d'adsorption a été mise en œuvre pour contrôler les émissions de GES. Le *Zeolitic Imidazolate Framework-8* (ZIF-8), une sous-catégorie de *Metal-Organic Frameworks* (MOFs), a été sélectionné comme matériau potentiel pour adsorber les GES en raison de sa porosité élevée, de sa grande surface, et de sa capacité pour adsorber d'autres gaz. Dans la présente étude, l'adsorption du CO_2, du CH_4 et du N_2O sur le ZIF-8 a été étudiée par des simulations de dynamique moléculaire (DM) en utilisant le champ de force MM3, qui a été adapté pour les structures de MOFs. Les simulations DM des trois gaz ont été effectuées individuellement dans un segment représentatif de ZIF-8. La comparaison de l'adsorption du CO_2 et du CH_4 calculée par MD avec les données rapportées dans la littérature a permis de valider la méthodologie développée dans ce travail, et a montré que DM produit, avec une certaine précision, des procédés physico-chimiques. La capacité d'adsorption du ZIF-8 a été analysée pour chaque gaz à 298 K et à différentes pressions. L'énergie moyenne d'adsorption a également été calculée pour chaque gaz. Les résultats ont indiqué que chaque gaz s'adsorbe avec une force différente sur le ZIF-8, montrant l'ordre suivant :

$CO_2 > N_2O > CH_4$. Cette étude contribue au contrôle des émissions de N_2O grâce à une analyse chimique-computationnelle efficace du procédé d'adsorption. L'utilisation de la MD permet de mieux comprendre les interactions et le comportement entre les GES et le ZIF-8, notamment le N_2O, avant de réaliser des tests expérimentaux.

CHAPTER 7. ADSORPTION OF CO_2, CH_4 and N_2O ON ZIF-8 BY MOLECULAR DYNAMICS SIMULATIONS

7.1. Introduction

Carbon dioxide (CO_2), methane (CH_4) and nitrous oxide (N_2O) are the three major greenhouse gases (GHGs) and the main cause of global warming. CO_2 is the GHG most emitted by humans, accounting for at least 60 % of all GHGs [2]. The principal sources of CO_2 emissions are from energy production, such as the burning of natural gas or coal for heat and power generation [3]. CH_4 is the second most abundant anthropogenic GHG, with about 16 % of the total GHG emissions, and N_2O is the third, with nearly 7 % [5]. CH_4 is emitted by rice growing, fossil fuel exploitation, landfill, biomass burning, etc. [88], and N_2O by agricultural activities, due to the use of nitrogen-based fertilizers and management of livestock manure [89]. Even if N_2O emissions are lower than those of CO_2 or CH_4, they must be reduced because it is one of the most ozone-depleting gases. In addition, its global warming potential is 298 times higher than CO_2, because it absorbs more infrared radiation than CO_2 and it persists longer in the atmosphere, for over 116 years [90]. Among the three GHGs, N_2O is the least studied, despite its big environmental impact.

Because GHGs emissions are increasing over the years, and causing numerous environmental problems, it is necessary to take action and reduce them. In order to mitigate GHG emissions effectively and economically, research has been directed towards improving current GHG capture and storage technologies [91]. Among them, the adsorption technique is highly promising because it has shown low energy consumption, high economic benefit, easy industrialization, and high efficiency [13]. One type of adsorbent that had been successfully used to mitigate GHGs emissions is the Metal-Organic Frameworks (MOFs) [92]. Zeolitic Imidazolate Frameworks (ZIFs) have been gaining particular attention as one of the most investigated MOFs since they are easy to fabricate, present remarkable stability, and have a special molecular sieving effect. ZIF-8, for example, has been studied for adsorbing and separating CO_2 and CH_4 [13]. Its high porosity, large surface area and strong mechanical strength, are ideal characteristics to be used as an adsorbent for GHGs [93].

The study of GHGs adsorption is mainly based on semi-empirical principles and it has traditionally focused on adsorption under high pressure (>100 atm). The knowledge of GHG adsorption under

atmospheric pressure is scarce and it can be obtained by both experimental assays, and molecular models of adsorption [48]. Molecular dynamics (MD) is a common method for modelling complex systems such as gas adsorption. It plays a key role in the structure determination of adsorbent materials like ZIF-8 and it can provide information about the adsorption capacity and thermodynamic properties of a whole system, e.g. the adsorption of GHGs (CO_2, CH_4, N_2O) on ZIF-8 [94]. The MD can be used as an analytical and predictive method to determine the optimal operating conditions for the adsorption of GHGs, without having to carry out complex and expensive experiments [62]. This method is very useful to simulate the interaction adsorbate-adsorbent and analyze the behavior of a system in which atoms and molecules interact for a period of time [32]. A visualization of the trajectory of the particles is generated by calculating the potential energy for each time interval in order to have a description of the different types of interactions occurring in the system [59]. This potential energy is calculated by a set of potentials and parameters called force fields that are used in MD to replace the complicated electronic interactions, and to estimate the forces acting on the atoms within molecules (intramolecular forces) and the forces between molecules (intermolecular forces) [67].

Currently, the developed force fields have a limited scope for the parametrization of specifics families of structures. For this reason, in some cases, it is important to adapt and/or optimize the force field parameters. For example, there is currently not a general force field for modelling gas adsorption process. However, it is possible to use the mathematical terms of an existing force field such as Molecular Mechanics 3 (MM3) and adapt all the parameters for a specific structure like ZIF-8 [95]. The MM3 force field, in particular, has been extended to a large number of important classes of organic compounds. In addition, it has been applied in the study of gas adsorption processes using porous materials such as MOFs [68].

Besides the importance of selecting a suitable force field, the type of parameters taken into account to carry out MD simulations is another key element to obtain more accurate results [96]. Usually, the internal flexibility of a complex structure (e.g., ZIF-8) is neglected. The intramolecular energies are not considered during simulations, resulting in a rigid structure, and only the intermolecular energies (dispersion-repulsion and electrostatic partial charges) are taken into account [97].

The main objective of the present study was to analyze the adsorption capacity of ZIF-8 by using MD simulation. The adsorption of CO_2 and CH_4 on ZIF-8 was analyzed and used to validate the MD simulation protocol which was developed for this study. The validated MD simulation was then

used to study the N_2O adsorption with ZIF-8 under atmospheric conditions (pressure and temperature), which is not well known. An adapted force field for MOFs was used, based on the existing MM3 force field. The excess uptake of the three gases was calculated, as a measure of the adsorption capacity of ZIF-8, to build the adsorption isotherms for each gas, as it is an important parameter to describe the performance of an adsorbent under certain operating conditions. The gas adsorption analysis included the calculation of the average adsorption energy for each gas as a key parameter of the interactions between the adsorbate and the adsorbent. This computational study is aimed to contribute to the control of the three major GHGs and especially N_2O, through an adsorption calculation technique using a representative segment of ZIF-8. The results will provide a better understanding of the interactions and behavior between N_2O and ZIF-8, showing the potential of a validated calculation method in order to avoid having to carry out experimental tests to determine adsorption parameters under non-studied operating conditions.

7.2. Materials and methodology

7.2.1. Simulation setup for molecular models

A segment of 8 unit cells (2×2×2) of ZIF-8 was used as an adsorbent volume, which was placed inside a simulation box of a symmetric cubic arrangement of 88 Å × 88 Å × 88 Å. These dimensions correspond to the size of the simulation box in the cartesian coordinates x, y, and z axes as part of the periodic boundary conditions applied for modeling the ZIF-8 structure. The size of the simulation box was defined to allow sufficient space to insert the adsorbent volume of ZIF-8 and the different loads of gas molecules.

The number of molecules in the adsorbent volume to enter in contact with ZIF-8 for the three gases varied from 50 to 1000 molecules during each dynamic simulation. Electrostatic cut-offs were applied to the end-atoms of the molecular structure of ZIF-8 to determine the coulombic interactions (attraction-repulsion) necessary to make the molecule roughly neutral [74]. Three simulation boxes were created to study the adsorption capacity of ZIF-8 with each of the three gases: 1) CO_2 + ZIF-8, 2) CH_4 + ZIF-8, and 3) N_2O + ZIF-8.

7.2.2. MM3-MOF force field

For this study, the MM3 force field adapted for MOFs was used to carry out the MD simulations. As part of the MM3-MOF force field, atom types were defined to represent every atom of the ZIF-8

as well as the atoms of the gas molecules (CO_2, CH_4, and N_2O) according to their binding and interaction properties.

In the case of the ZIF-8 adsorbent, the atom types were defined based on the study of Dürholt *et al*. [98] who considered the carbon and hydrogen atoms as distinct functional groups in the imidazolate linkers, as shown in Fig. 7.1. Every type of atom (C1, C2, C3, H1, H3, N1 and Zn) was assigned with a unique number to build the ZIF-8 structure, using the MM3-MOF force field, as is shown in Table A.1.
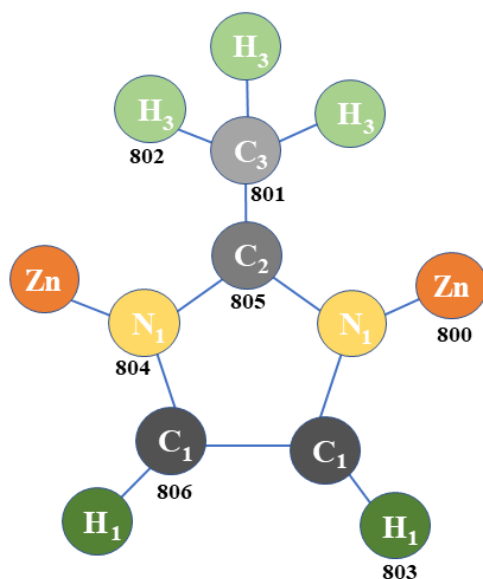
Figure 7.1 Chemical structure and atom type definition of a unit of ZIF-8 used in MM3-MOF force field. Carbon (C1, C2, and C3) in gray; Hydrogen (H1, H3) in green; Nitrogen (N1) in yellow; Zinc (Zn) in orange.

The mathematical terms of the existing MM3 force field were used as a base, but the parameters for bonded and non-bonded interactions of ZIF-8 were taken from Dürholt *et al*. [98] and adapted to the software of molecular modeling Tinker 8. As part of this adaption of the MM3-MOF force field, the internal flexibility of the molecular structure of ZIF-8 was considered during simulations. This included intramolecular forces (bonded terms), not just intermolecular forces (non-bonded terms). The bonded terms considered were bond stretching, angle bending, dihedral torsion and out-of-plane bending. Because the ZIF-8 has an imidazole ring in its molecular structure, some additional parameters were considered for this particular 5-ring structure being part of the bond stretching, the angle bending and the dihedral torsion terms. The non-bonded terms considered

included were the van der Waals potentials and the electrostatic partial charges, shown in Tables A.6 and A.7.

Electrostatic cut-offs were applied on the end-atoms of the molecular structure of ZIF-8. Specific atom types were defined as shown in Fig. 7.2, with the corresponding parameters, to differentiate this part of the structure. C4, H4, and N2 were assigned with a unique number as part of the end-atoms that constitute the ZIF-8 structure. The atom types and the corresponding parameters were taken from the adapted MM3-MOF force field and they are listed in Tables A.8-A14.
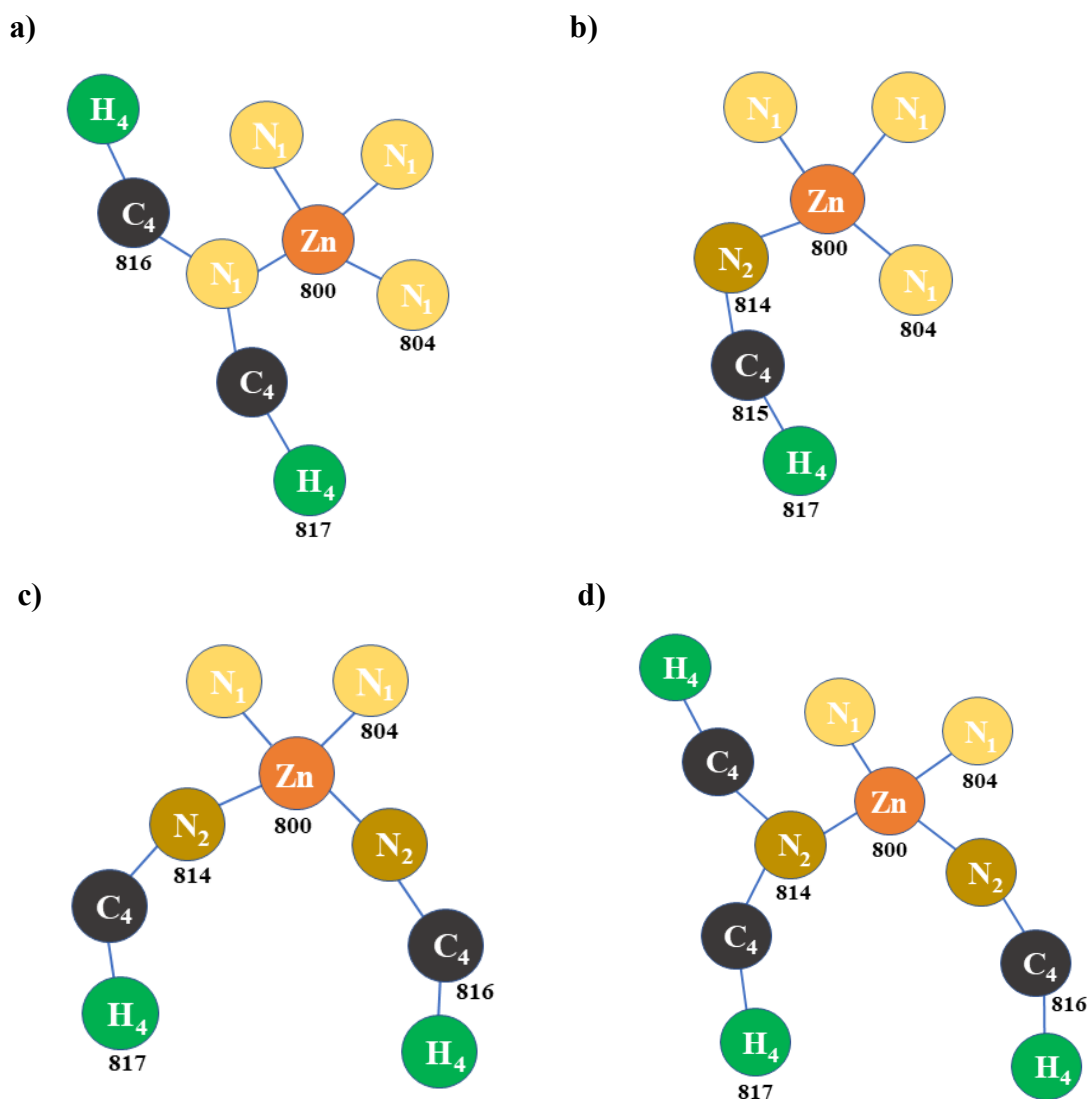
Figure 7.2 Four scenarios of the cut-off ends of ZIF-8 and the corresponding atom types used in MME-MOF force field. Carbon (C4) in gray; Hydrogen (H4) in green; Nitrogen (N1, N2) in yellow; Zinc (Zn) in orange.

Due to the charge effect produced by the electrostatic cut-offs to use a fragment of the molecular structure of ZIF-8, an atomic charge distribution was applied following the methodology of Sladekova *et al*. [99]. The remaining charge of the fragment of ZIF-8 was uniformly distributed over all the atoms to bring the framework to a non-zero overall charge.

In the case of the gas molecules (CO_2, CH_4, and N_2O), a similar method was used with some force field parameters available from the literature. For example, the CO_2 has a symmetrical structure, as shown in Fig. 7.3 (a), so the two oxygen atoms of CO_2 were defined with the same atom type because they have an equal electronegativity. The atom types of CH_4 were defined as Fig. 7.3 (b) illustrates. A single atom type was needed to define the hydrogen atoms. Unlike CO_2, to define the atom types of N_2O, it was necessary to differentiate one nitrogen from the other (N1 and N2) due to their charges and valence numbers. The molecular structure of N_2O based on the atom types is shown in Fig. 7.3 (c). The details about the atom types of the three gases are defined in Table A15.
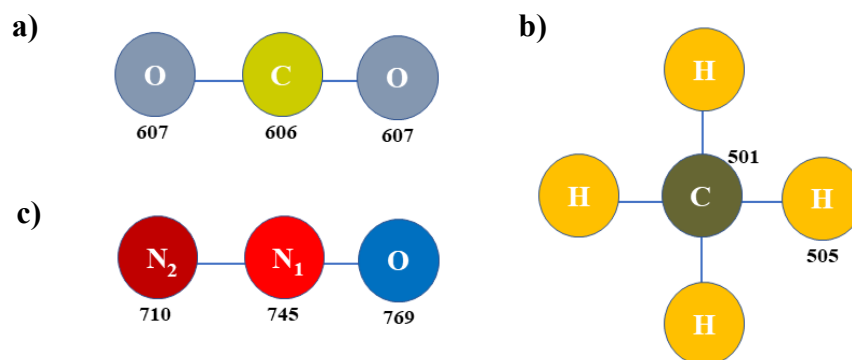
Figure 7.3 Chemical composition and atom type definition of a) CO_2, b) CH_4, and c) N_2O used in MM3-MOF force field. Oxygen (O) in blue; Carbon (C) in green; Hydrogen (H) in yellow; Nitrogen (N1, N2) in red.

Some parameters for the CO_2 and N_2O molecules were obtained from the study of Hansen *et al*. [7] (TraPPE model), and for the CH_4 molecules, some of the parameters were obtained from the study of Naeiji *et al*. [100] (TraPPE model). Due to their molecular structure, only bond stretching and angle bending parameters were required as part of the bonded terms. For CO_2 and CH_4, the bond stretching constant k_b and the angle bending constant k_a were obtained directly from the MM3 force field. However, in the case of N_2O, the bond stretching constant k_b was considered as the spring constant which is related to Hooke's Law equation: $F = -kr$ and the corresponding potential energy: $E_p = \frac{1}{2}kr^2$; where F is the restoring force (kcal·Å/mol); k is the spring constant (kcal/mol·Å^2); r is the displacement of the spring's end from its equilibrium position (Å); and E_p is

the potential energy (kcal/mol). The energy E_p was calculated using Density Functional Theory (DFT B3LYP-D3 6-31G*), as a function of the distance r, and replaced in the equation to solve for k. The bond stretching constant k_b calculated for N_2O was converted to units in mdyne/Å, and then compared to the one found in the MM3 force field. Van der Waals potentials and the electrostatic partial charges were considered for the non-bonded terms of the three gases (See Tables A.18 and A.19). Specifically, the electrostatic charges found in the literature [7], [100] were validated by calculating them applying the electrostatic method of Density Functional Theory (DFT B3LYP 6-311+G**).

7.2.3. Molecular dynamics simulation method

The adsorption capacity of ZIF-8 as a function of gas pressure (CO_2, CH_4, and N_2O), was obtained by MD simulations using the MM3-MOF force field. All adsorption simulations were carried out in the simulation boxes using a molecular modeling software: Tinker 8 (V8.7) from Ponder Lab [101]. The interactions of each gas with ZIF-8 were studied.

The structures of the molecular models in the three initial simulation boxes (N_2O + ZIF-8, CO_2 + ZIF-8 and CH_4 + ZIF-8) were minimized with a convergence criterion of 0.4-0.5 prior to dynamic simulations. During minimization phase, none of the Zn atoms of ZIF-8 were fixed, to allow the molecular structure to relax correctly.

All MD simulations were set in the canonical ensemble NVT at 298 K, using the Bussi thermostat, and a time step of 1 fs to examine the pressure effect created by the number of molecules on the adsorption capacity of ZIF-8. The adsorption simulations were divided in two main phases: 1) Equilibration, and 2) Production I and II. The molecular structure of ZIF-8, during equilibration and production I, was considered partially rigid by fixing, symmetrically, some of the Zn atoms to their original positions to avoid any kind of structural deformation and to keep the ZIF-8 in the middle of the simulation box. The equilibration phase was considered complete after 1 ns (1 000 000 steps). Another 1 ns was run to complete production phase I and identify the total number of guest gas molecules adsorbed on ZIF-8. For production phase II, 0.3 ns (300 000 steps) were run to measure the total pressure of the system in atm at every 100 000 steps. During production phase II, the Zn atoms of ZIF-8 were unfixed.

7.2.4. Adsorption capacity of ZIF-8

After carrying out all MD simulations, the adsorption capacity of ZIF-8 for each gas (CO_2, CH_4, and N_2O) was determined by means of the adsorption isotherms which depend on the excess uptake and total pressure of the system.

Excess uptake is a computational measure of the adsorption capacity of ZIF-8 according to the number of guest gas molecules adsorbed, the total pressure of the system and the size of the ZIF-8 segment.

The excess uptake (mg/g) was calculated after production phase II with the following equation [17]:

$$Excess\ uptake = \frac{\frac{N_g \cdot m_g}{N_A} - \frac{\rho_g \cdot V_{free} \cdot M_{ZIF-8}}{N_A}}{\frac{M_{ZIF-8}}{N_A}}\ x\ 1000 \tag{7.1}$$

where,

N_g (mol) is the number of gas molecules adsorbed on the ZIF-8 at the end of production phase I; m_g (g/mol) is the molecular weight of the gas; ρ_g (g/cm^3) is the density of the gas at the total pressure of the system (determined at the end of the production II phase); V_{free} (cm^3/g) is the available volume in the ZIF-8 segment for adsorbing gas molecules (V_{free} = 0.485 cm^3/g, obtained from [102]); M_{ZIF-8} (g/mol) is the molecular weight of the ZIF-8 segment (2×2×2 = 10 587.48 g/mol), calculated by a molecular modeling software (Spartan'18 (V1.4.5)); and N_A is the Avogadro's number (6.0221×10^{23}/mol).

Three different adsorption isotherm curves (CO_2 + ZIF-8, CH_4 + ZIF-8, and N_2O + ZIF-8) were created using the results of the excess uptake (mg gas/g ZIF-8) for each total pressure (atm).

The Radial Distribution Functions (RDFs) were calculated with the plugin function included in the molecular visualization program (Visual Molecular Dynamics: VMD (V1.9.3)). The maximum distance of adsorption in the first layer between the gas molecule and the ZIF-8 was determined by the RDFs and used to establish two cut-offs for adsorption (electrostatic charge and Van der Waals) for calculating the adsorption energies in all simulation sets.

The total adsorption energies for each molecular system, also defined as intermolecular energies, were calculated using the molecular modeling software Tinker 8. The adsorption energies (E_{ads}) per

molecule of gas were determined dividing the total adsorption energies by the number of adsorbed gas molecules, previously identified. An average of all E_{ads} was determined for each gas.

7.3. Results and discussion

7.3.1. Simulation boxes: CO_2 + ZIF-8, CH_4 + ZIF-8, and N_2O + ZIF-8

The molecular structure of a representative segment of ZIF-8 ($2\times2\times2$) as well as the gas molecules (CO_2, CH_4, and N_2O) were constructed using the interface of the molecular modeling software Tinker 8 and the MM3-MOF force field. Regarding the MM3-MOF force field parameters, the calculated k_b (bond stretching constants) for N_2O was 19.253 mdyne/Å for the N2-N1 bond and 10.417 mdyne/Å for the N1-O bond. They were similar to those found in the MM3 force field (17.330 and 8.800 mdyne/Å, respectively). The partial charges calculated for CO_2 and N_2O were similar to the ones reported by Hansen *et al.* [7]; however, the calculated partial charges in CH_4 were different from those reported in the literature by Naeiji *et al.* [100]. The detailed results of the partial charges for the three gases are shown in Table A.19.

The simulation box was used to apply periodic boundary conditions and control the initial conditions to perform dynamic simulations. Since the molecular system is large and complex, the use of periodic boundary conditions simplifies the analysis of the simulation box representing the behavior and the characteristics of an infinitive molecular system (adsorbate-adsorbent) [74]. Each of the three simulation boxes contained the same segment of ZIF-8 and a specific number of molecules that varied in each dynamic simulation set.

After creating the simulation box for each gas, energy minimization was applied to all atoms before starting the dynamic simulation set, in order to relax the initial structures and remove any steric clashes or poor configurations arising from the initial distribution of gas molecules near the ZIF-8 in the simulation box. The minimization phase is an important step to carry out the MD simulation correctly, and it has to be repeated for each dynamic simulation. The convergence criterion of 0.4-0.5 for minimization was chosen to avoid a structural deformation of ZIF-8.

For the three simulation boxes of CO_2 + ZIF-8, CH_4 + ZIF-8 and N_2O + ZIF-8, the first MD simulation began with 50, 100 and 50 gas molecules randomly distributed into the simulation boxes, respectively. At the end of each simulation set, additional molecules were added to the remaining system from the previous simulation to run a new dynamic simulation. The number of molecules

for the CO_2 simulations was 50, 100, 200, 300, 400, 500, 750 and 1000; for CH_4, the number of molecules used was 100, 200, 300, 400, 500, 600, 700 and 800; and for N_2O, the number of molecules was 50, 100, 200, 300, 400, 500, 600, 800 and 1000. Fig. 7.4 illustrates three different gas loads as part of the sequence followed to carry out the simulations for N_2O adsorption on ZIF-8. The distribution of gas molecules into the simulation box is clearly visible as well as the progressing saturation due to the gas molecules.
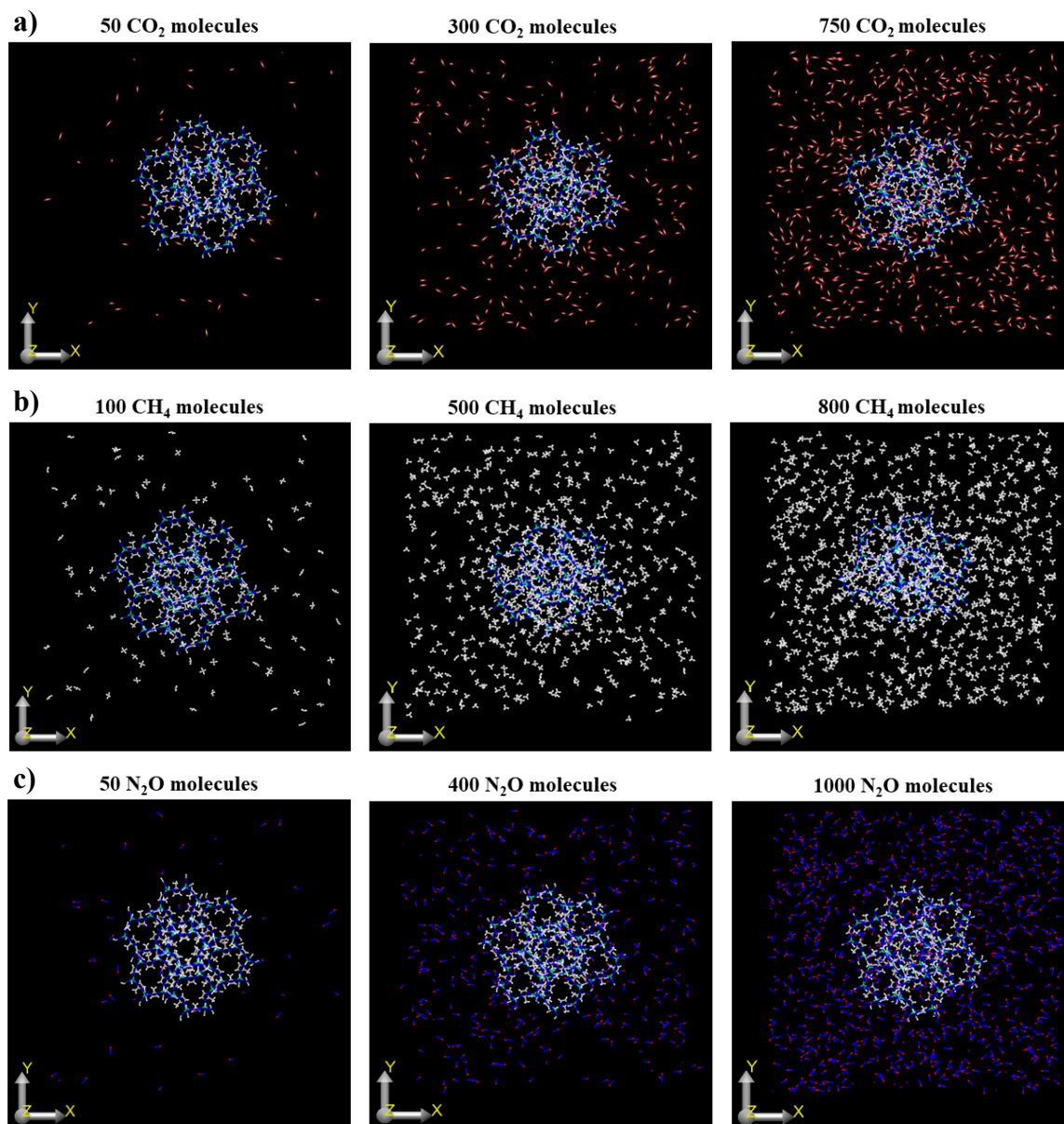
Figure 7.4 Simulation boxes with the segment of ZIF-8 and three different loads of a) CO_2, b) CH_4, and c) N_2O.

As it is shown in the figure, the simulation box with 50 CO_2, 100 CH_4 and 50 N_2O molecules is the only one that shows the original position of the molecules before being adsorbed on the ZIF-8. In the following two images for the three gases, some of the molecules have already been adsorbed on the surface of ZIF-8.

7.3.2. Adsorption capacity of ZIF-8 described by adsorption isotherms

The adsorption capacity of ZIF-8 for each gas (CO_2, CH_4, and N_2O) was determined through adsorption isotherms in which the total pressure of the system and the excess uptake for every gas was calculated in a series of MD simulations sequences. The resulting output of each MD simulation was used to create the input for the next simulation, maintaining fixed, during simulation, the number of gas molecules, the volume of the simulation box ($88 \times 88 \times 88$ Å) and the temperature (298 K), so the pressure was the only variable to be calculated by MD simulations.

For all simulation sets, 1 ns was enough to consider that the system reached equilibration. However, production phase I helped to back up the equilibrium because all initial settings of the dynamic simulation remained the same during production I. Past 2ns the pressure did not vary anymore, and the number of adsorbed molecules was identified. During dynamic simulations, the ZIF-8 maintained its original structure by fixing some of the Zn atoms symmetrically while allowing small rearrangement of the other atoms. Production phase II did not require as much time as equilibration or production I because the system was already stable. Different pressures were calculated as a result of the increase in the number of gas molecules in the simulation box at the beginning of every simulation set.

The excess uptake was calculated according to every pressure using Eq. 7.1. The number of molecules as well as the density varied based on the different pressures obtained.

Because the adsorption of N_2O using ZIF-8 has not been well studied and there is no available information to compare with in the literature, the adsorption capacity of ZIF-8 with CO_2 and CH_4 was analyzed by MD simulations, since this adsorbent has already been studied with these two gases. The simulated adsorption isotherms of CO_2 and CH_4 were compared to those obtained by experimentation reported in the literature [56] in order to validate the MD simulations and the calculation methodology developed in this study. This comparison was backed up with a statistical analysis based on an ANOVA test to determine whether there was a significant difference between the data obtained by the simulations and those from the literature.

The isotherms calculated by MD and the isotherms reported in literature for CO_2 and CH_4 at room temperature are shown in Fig. 7.5. Each point of the isotherm was calculated by a dynamic simulation and corresponds to different gas loads. These calculated points are plotted to fit the Langmuir adsorption model for gas adsorption [56]. Regarding the adsorption of these two gases, at low pressures, the excess uptake of CO_2 increased faster than that one for CH_4. The maximum excess uptake for CO_2 (Fig. 7.5 (a)) was 363 mg CO_2/g ZIF-8 at 41 atm, and for CH_4 106 mg CH_4/g ZIF-8 at 42 atm (Fig. 7.5 (b)). For both gases, these were the maximum pressures used, and they did not become constant. This suggest that the saturation point was not reached.
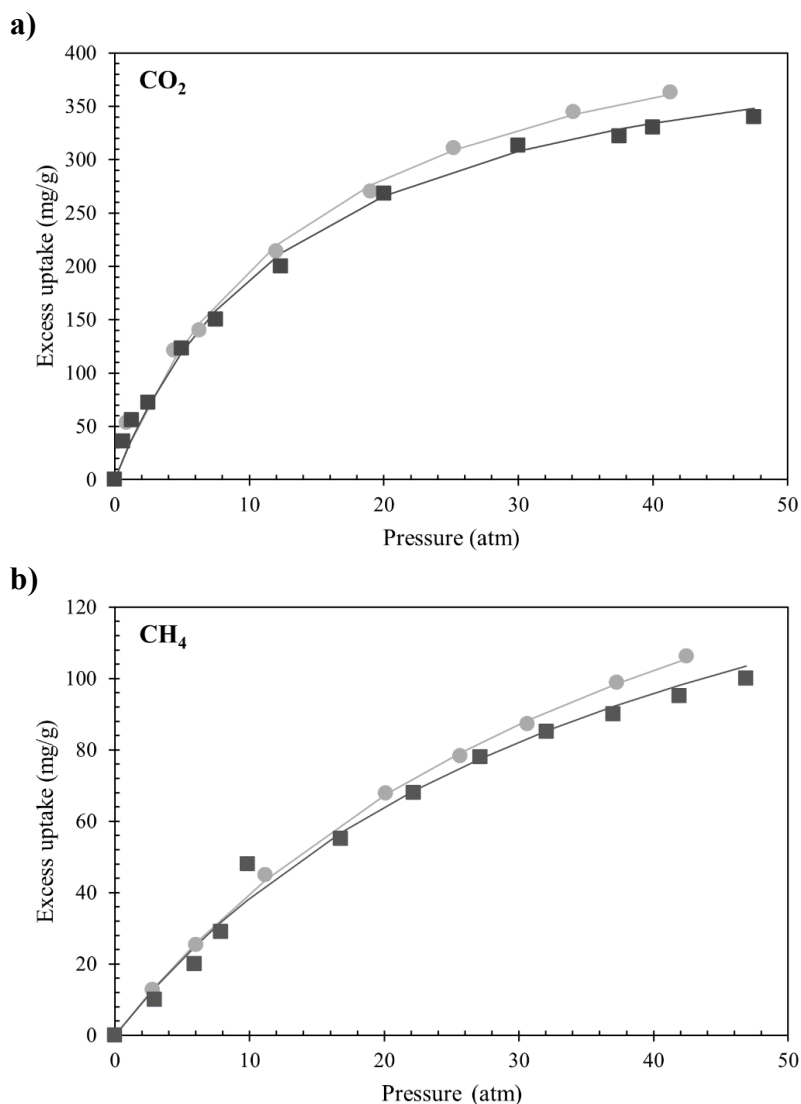
Figure 7.5 Adsorption isotherms of a) CO_2 and b) CH_4 on ZIF-8 at 298 K. Comparison between simulations and experiments. Circle ● symbols represent the simulation results of this work; Square ■ symbols represent the experimental data reported by *Zhu et al.* [56]. The solid line is the fitted Langmuir adsorption equation.

74

The simulated and experimental isotherms for both CO_2 and CH_4 are very similar in terms of values and trend. The results of the statistical analysis, shown in Table 7.1, indicate that there are no differences between the isotherm parameters from simulation and experimental determination.

Table 7.1 Statistical analysis based on ANOVA test for adsorption isotherms of CO_2 and CH_4.

Gas	Source of Variation	SS	df	MS	F	P-value	F crit
CO_2	Between Groups	19 888.8	1	19 888.8	1.3936	0.2550*	4.4940
	Within Groups	228 340.2	16	14 271.3			
	Total	248 229.0	17				
	Between Groups	913.6	1	913.6	0.7522	0.3986*	4.4940
CH_4	Within Groups	19 433.4	16	1 214.6			
	Total	20 347.0	17				

* Significant at 5% level ($P \leq 0.05$)

The isotherms obtained by simulation are slightly higher than the experimental ones. This could be due to several factors such as the purity, crystallinity, and structure of the adsorbent in real conditions, which will affect the adsorption. For example, it is highly probable that the adsorption decreases when pores are blocked, or when the adsorbent contains impurities, which will interfere with molecular attractions. Also, in some adsorption experimental techniques, access of the gas molecules to the entire ZIF-8 structure is not maximized.

The N_2O was also adsorbed on ZIF-8 at room temperature. Fig. 6 shows the adsorption isotherm of N_2O on ZIF-8. As mentioned before, total pressure increases with the number of molecules, and the excess uptake of N_2O increases with total pressure. According to the adsorption isotherm, the ZIF-8 was saturated at a total pressure of around 36 atm, which corresponded to the maximum adsorption of N_2O of 211 mg N_2O/g ZIF-8. Above this pressure, the excess uptake remains nearly constant.
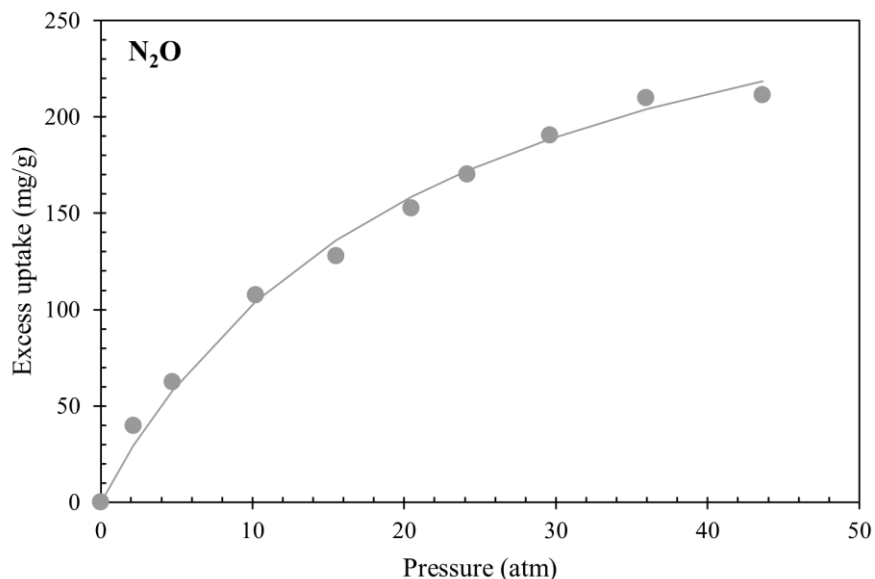
Figure 7.6 Simulated adsorption isotherm of N_2O on ZIF-8 at 298 K from MD calculations. Circle ● symbols represent simulation results of this work. The solid line is the fitted Langmuir adsorption equation.

For the three gases, the maximum adsorption was obtained at pressures of around 40 atm. Results show that the ZIF-8 presents different adsorption capacities for each gas. For example, at 1 atm, CO_2 is the one that can be most adsorbed by ZIF-8 at 55 mg CO_2/g ZIF-8, while CH_4 is the gas least adsorbed by ZIF-8 at 4 mg CH_4/g ZIF-8. However, ZIF-8 can adsorb the N_2O at a rate of 18 mg N_2O/g ZIF-8, which can be considered as moderate adsorption compared with the other two gases. Based on the simulation results presented in this work, it can be concluded that ZIF-8 adsorbs the three gases in the following order based on the mass capacity: $CO_2>N_2O>CH_4$.

7.3.3. Radial Distribution Functions (RDFs) and adsorption energies

The radial distribution function (RDF) is a measure of the probability of finding a gas molecule at a distance r from any part of ZIF-8 [103]. For the present work, this function was used to define the maximum adsorption distance and determine the cut-offs for adsorption (electrostatic charge and Van der Waals) necessary to calculate the adsorption energies (E_{ads}) of CO_2, CH_4 and N_2O on ZIF-8.

The RDFs of the three gases (CO_2, CH_4, and N_2O) with ZIF-8 were created using the molecular visualization program VMD. To generate these graphs, all atoms from the gas molecules (N, O, C, H) were considered in the calculation. Fig. 7.7 shows some of the RDFs created with different loads of N_2O gas molecules. The first peak in all graphs corresponds to the maximum distance at which the gas atoms were considered adsorbed. For example, the maximum distances to adsorb CO_2 and

CH$_4$ were 6.3 Å and 6.5 Å, respectively. For N$_2$O, the distance was 6.3 Å. Thus, the peak and shape of the RDFs differ with each type of gas. The position of the first peak in the RDFs represents the first adsorption layer where the gases were located on ZIF-8.

a)

b)

c)
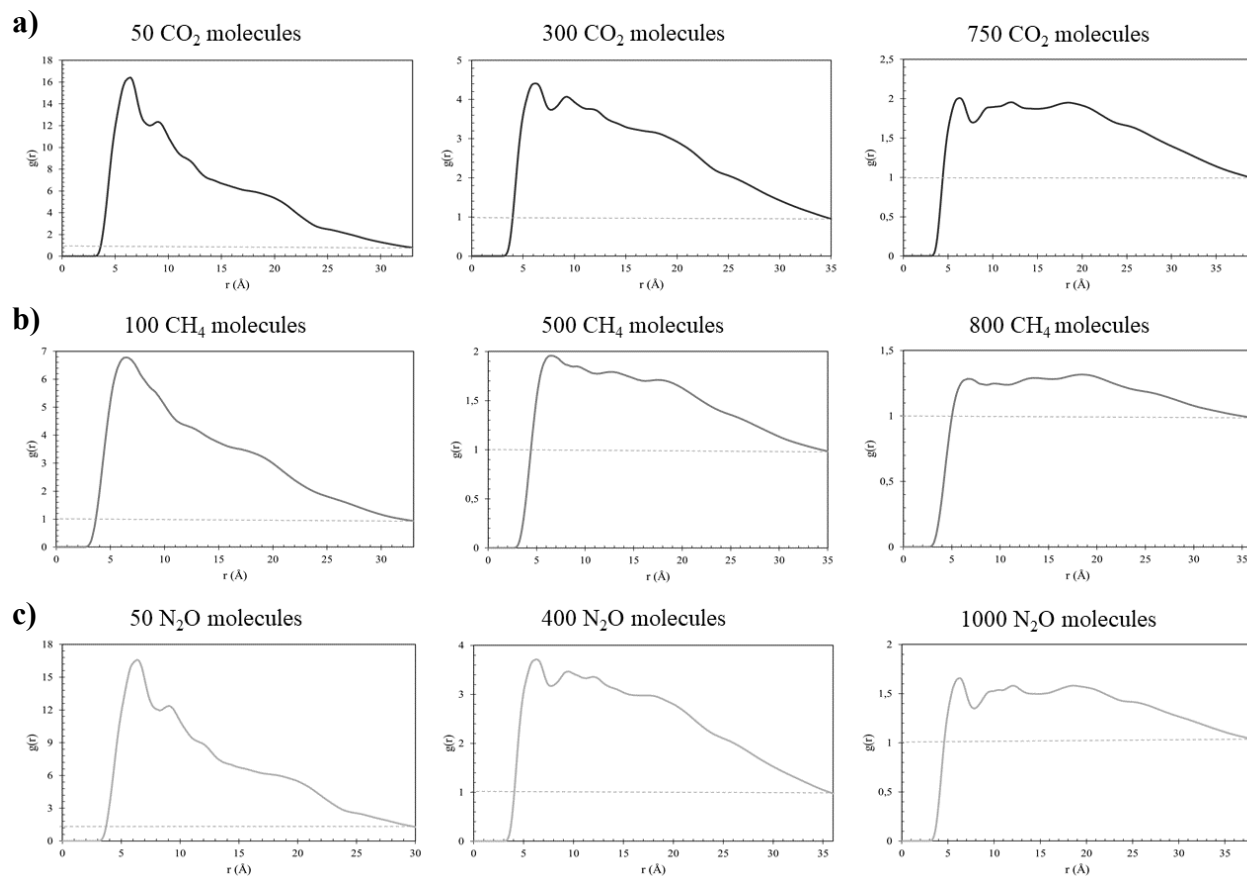
Figure 7.7 Radial distribution functions of a) CO$_2$, b) CH$_4$, and c) N$_2$O molecules with ZIF-8 at different gas loads.

With the sequence of dynamic simulations and the increase in the number of molecules, other peaks in the graphs appeared. These peaks may be due to a second or third adsorption layer, but those are not well defined in Fig. 7.7. All RDFs converge toward one (horizontal dotted line shown in the figure) because for higher distances, the interactions between atoms can be considered as negligible, and at this point, the density of the gas corresponds to the density of an ideal gas.

In the calculation of the E$_{ads}$, the cut-offs for adsorption, that represent the intermolecular forces (electrostatic charge and Van der Waals), are important for the analysis. The maximum adsorption distances of the gas molecules are reflected in these cut-offs. To calculate E$_{ads}$, it is necessary to

define the distance at which the molecules are considered adsorbed, excluding any molecule outside this perimeter.

E_{ads} was calculated at the end of each simulation to analyze the interaction stability between adsorbate and adsorbent. The results of E_{ads} varied slightly due to the different gas loads during simulations. Thus, an average interaction energy was calculated for the three gases; the results of these calculations are shown in Table 3. The average E_{ads} for CO_2, CH_4, and N_2O were -23.7 kJ/mol, -14.1 kJ/mol and -22.8 kJ/mol, respectively. In the case of CO_2, the average E_{ads} was very close to the one reported by Fischer and Bell [52], i.e. -24.6 kJ/mol. Likewise, the E_{ads} for CH_4 was similar to the E_{ads} reported by Li *et al.* [104] of -16.5 kJ/mol. Both E_{ads} issued from the literature were obtained by carrying out DFT calculations.

Table 7.2 Average calculation of the adsorption energy of the three guest gases (N_2O, CO_2 and CH_4) on ZIF-8.

Guest gases	Average adsorption energy (kJ/mol)	
	Present study	Literature
CO_2	-23.7	-24.6[a]
CH_4	-14.1	-16.5[b]
N_2O	-22.8	-

[a] Fischer and Bell [52]
[b] Li *et al.* [104]

The strength of the interactions between adsorbate and adsorbent is an important parameter in the gas adsorption. The previous affinity of the three gases adsorbed on the surface of ZIF-8 can be associated to their E_{ads}. In this way, the excess uptake was in the same order as the adsorption energies: $CO_2 > N_2O > CH_4$. This study confirms that the analysis of the interaction effectiveness of the three gases with ZIF-8 can be defined according to these two properties.

7.4. Conclusion

The adsorption capacity of ZIF-8 was mainly studied with N_2O by MD simulations using the MM3 force field, adapted for MOFs. Because the adsorption of N_2O on ZIF-8 has not been studied in depth, the methodology used in this work was validated by simulating the adsorption of CO_2 and CH_4 on ZIF-8 and comparing the results obtained with the experimental data reported in the literature. The three gases were studied individually with a segment of ZIF-8 in simulation boxes of 88 Å × 88 Å × 88 Å, applying periodic boundary conditions.

The excess uptake of the three gases was calculated under the effect of pressure to build the adsorption isotherm curves for each gas at 298 K. The adsorption capacity of ZIF-8 followed the order $CO_2 > N_2O > CH_4$, corresponding to an excess uptake of 363 mg/g, 211 mg/g, and 106 mg/g respectively. The results showed that the maximum excess uptake was obtained at pressures of around 40 atm for the three gases. The average adsorption energy was also calculated for each of the three gases to complement the previous analysis, using the RDF to define the distance at which the molecules are considered adsorbed. As a result, CO_2 showed the highest adsorption energy of the three gases with -23.7 kJ/mol, followed by N_2O with -22.8 kJ/mol and CH_4 with -14.1 kJ/mol, reflecting the affinity of the gases to be adsorbed on the surface of ZIF-8. This analysis followed the same order: $CO_2 > N_2O > CH_4$ as the adsorption isotherms results.

The present work focuses on the study of the adsorption of N_2O on ZIF-8, as it is a harmful GHG not extensively studied. This study aims to contribute to the control of N_2O emissions through a computational approach as a preliminary step to experimentation in order to have a better understanding of the interaction and the behavior of N_2O with ZIF-8.

CHAPTER 8. GRAVIMETRIC ADSORPTION OF CO_2 ON ZIF-8 AT ATMOSPHERIC CONDITIONS

8.1. Introduction

It is widely acknowledged that carbon dioxide (CO_2) emissions play a major role in global warming and they are related to climate change issues, since CO_2 is the most important greenhouse gas (GHGs) [55], [105]. To reduce the amount of CO_2 released into the atmosphere, different technologies have been developed in order to be applied to large point sources of CO_2, such as pre and post-combustion power plants, and in large industrial process to separate CO_2 from natural gas, coal bed methane or biogas [106]. Some of these technologies are based on adsorption techniques, which have been considered as one of the most promising approaches for capturing GHGs like CO_2 [107]. Due to this, the importance of porous materials like Metal-Organic Frameworks (MOFs) and Zeolitic Imidazolate Frameworks (ZIFs; subclass of MOFs) has increased in order to be used as adsorbents in CO_2 capture [77]. In the adsorption technique, a suitable adsorbent must be cheap, selective for the target gas, have a high surface area, a big pore volume with fast intraparticle diffusion and reversible adsorption (ideally upon pressure swings) [106]. Zeolitic Imidazolate Framework-8 (ZIF-8), for example, has shown to have all these characteristics and it has been studied to adsorb some of the GHGs, especially CO_2, under different operating conditions. Besides, ZIF-8 is already commercially available which makes easier the use of this material in gas adsorption application techniques [108].

Thermogravimetric analysis is a method commonly used to study gas-solid interactions. This method is also applied in the fields of fuels, catalysis, polymers, and chemical synthesis. Thermogravimetric analysis covers a wide spectrum of thermoanalytical techniques, which monitor one or more physical properties of a substance that is undergoing a temperature programmed heating as a function of time or temperature [109]. The advantage of using a gravimetric measurement for adsorption processes is that it can detect the adsorption equilibrium in gas-solid sorbent systems [110]. Also, this method allows to study the adsorbate-adsorbent interactions under atmospheric conditions (pressure and temperature), which is interesting since most of the CO_2 adsorption tests reported in the literature have been carried out at high pressures and GHGs emissions are mostly emitted at atmospheric pressure and ambient temperature [111].

The main objective of the present study was to determine the physicochemical properties of ZIF-8 which affect the adsorption of gases and to investigate the adsorptive properties of CO_2 on ZIF-8 under atmospheric pressure and ambient temperature. In the present work, a morphological and structural comparison between the synthetized and commercialized ZIF-8 was carried out. The adsorption capacity of ZIF-8 with CO_2 was investigated under atmospheric conditions by a thermogravimetric adsorption-desorption method. As part of this, the amount of CO_2 adsorbed was calculated from the sample weight changes measured by the thermogravimetric analysis (TGA) as a function of different CO_2 flow rates. By carrying out experimental analyses, this work aims to validate the previous computational study of CO_2 adsorption on ZIF-8 (chapter 7). Therefore, the experimental results obtained allow to analyze the efficiency of commercialized ZIF-8 to adsorb CO_2 under atmospheric conditions. The developed methodology can be extended to the study of other GHGs adsorption such as CH_4 and N_2O as it establishes the experimental basis of adsorption-desorption process in a gravimetric system.

8.2. Experimental methodology

8.2.1 Materials

Three chemical reagents were used to synthesize ZIF-8 crystals: Zinc nitrate hexahydrate ($Zn(NO_3)_2 \cdot 6H_2O$, 98 % purity), methanol (MeOH, 99.9 % purity), and 2-methylimidazole (2-mIm, 99 % purity). $Zn(NO_3)_2 \cdot 6H_2O$ and 2-mIm were purchased from Sigma-Aldrich (USA) and MeOH was purchased from Thermo Fisher Scientific Inc. (New Jersey, USA). The commercial compound ZIF-8 (2-methylimidazole zinc salt, 99.9 % purity), used to carry out the gas adsorption-desorption tests, was purchased from ACSYNAM (Montreal, Canada). All chemicals were used as received without further purification.

8.2.2 Synthesis of ZIF-8

ZIF-8 was obtained by a solvothermal synthesis taken from Delgado *et al.* [112]. A quantity of 0.66 g of $Zn(NO_3)_2 \cdot 6H_2O$ was dissolved by stirring in 28 ml of MeOH. A quantity of 1.20 g of 2-mIm was then dissolved by stirring in 28 ml of MeOH. After 5 min, both solutions were mixed and stirred for 1h at stirring rate of 640 rpm and aging without stirring for 1 h at room temperature (25 ± 5 ºC). For solvothermal synthesis, the precursor solution was transferred in an autoclave and heated at 150 ºC for 5 h. The ZIF-8 crystals were washed with MeOH and collected by

centrifugation (4500 rpm for 20 min), repeating it three times. The crystals were dried at 80 ºC over-night.

8.2.3 Characterization of ZIF-8

The morphology and components of ZIF-8 (synthetized and commercialized) were characterized by thermogravimetric analysis (TGA), X-ray diffraction pattern (XRD), Fourier transform infrared spectroscopy (FTIR), zeta potential analysis (Zetasizer) and nanoparticle tracking analysis (NTA-Nanosight). The results of characterization of both ZIF-8 (synthetized and commercialized) were compared with data reported in the literature.

The thermal stability of ZIF-8 was investigated with the thermogravimetric analysis (TGA) by a TGA/DSC 3+ analyzer (Mettler Toledo, Switzerland). A quantity of 5 mg of ZIF-8 powder was conducted, in alumina pan, from 25 to 800 ℃ with a heating rate of 10 ℃/min under nitrogen atmosphere. The flow rate of N_2 was 30 ml/min.

The crystallinity of ZIF-8 particles was identified by a XRD analysis with Cu kα radiation (wavelength of $\lambda = 1.54184$ Å at 30 kV and 10 mA) at step time 1 s and step size of 0.1° by scanning 2θ angle range between 5 and 80° with an X-ray D2 PHASER diffractometer (Burker AXS, Germany). For determining the type of groups and ligands that constitute the ZIF-8 structure, FTIR spectra was recorded using a FTIR Nicolet iS5 spectroscopy (Thermo Scientific, USA) in the range of 400-4000 cm^{-1} at an average of 32 scans with a resolution of 4 cm^{-1}. For both techniques, XRD and FTIR, ZIF-8 powder was dried at 150 °C in oven for 1 h before analysis.

Nanoparticle tracking analysis (NTA) was performed on a NanoSight LM10 NTA system (Malvern, U.K.) to analyze the particle size distribution of ZIF-8. The camera was manually set and kept the same for all samples with a slider shutter 1232 and slider gain 219. Videos of 1 min were recorded, and the number of captures was 3. The detection threshold was set to 5, and blur and max jump distance were automatically set. The surface zeta potential of ZIF-8 particles was determined using a Zetasizer NANO-ZS ZEN3600 analyzer (Malvern, U.K.) at different pH values. The pH adjustment was done in acidic and basic conditions, using 0.1 M hydrochloric acid (HCl) and sodium hydroxide (NaOH), from a range of 2-12 to analyze the effect of the pH on the electronic charge of ZIF-8. Prior to Nanosight and Zetasizer measurement, ZIF-8 powder was dispersed in water by agitation and sonication for 2 h with a concentration of 1 mg ZIF-8/100 ml water and

10 mg ZIF-8/100 ml water, respectively. The temperature was maintained at 20 °C to perform both analyses.

8.2.4 Thermogravimetric adsorption-desorption method

Adsorption tests of CO_2 were performed using a thermogravimetric adsorption-desorption method in a TGA/DSC 3+ analyzer (Mettler Toledo, Switzerland) with continuous monitoring of the mass changes. ZIF-8 commercialized was used as the adsorbent material. All the experimental tests were carried out in five phases: 1) Stabilization, 2) Pretreatment, 3) Cool down, 4) Adsorption, and 5) Desorption, at atmosphere pressure under controlled temperature.

Around 5 mg (initial weight) of ZIF-8 commercialized sample was placed and loaded in an alumina pan to perform all the adsorption tests. The gas N_2 (99.999 % purity) was used for the stabilization, pretreatment, cool down and desorption phases, while CO_2 (99.99 % purity) was used for carrying out the adsorption phase only. The gas N_2 was purchased from Messer Canada Inc. and the gas CO_2 was purchased from Linde Canada Inc. Before carrying out a test, a stabilization phase was programmed for a few minutes to set up the initial temperature (25 °C). As part of the pretreatment phase, the sample was heated up at a rate of 10 °C/min to 300 °C under a N_2 flow rate of 100 ml/min and was maintained constant for 1.5 h to remove the moisture and any pre-adsorbed gases. The temperature was then cooled down to the selected adsorption temperature at 25 °C. After the temperature became stable at 25 °C for 30 min, N_2 flow stopped and CO_2 was then introduced for 3 h. Different flow rates of CO_2 were used in each adsorption test, varying from 50 to 300 ml/min. After the adsorption phase, the gas was switched to N_2 at a flow rate of 100 ml/min for 1.5 h to perform the desorption phase at 300 °C with a heating rate of 10 °C/min.

For evaluating the adsorption capacity of ZIF-8 with CO_2, the weight changes were calculated in mg/g (adsorbate/adsorbent) from the thermogravimetric adsorption-desorption method. The amount of CO_2 adsorbed was calculated based on the following equation [77]:

$$Gas\ uptake = \frac{w_t - w_{t=0}}{m_g \cdot w_{t=0}}\ x\ 1000 \tag{8.1}$$

where,

$Gas\ uptake$ (mmol/g) is the amount of gas adsorbed on ZIF-8; w_t (mg) is the equilibrium weight of ZIF-8 after adsorption; $w_{t=0}$ (mg) is the initial weight of ZIF-8 before adsorption; and m_g (mg/mol) is the molecular weight of the gas.

A CO_2 adsorption profile curve at constant temperature was created using the results of the gas uptake (mmol gas/g ZIF-8), over time, corresponding to each CO_2 flow rate (ml/min) used for carrying out the adsorption tests.

8.3. Results and discussion

8.3.1 Morphological and structural characterization of ZIF-8

The thermal stability of synthetized and commercialized ZIF-8 determined by the TGA analysis is shown in Fig. 8.1. The thermogravimetric curves show the weight loss of both ZIF-8 due to the structural degradation of the material with increasing temperature. Results from both curves were compared with the literature. A considerable difference in the weight loss between the synthetized ZIF-8 and the commercialized ZIF-8 is clearly visible in the figure.
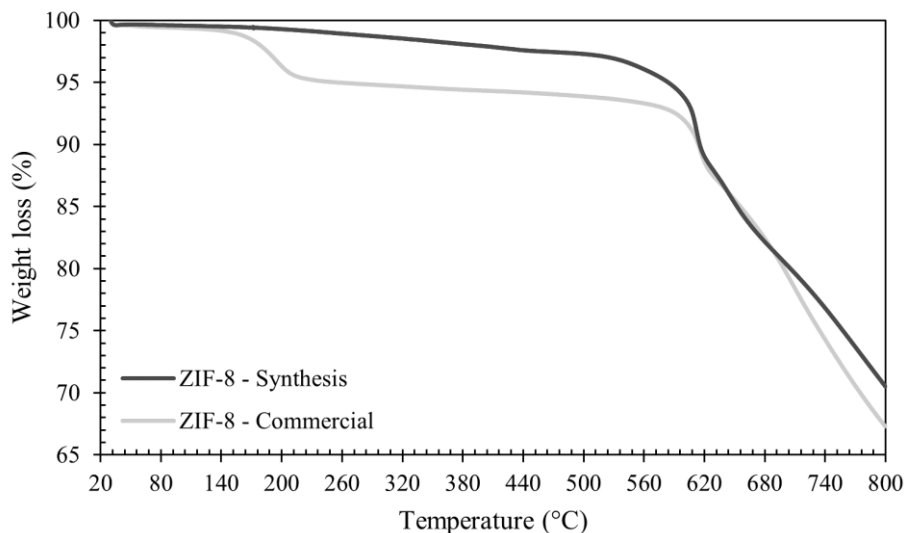
Figure 8.1 TGA curves of the total mass loss of synthetized ZIF-8 and commercialized ZIF-8 under N_2 atmosphere.

The synthetized ZIF-8 showed a slight weight loss up to 500 °C. In the case of the commercialized ZIF-8, the TGA curve exhibited only a very weak weight loss of less than 0.5 wt% from 25 to 150 °C. This weight loss can be attributed to the evaporation of the remaining solvent used in the synthesis of ZIF-8 (i.e. methanol) and the removal of guest molecules like pre-adsorbed gases due to exposure to atmosphere during the synthesis process [77], [113], [114] . However, from 150 to 220 °C, the commercialized ZIF-8 showed a major mass loss corresponding to evaporation of adsorbed water molecules from ZIF-8 cavities [115], [116]. The difference of the initial weight loss between both ZIF-8 (synthetized and commercialized) could be explained by the type of synthesis

used for producing the adsorbents because the solvothermal synthesis allowed to dry the ZIF-8 during its production.

According to the thermogravimetric curves, a slight loss weight was observed from 200 to 500 °C, corresponding to the carbonization of unreacted 2-mIm [115]. At temperatures below 500 °C, the ZIF-8 structure showed a good stability. However, ZIF-8 organic linkers started to decompose at temperatures around 500-600 °C [113]–[115]. Thus, the structure of the synthesized ZIF-8 was stable up to 520 °C, while the commercialized ZIF-8 presented a thermal decomposition after 565 °C which shows a better thermal stability between both ZIF-8. When temperature was over 600 °C, a sharp weight loss occurred in both TGA curves, corresponding to the collapse of the backbone of ZIF-8 [114]. At 800 °C, the remaining weight was of approximately 29 and 32 wt% for the synthetized ZIF-8 and the commercialized ZIF-8, respectively.

The crystallinity of the ZIF-8 structure was investigated by the XRD analysis from 2θ values of 5 to 80°. Fig. 8.2 (a) shows a comparison of the XRD patterns of the synthetized ZIF-8 and the commercialized ZIF-8 only between 2θ values of 6 and 40° which are the most representative for this type of structure. The peak broadening observed indicates the formation of ZIF-8 crystals. The main diffraction peaks from left to right were at 2θ = 7.5, 10.5 , 12.8, 14.8, 16.6, 18.2, 24.6, and 26.9° for the synthetized ZIF-8, and at 2θ = 7.3, 10.4, 12.7, 14.7, 16.5, 18.0, 24.5, and 26.7° for the commercialized ZIF-8, corresponding, respectively, to the planes 110, 200, 211, 220, 310, 222, 332, and 431 of ZIF-8 crystal structure. The relative intensities and prominent peak positions confirmed the sodalite structure corresponding to the typical structure of ZIF-8. The well-defined peaks also revealed the high crystallinity and the purity of the material. Even if the commercialized ZIF-8 showed more prominent peaks than the synthetized ZIF-8, the results were pretty similar between them, and the overall XRD patterns with the corresponding peaks were in good agreement with the literature [113], [114], [117]–[121].
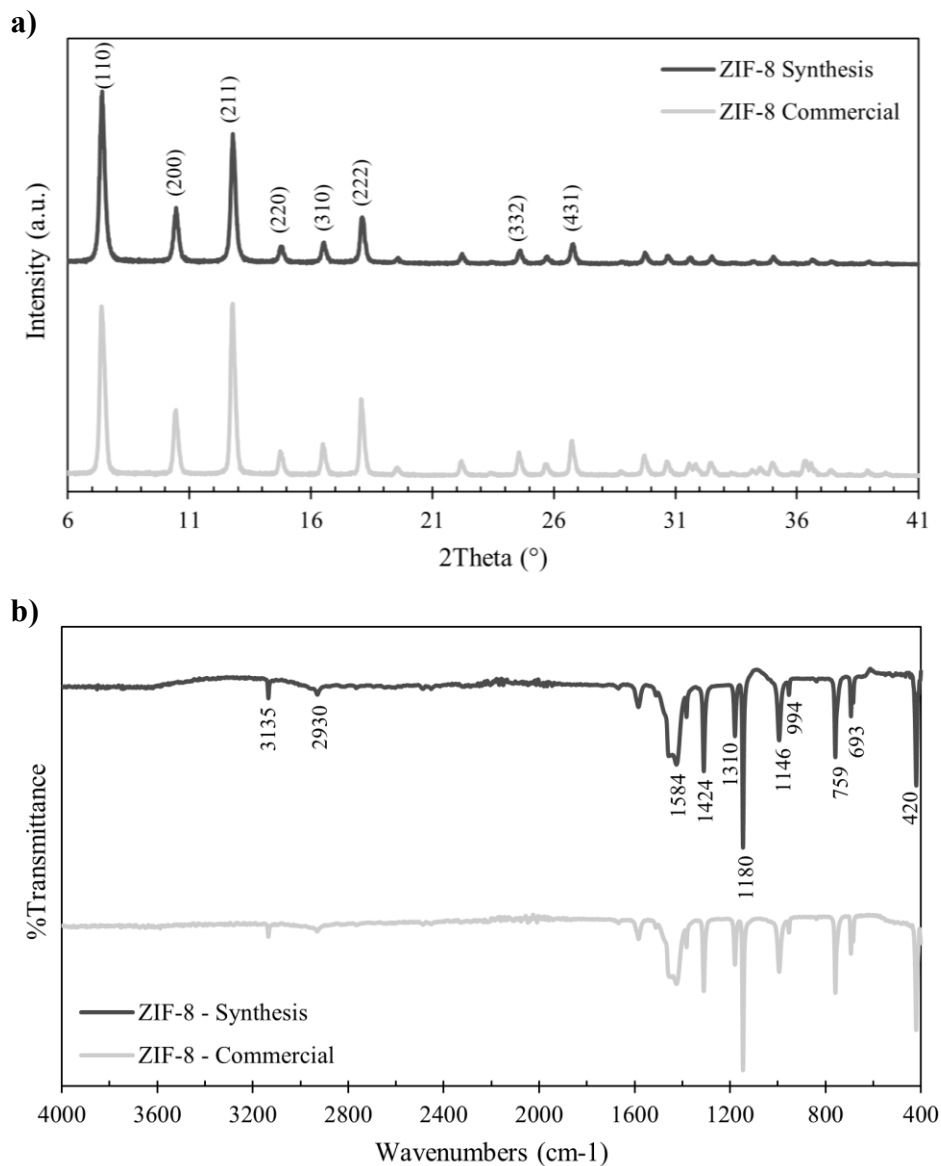
Figure 8.2 a) XRD patterns (2θ = 6-40°) and b) FTIR spectra of ZIF-8. Comparison between synthetized ZIF-8 and commercialized ZIF-8.

The FTIR spectra of the ZIF-8 crystals is shown in Fig. 8.2 (b) to analyze the type of functional groups and the ligands that constitute the chemical structure of ZIF-8, comparing the synthetized and the commercialized ZIF-8. Different surface functionalities can be understood by assigning the various peaks. Results of the FTIR spectra for both ZIF-8 (synthetized and commercialized) differed by decimals. At 3135 and 2930 cm^{-1}, a characteristic absorption for both ZIF-8 is present, which can be attributed to the C–H aromatic and aliphatic asymmetric stretching of the methyl group present in the linker [116], [120]. The peak at 1584 cm^{-1} for both ZIF-8 corresponds to the C=N stretching mode [115], [116], [120], [122]. Further, the frequency region from 1424 to 1180 cm^{-1}

constitutes the stretching and bending vibrations of the entire imidazole ring [115], [116], [119], [120], [122]. The absorption bands at 1146 and 994 cm^{-1} are attributed to C–N stretching and bending modes, respectively, while the absorption peaks at 759 and 693 cm^{-1} are related to the aromatic sp^2 C–H bending [120]. Besides, the peak at 420 cm^{-1} corresponds to the Zn–N stretching vibration mode, establishing the direct bonding between Zn and N atoms from the imidazole linker [115], [116], [119]–[121].

The particle size distribution of both ZIF-8 (synthesized and commercialized) is illustrated in Fig. 8.3. The dilute ZIF-8 suspension exhibited a particle size distribution in a range of 100 to 500 nm. The mean particle size of 209.2 ± 4.3 nm and 214.4 ± 13.4 nm was calculated from the distribution curves of the synthetized and commercialized ZIF-8, respectively. These results are similar to data reported in the literature [119], [123], [124]. Even if the mean particle size for both ZIF-8 is similar, the particle size distribution differed. For the synthetized ZIF-8 most of the particles have a size of 175 nm (Fig. 8.3 (a)), while for the commercialized ZIF-8, most of the particles have a size of 71 and 307 nm (Fig. 8.3 (b)). This difference in particle distribution can be explained by the type of synthesis that was used to produce both ZIF-8.
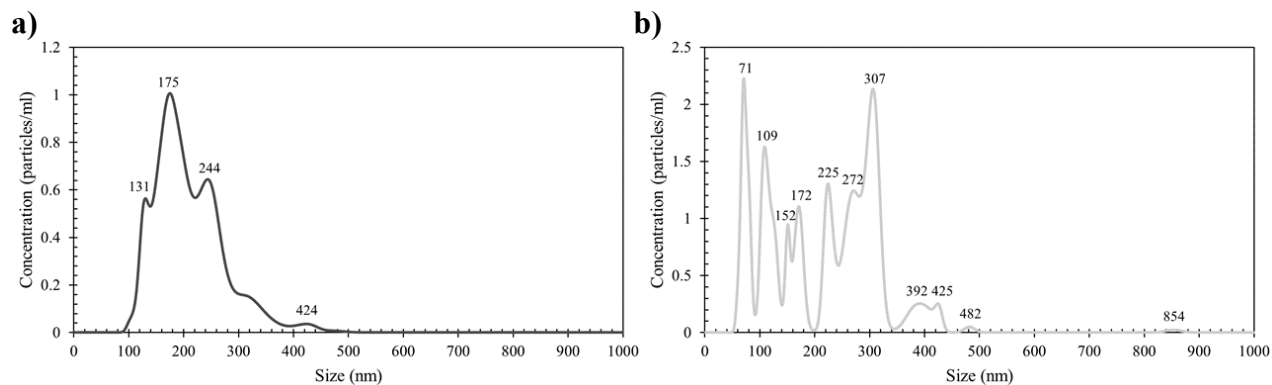
Figure 8.3 Particle size distribution in water of a) synthetized ZIF-8 and b) commercialized ZIF-8.

Zeta potential of commercialized ZIF-8 was measured from a pH range of 2-12, for evaluating the effect of the pH on the surface electronic charge of ZIF-8. The surface charge of ZIF-8 varied from positive to negative according to the acidic or alkaline conditions done with a pH adjustment. However, Fig. 8.4 shows only the results obtained in a pH range between 7 and 11, since ZIF-8 is not stable in acidic conditions [116].
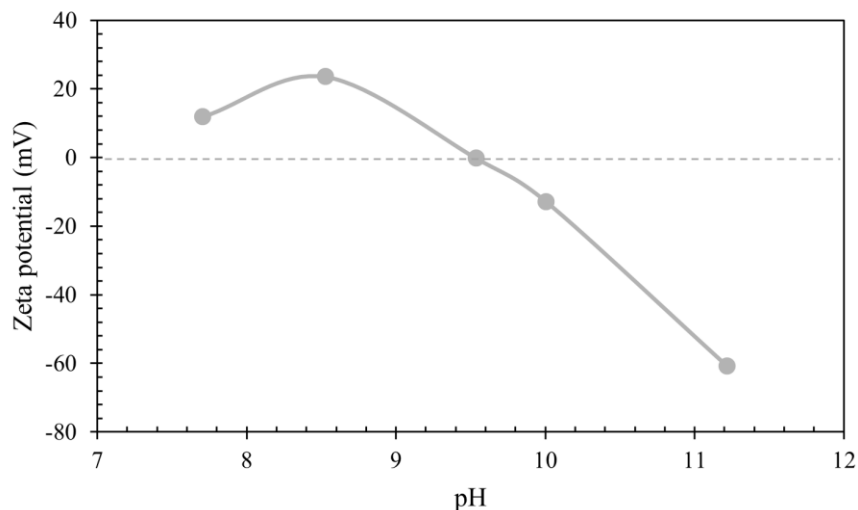
Figure 8.4 Zeta potential of commercialized ZIF-8 over the range pH = 7-11.

The zero-point charge (pH_{ZPC}), at which the zeta potential is zero, is an important factor used to determine the adsorption ability of the surface [116]. For the commercialized ZIF-8, the pH_{ZPC} was at a pH around 9.5, similar to results reported in the literature [121], [122], [124]. As it can be seen from the figure, the value of pH_{ZPC} implied that the surface of ZIF-8 was positively charged when solution pH was below 9.5 (acidic and neutral region), while the surface charge of ZIF-8 become negative at solution pH above 9.5 (alkaline region). The surface potential helps to analyze whether the electrostatic interaction facilitates adsorption or not [119].

8.3.2 Thermogravimetric analysis of CO_2 adsorption on ZIF-8

The adsorption capacity of commercialized ZIF-8 with CO_2 was studied at atmospheric pressure (101.30 kPa) and ambient temperature (25 °C) by a thermogravimetric analysis. Different CO_2 flow rates were considered for carrying out the adsorption tests. The CO_2 uptake was calculated, using Eq. 8.1, for determining the adsorption capacity of ZIF-8. The results of the CO_2 uptakes obtained at different flow rates are shown in Fig. 8.5. An evolution of the adsorption process of CO_2 is clearly illustrated in Fig. 8.5 (a), showing an increase in the amount of the adsorbed mass of CO_2 over time, corresponding to the 3 h of the adsorption phase. The adsorption increment is shown staggered due to the way the TGA measures mass changes. A better view of CO_2 uptake corresponding to each CO_2 flow rate is shown in Fig. 8.5 (b).
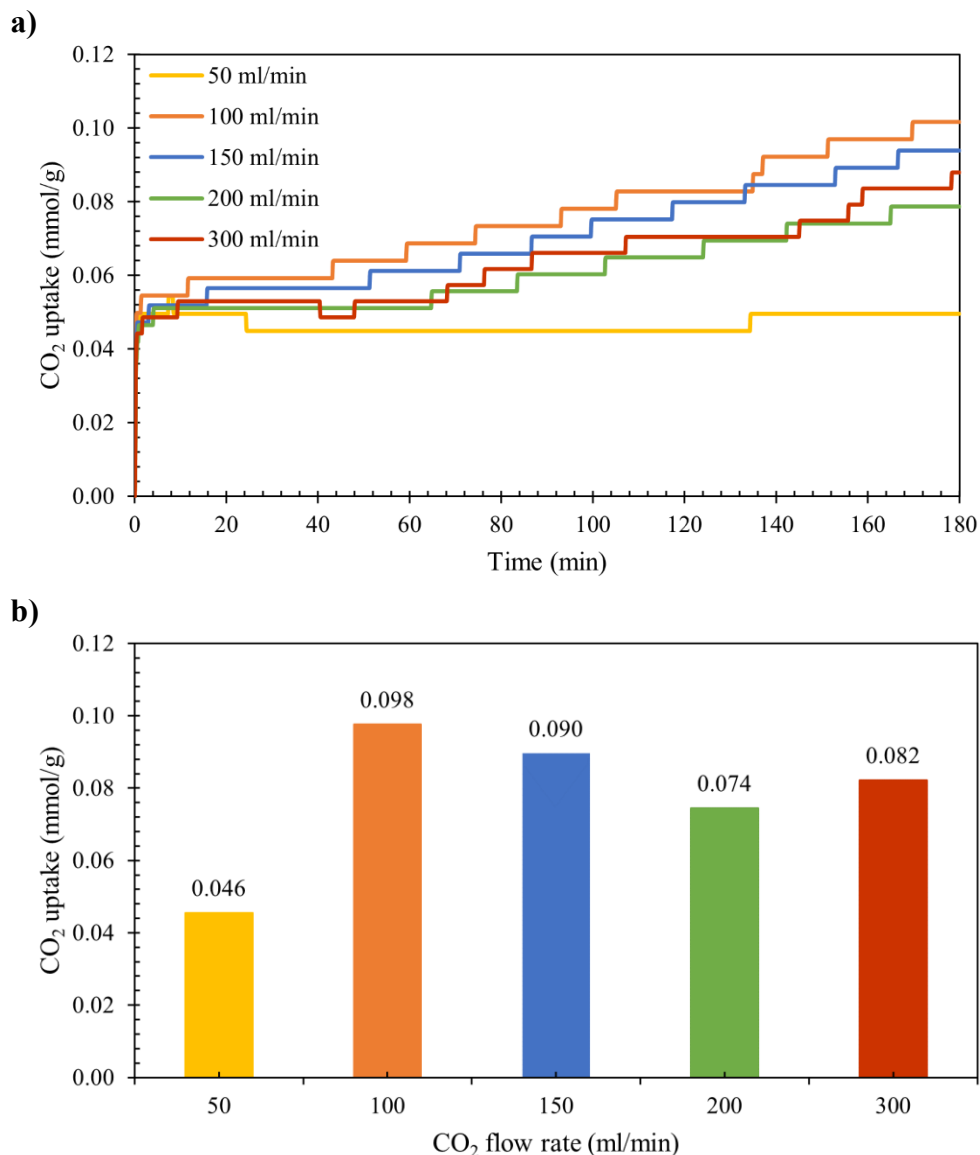
Figure 8.5 (a) Evolution over time and (b) Variation of CO_2 adsorption on ZIF-8 under different flow rates of pure CO_2 at atmospheric conditions (P = 101.30 kPa; T = 25 °C).

An effect of the different flow rates on CO_2 adsorption can be seen from both graphs. The lowest CO_2 uptake of 0.046 mmol/g corresponded to a flow rate of 50 ml/min which was the smallest flow rate used for performing the tests. By increasing the CO_2 flow rate, an increase in CO_2 adsorption was observed. At a flow rate of 100 ml/min, the highest CO_2 uptake was obtained with 0.098 ± 0.02 mmol/g even if the flow rate was not the highest used. For the flow rate of 150 ml/min, the CO_2 uptake decreased slightly resulting in 0.090 mmol/g. A continue decrease was observed with the flow rate of 200 ml/min, obtaining a CO_2 uptake of 0.074 mmol/g. However, the CO_2 uptake increased lightly again resulting in 0.082 mmol/g, by increasing the flow rate at 300 ml/min.

The general relationship between adsorption and flow rate of CO_2 could be explained by a possible variation of the pressure. Although the TGA pressure was set at 101.30 kPa, the different flow rates might cause a small fluctuation in the internal pressure, influencing the amount of CO_2 adsorbed.

As it was observed, the highest CO_2 uptake resulted with a flow rate of 100 ml/min. This could be related to the N_2 flow rate used in the other phases (pretreatment, cooldown, and desorption) which was 100 ml/min. As the whole thermogravimetric adsorption-desorption process was carried out under the same flow rate (100 ml/min), the system permitted equal changes of adsorption for both gases with a thermogram signal more stable, resulting in a higher adsorption of CO_2. Besides, by varying the CO_2 flow rate in the adsorption phase, the gas velocity also varies, and this could affect the adsorption of CO_2 on the ZIF-8. Thus, for the thermogravimetric system, a flow rate of 100 ml/min and an adsorption time of 3 h seem to be the ideal conditions for allowing the ZIF-8 to adsorb better the CO_2 at atmospheric conditions.

The CO_2 uptakes obtained experimentally (4.3 mg CO_2/g ZIF-8) resulted lower than the ones reported in the literature (31 mg CO_2/g ZIF-8) [108], [125]. These experimental results were also smaller to the ones obtained by MD simulations (55 mg CO_2/g ZIF-8; Chapter 7). This could be due to the fact that in MD simulations, all the adsorption system is considered as ideal. All the pores of ZIF-8 are completely free and there is no gas previously adsorbed, while in experiments, there are already gases adsorbed on the ZIF-8. Besides, MD simulations were performed only with CO_2 molecules. Nevertheless, using a thermogravimetric adsorption-desorption method, this is not possible because for carrying out the whole analysis, the ZIF-8 comes into contact with N_2 and CO_2. Although N_2 has been used as purge gas and only CO_2 has been introduced in the adsorption phase, the ZIF-8 has been adsorbed a certain amount of N_2 before the adsorption phase, which could cause a partial saturation of the ZIF-8 with N_2. According to literature, during adsorption process a selectivity phenomenon can occur when two or more gases are in contact with ZIF-8 [55], [126]. Even if a binary mixture (CO_2/N_2) was not specifically used in the adsorption phase, both gases can be adsorbed in different amounts on ZIF-8 because N_2 has shown to have only a small affinity for the ZIF-8 [126]. Therefore, at atmospheric conditions, CO_2 might take the sites available in ZIF-8, leaving the few N_2 molecules that have been adsorbed before the adsorption phase.

8.4. Conclusion

The ZIF-8 is a potential gas adsorbent that can be produced by relatively simple synthesis method, such as solvothermal synthesis. Because of the good characteristics of ZIF-8 as adsorbent material and the way to produced, it is commercially available. The morphology and structure of both synthetized and commercialized ZIF-8 was analyzed by a thermogravimetric analysis, X-ray diffraction spectrum, Fourier-transform infrared spectroscopy, zeta potential analysis and nanoparticle tracking analysis. Characterization results showed that commercial ZIF-8 is as pure as ZIF-8 synthesized using high purity reagents. In addition, the adsorption capacity of ZIF-8 with CO_2 was studied at atmospheric conditions under different CO_2 flow rates using a thermogravimetric adsorption-desorption method. The different flow rates showed an influence in the adsorption of CO_2. However, the adsorbed amount of CO_2 did not increase linearly according to each flow rate, obtaining the highest CO_2 uptake (0.098 ± 0.02 mmol/g) with a flow rate of 100 ml/min. Although the experimental results allowed to analyze the efficiency of commercialized ZIF-8 to adsorb CO_2 under atmospheric conditions, the CO_2 uptake obtained experimentally resulted lower than the one obtained by MD simulations. A series of elements like the purity of ZIF-8, the purity of CO_2, the adsorption-desorption cycle using N_2 and CO_2 and the selectivity phenomenon (CO_2/N_2)could cause the difference between both adsorption results.

The present work focuses on the study of the adsorption of CO_2 on ZIF-8 at atmospheric conditions, as this gas is reported as the most important anthropogenic GHG and is widely emitted under these conditions. This experimental study was performed with the aim to develop an experimental method to corroborate the computational study (MD simulations) and extend the methodology for future works related to the adsorption of other GHGs like CH_4 and N_2O on ZIF-8.

CHAPTER 9. CONCLUSION

The physical adsorption process of N_2O has been studied using molecular modeling and computational chemistry, and it has been divided in three parts: 1) Quantum mechanics (QM) simulations, 2) Molecular dynamic (MD) simulations, and 3) Experimental analysis. ZIF-8 has been used in this study as the adsorbent material, and its adsorption capacity has been investigated under different operating conditions. The adsorption of CO_2 and CH_4 on ZIF-8 has been also analyzed and compared to the literature with the purpose of validating the methodology developed in this work to mainly study the adsorption of N_2O on ZIF-8.

1) The main conclusions for QM simulations using a combination of the mathematical models Semi-Empirical Method PM6 and Density Functional Theory DFT B3LYP-D3 6-31G* are the following:

- The molecular adsorption interactions between N_2O and ZIF-8 mainly occur in three sites of the ZIF-8 structure: Center, Side and Methylcenter, for both pores (small and big) of ZIF-8;

- The six-membered window of ZIF-8 seems to be the pore where the most stable interactions occur based on the adsorption energy and the approach distance;

- The Center of the six-membered window (big pore) is considered the adsorption site where N_2O finds firstly the interaction stability, showing the shortest approach distance of 0.1 Å and a corresponding adsorption energy of -43.9 kJ/mol;

- N_2O molecule can be adsorbed via oxygen atom (–ONN) or terminal nitrogen atom (–NNO). The –ONN configuration produces more stable interactions with the surface of ZIF-8 than –NNO configuration;

- Approximately, the adsorption energies vary from -20 to -40 kJ/mol. However, the highest adsorption energy is -61.8 kJ/mol, corresponding to the –NNO configuration and the Side site of the big pore, with an approach distance of 5.6 Å;

- The adsorption energies obtained in this study are in the range of energies reported in other studies for the adsorption of N_2O using other adsorbents (Chapter 6, See Table 6.1).

2) The main conclusions for MD simulations using the existing Molecular Mechanics 3 (MM3) force field, adapted for MOFs, are the following:

- The adsorption capacity of ZIF-8 with N_2O, CO_2 and CH_4 increases with pressure according to adsorption isotherm curves obtained at 298 K. The maximum adsorption occurs at pressures around 40 atm when ZIF-8 is saturated with each of the three gases individually;

- The adsorption capacity of ZIF-8, at the adsorption saturation pressure of 40 atm, follows the order $CO_2 > N_2O > CH_4$, corresponding to an excess uptake of 363 mg/g, 211 mg/g and 106 mg/g, respectively;

- At atmospheric pressure (1 atm) and ambient temperature (298 K) , the adsorption capacity of ZIF-8 with CO_2, CH_4 and N_2O is 55 mg/g, 4 mg/g and 18 mg/g, respectively.

- The N_2O excess uptake varies between 50 and 200 mg/g;

- The average adsorption energy for CO_2 is -23.7 kJ/mol, for CH_4 is -14.1 kJ/mol, and for N_2O is -22.8 kJ/mol;

- The adsorption isotherms curves and the adsorption energies of CO_2 and CH_4 obtained in this study are similar to the ones reported in the literature. The statistical analysis (ANOVA) indicated that there was no difference among the isotherm parameters for simulation and experimental determination. The isotherm curves obtained by simulations are slightly above the experimental ones reported in the literature because the purity and the crystallinity of the adsorbent are not ideal (Chapter 7, See Fig. 7.5). The adsorption energies calculated are slightly smaller than the ones reported in the literature (Chapter 7, See Table 7.3).

3) The main conclusions for the experimental analysis, using the thermogravimetric adsorption-desorption method, are the following:

- The ZIF-8 structure is stable at temperatures below 500 °C, approximately. The synthesized ZIF-8 shows a thermal stability up to 520 °C, while the thermal stability of the commercialized ZIF-8 is reached up to 565 °C;

- The crystallinity and the sodalite structure of synthetized and commercialized ZIF-8, as well as the main type of groups and ligands (C–H, C–N, C=N, N–H, Zn–N and imidazole ring, including the stretching and bending vibration modes) correspond to the typical structure of ZIF-8;

- The particle size of the synthetized ZIF-8 is 209.2 ± 4.3 nm, while the particle size of the commercialized ZIF-8 is around 214.4 ± 13.4 nm;

- The ZIF-8 material is unstable in acidic pH. The zero-point charge (pH_{ZPC}) of ZIF-8 corresponds to a pH around 9.5, evidencing that ZIF-8 is stable in alkaline conditions;

- The whole characterization of both ZIF-8 (synthetized and commercialized) obtained in this study agrees with the literature (Chapter 8, See Fig. 8.1-8.4);

- The adsorption capacity of ZIF-8, based on CO_2 uptake, varies under different CO_2 flow rates. However, the relation between these variables is not linear. At atmospheric conditions (P = 101.30 kPa; T = 25 °C), the highest CO_2 uptake was 0.098 ± 0.02 mmol/g, obtained with a flow rate of 100 ml/min;

- The adsorption capacity of ZIF-8 with CO_2 obtained experimentally (4.3 mg/g) is smaller than the one obtained by simulations (55 mg/g) due to the purity of ZIF-8, the purity of CO_2, the gases that are in contact with ZIF-8 (CO_2 and N_2) and the selectivity phenomenon (CO_2/N_2).

The general conclusions of this study are the following:

- The combination of the mathematical methods (PM6 and DFT B3LYP-D3 6-31G*) helps to optimize the time of QM simulations;

- The mathematical terms of the MM3 force field can be extended for MOFs, adapting the parameters for the ZIF-8 structure. The MM3-MOF force field, used in MD, can simulate the multiple types of bonded and non-bonded interactions occurred within the atoms of a molecule (intramolecular forces) and between molecules (intermolecular forces);

- The electrostatic cut-offs and the periodic boundary conditions are two important and useful elements in MD to simulate large molecules like ZIF-8 and complex systems like gas adsorption process. They also help to optimize the time of MD simulations;

- The RDFs are useful to calculate the maximum adsorption distance of gas molecules and therefore, to calculate the adsorption energies;

- The ZIF-8 can adsorb individually the three main GHGs (CO_2, CH_4 and N_2O) but in different amounts due to the adsorbate-adsorbent molecular interactions, the size and the affinity of the gas molecules. Adsorption of N_2O is higher than the one of CH_4, but smaller than the adsorption of CO_2;

- The order $CO_2 > N_2O > CH_4$ for the excess uptake from the adsorption isotherms is the same than for the adsorption energies. In this way, the analysis of the interaction effectiveness of the three gases on ZIF-8 can be described with these two properties;

- The physicochemical properties of synthetized and commercialized ZIF-8 are similar which confirms that the commercialized ZIF-8 can be used to perform adsorption tests;

- The thermogravimetric analysis is a useful technique for studying gas-solid interactions like CO_2 adsorption on ZIF-8. This method establishes the experimental basis of adsorption-desorption process in a gravimetric system and can be extended to the study of other GHGs adsorption such as CH_4 and N_2O on ZIF-8;

- Experimental and simulation results show certain differences because MD simulations consider the adsorption system as ideal, while in experimentation, there are some factors that can affect the performance of the material for adsorbing the gases, e.g., the purity and the crystallinity of the material as well as the exposure of the material to atmosphere during synthesis and manipulation. However, a combined experimental and theoretical approach is useful to deepen the understanding of molecular interactions between the gas and the adsorbent material before carrying out experimental tests.

CONCLUSION

Le procédé d'adsorption physique du N_2O a été étudié à l'aide de la modélisation moléculaire et de la chimie computationnelle. Il a été divisé en trois parties : 1) Simulations de mécanique quantique (*Quantum Mechanics* (QM) *simulations*), 2) Simulations de dynamique moléculaire (*Molecular dynamics* (MD) *simulations*) et 3) Analyse expérimentale. Le ZIF-8 a été utilisé dans cette étude comme matériau adsorbant, et sa capacité d'adsorption a été étudiée sous différentes conditions d'opération. L'adsorption du CO_2 et du CH_4 sur le ZIF-8 a été également analysée et comparée avec la littérature dans le but de valider la méthodologie développée dans ce travail pour étudier principalement l'adsorption du N_2O sur le ZIF-8.

1) Les principales conclusions des simulations de mécanique quantique en utilisant une combinaison des modèles mathématiques *Semi-Empirical Method* PM6 et *Density Functional Theory* DFT B3LYP-D3 6-31G* sont les suivantes :

- Les interactions d'adsorption moléculaire entre le N_2O et le ZIF-8 se produisent principalement dans trois sites de la structure du ZIF-8 : *Center*, *Side* et *Methylcenter*, pour les deux pores (petit et grand) du ZIF-8 ;

- Le grand pore du ZIF-8 semble être le pore où se produisent les interactions les plus stables en fonction de l'énergie d'adsorption et de la distance d'approche ;

- Le centre (*Center*) du grand pore est considéré comme le site d'adsorption où le N_2O trouve d'abord la stabilité d'interaction, présentant la distance d'approche la plus courte de 0,1 Å et une énergie d'adsorption correspondante de -43,9 kJ/mol ;

- La molécule de N_2O peut être adsorbée par l'atome d'oxygène (–ONN) ou par l'atome d'azote terminal (–NNO). La configuration –ONN produit des interactions plus stables sur la surface du ZIF-8 que la configuration –NNO ;

- Les énergies d'adsorption varient entre -20 et -40 kJ/mol. Cependant, l'énergie d'adsorption la plus élevée est de -61,8 kJ/mol, correspondant à la configuration –NNO et au site *Side* du grand pore, avec une distance d'approche de 5,6 Å ;

- Les énergies d'adsorption obtenues dans cette étude sont dans la gamme des énergies rapportées dans d'autres études pour l'adsorption du N_2O en utilisant d'autres adsorbants (Chapitre 6, voir Tableau 6.1).

2) Les principales conclusions pour les simulations de dynamique moléculaire en utilisant le champ de force existant appelé *Molecular Mechanics 3* (MM3), adapté aux Réseaux Métallo-Organiques (*Metal–Organic Frameworks* (MOFs)), sont les suivantes :

- La capacité d'adsorption du ZIF-8 avec le N_2O, le CO_2 et le CH_4 augmente avec l'augmentation de la pression selon les courbes d'isothermes d'adsorption obtenues à 298 K. L'adsorption maximale se produit à des pressions autour de 40 atm lorsque le ZIF-8 est saturé avec chacun des trois gaz individuellement ;

- La capacité d'adsorption du ZIF-8, à la pression de saturation d'adsorption de 40 atm, suit l'ordre $CO_2 > N_2O > CH_4$, correspondant à une adsorption en excès de 363 mg/g, 211 mg/g et 106 mg/g, respectivement ;

- Sous pression atmosphérique (1 atm) et à température ambiante (298 K), la capacité d'adsorption du ZIF-8 avec le N_2O, le CO_2 et le CH_4 est de 18 mg/g, de 55 mg/g et de 4 mg/g, respectivement ;

- L'adsorption en excès du N_2O varie entre 50 et 200 mg/g ;

- L'énergie d'adsorption moyenne pour le N_2O est de -22,8 kJ/mol, pour le CO_2 de -23,7 kJ/mol et pour le CH_4 de -14,1 kJ/mol ;

- Les courbes d'isothermes d'adsorption et les énergies d'adsorption du CO_2 et du CH_4 obtenues dans cette étude sont similaires à celles rapportées dans la littérature. Les courbes d'isotherme obtenues par simulations sont supérieures aux courbes expérimentales rapportées dans la littérature car la pureté et la cristallinité de l'adsorbant ne sont pas idéales (Chapitre 7, Voir Fig. 7.5). Les énergies d'adsorption calculées sont légèrement inférieures à celles rapportées dans la littérature (Chapitre 7, voir Tableau 7.3).

3) Les principales conclusions de l'analyse expérimentale par la méthode thermogravimétrique d'adsorption-désorption sont les suivantes :

- La structure du ZIF-8 est stable à des températures inférieures à 500 °C. Le ZIF-8 synthétisé montre une stabilité thermique jusqu'à 520 °C, tandis que la stabilité thermique du ZIF-8 commercialisé est atteinte jusqu'à 565 °C ;

- La cristallinité et la structure de la sodalite ZIF-8 synthétisé et commercialisé, ainsi que leurs principaux types de groupes et de ligands (C–H, C–N, C=N, N–H, Zn–N et imidazole

anneau, y compris les modes de vibration d'étirement et de flexion) correspondent à la structure typique du ZIF-8 ;

- La taille des particules du ZIF-8 synthétisé est de 209,2 ± 4,3 nm, tandis que la taille des particules du ZIF-8 commercialisé est d'environ 214,4 ± 13,4 nm ;

- Le matériau ZIF-8 est instable en pH acide. La charge du point zéro (pH_{ZPC}) du ZIF-8 correspond à un pH d'environ 9,5, ce qui prouve que le ZIF-8 est stable dans des conditions alcalines ;

- L'ensemble de la caractérisation des deux ZIF-8 (synthétisé et commercialisé) obtenu dans cette étude est en accord avec la littérature (Chapitre 8, Voir Fig. 8.1-8.4) ;

- La capacité d'adsorption du ZIF-8, basée sur l'adsorption du CO_2, varie selon les différents débits de CO_2. Cependant, la relation entre ces variables n'est pas linéaire. Sous des conditions atmosphériques (P = 101,30 kPa ; T = 25 °C), l'adsorption du CO_2 la plus élevée était de 0,098 ± 0,02 mmol/g, laquelle a été obtenue avec un débit de CO_2 de 100 ml/min ;

- La capacité d'adsorption du ZIF-8 avec le CO_2 obtenue expérimentalement est inférieure à celle obtenue par simulations en raison de la pureté du ZIF-8, la pureté du CO_2, les gaz qui sont en contact avec le ZIF-8 (CO_2 et N_2) et le phénomène de sélectivité (CO_2/N_2).

Les conclusions générales de cette étude sont les suivantes :

- La combinaison des méthodes mathématiques (*Semi-Empirical Method* PM6 and *Density Functional Theory* DFT B3LYP-D3 6-31G*) permet d'optimiser le temps des simulations de mécanique quantique ;

- Les termes mathématiques du champ de force MM3 peuvent être appliqués aux Réseaux Métallo-Organiques (MOFs), en adaptant les paramètres pour la structure du ZIF-8. Le champ de force MM3-MOF, utilisé dans la dynamique moléculaire, peut simuler les multiples types d'interactions liées et non liées qui se produisent au sein des atomes d'une molécule (forces intramoléculaires) et entre les molécules (forces intermoléculaires) ;

- Les distances limites électrostatiques (*electrostatic cut-offs*) et les conditions aux limites périodiques (*periodic boundary conditions*) sont deux éléments importants et utiles dans la dynamique moléculaire pour simuler de grosses molécules comme le ZIF-8 et des systèmes complexes comme le procédé d'adsorption de gaz. Ils permettent aussi d'optimiser le temps des simulations de dynamique moléculaire ;

- Les fonctions de distribution radiale (*Radial Distribution Fonctions* (RDFs)) sont utiles pour calculer la distance maximale d'adsorption des molécules de gaz et donc, pour calculer les énergies d'adsorption ;

- Le ZIF-8 peut adsorber individuellement les trois principaux GES (CO_2, CH_4 et N_2O) en quantités différentes en raison des interactions moléculaires adsorbant-adsorbat et de la taille des molécules de gaz. L'adsorption du N_2O est supérieure à celle du CH_4, mais inférieure à celle du CO_2 ;

- L'ordre $CO_2>N_2O>CH_4$ pour l'adsorption en excès des isothermes d'adsorption est le même pour les énergies d'adsorption, donc l'analyse de l'efficacité des interactions des trois gaz sur le ZIF-8 peut être décrite avec ces deux propriétés ;

- Les propriétés physico-chimiques du ZIF-8 synthétisé et commercialisé sont similaires, ce qui confirme que le ZIF-8 commercialisé peut être utilisé pour effectuer des tests d'adsorption ;

- La méthode d'adsorption-désorption thermogravimétrique est une technique utile pour étudier les interactions gaz-solide comme l'adsorption du CO_2 sur le ZIF-8. Cette méthode établit la base expérimentale du processus d'adsorption-désorption dans un système gravimétrique et peut être étendue à l'étude d'adsorption d'autres GES tels que le CH_4 et le N_2O sur le ZIF-8 ;

- Les résultats expérimentaux et de simulation montrent certaines différences car les simulations de dynamique moléculaire considèrent le système d'adsorption comme idéal, tandis qu'aux niveaux des expérimentations, certains facteurs peuvent affecter les performances du matériau pour adsorber les gaz; par exemple, la pureté et la cristallinité du matériau ainsi que l'exposition du matériau à l'atmosphère pendant sa synthèse et la manipulation de celui. Une approche combinée expérimentale et théorique est utile pour approfondir la compréhension des interactions moléculaires entre le gaz et le matériau adsorbant avant de réaliser des tests expérimentaux.

APPENDIX A. MOLECULAR MECHANICS FORCE FIELD TERMS

A.1. Bonded terms

The bonded terms depend on bond stretching, angle bending and dihedral torsions parameters.

Bond stretching represents a covalent bond made up of a spring [95]:

$$E_{bond} = \frac{1}{2} k_b (r_b - r_0)^2 \tag{A.1}$$

where,

k_b is a force constant that gives a measure of the strength of the spring, i.e., the bond (mdyne/Å). A double bond will have a larger value of k_b than a single bond; r_b is the bond length distance value (Å); and r_0 is a reference value of the stretch corresponding to the equilibrium structure of the molecule (Å).

Angle bending represents the angle formed by three consecutive atoms at their minimum energy position [95]:

$$E_{angle} = \frac{1}{2} k_a (\theta_a - \theta_0)^2 \tag{A.2}$$

where,

k_a is a force constant that describes the potential energy changes due to angle bending (mdyne*Å/rad²); θ_a is the angle between two bonds, resulting in a bending position (°); and θ_0 is a reference value of the bend corresponding to the equilibrium structure of the molecule (°).

Dihedral torsion is generated by atoms that are separated by three bonds from each other [68]:

$$E_{dihedral} = k_{dihedral} \left[1 + cos(n(\phi - \phi_0)) \right] \tag{A.3}$$

where,

$k_{dihedral}$ is a constant that represents the energy barrier of the system to rotate around a central bond, defining the torsion angle (kcal/mol); n is an integer value that defines the periodicity of rotation; ϕ is the torsion angle that represents the dihedral angle defining the relative orientation of the atoms (°); and ϕ_0 is the ideal torsion angle relative to a staggered conformation of two atoms (°).

Out-of-plane bending (E_o) coordinate calculates the forces for trigonal centers which consists in four atoms with three valence bonds formed to one center atom [67]:

$$E_o = \frac{1}{2} k_o \gamma_o^2 \tag{A.4}$$

where,

k_o is the force constant related to the out-of-plane angle deformation (mdyne*Å/rad^2); and γ_o is an average of the three angles associated with the out-of-plane center (°).

A.2. Non-bonded terms

The nonbonded terms depend on the electrostatic partial charges and on the van der Waals potentials.

The dispersion-repulsion energy between two force centers is represented by the Lennard-Jones (LJ) potential [67]:

$$E_{vdW} = \varepsilon \left[1.84 x 10^5 \, exp \left(\left(-12 \frac{\sigma_{ij}}{r_{ij}} \right) - 2.25 \left(\frac{\sigma_{ij}}{r_{ij}} \right)^6 \right) \right] \tag{A.5}$$

where,

ε_{ij} refers to the polarizability of the atoms and describes the strength of the interaction between two atoms considered and it is the van der Waals minimum energy value (kcal/mol); σ_{ij} is the distance at which the potential energy is equal to zero (Å); and r_{ij} is the distance of the two atoms of interaction (Å).

In the case of binary interactions involving different force centers i and j like cross term pairwise Lennard-Jones interactions, Lorentz–Berthelot combination rules (arithmetic mean for minimum distance and geometric mean for the well depth of non-equal atom pairs) are used to improve the agreement with the reference vibrational frequencies [67]:

$$\varepsilon_{ij} = \sqrt{\varepsilon_i \varepsilon_j} \quad \& \quad \sigma_{ij} = \frac{\sigma_i + \sigma_j}{2}$$

The Coulomb interaction term is described as follows assuming that the molecules bear electrostatic point charges, measuring the effect of a charge between two points [95]:

$$E_{electrostatic} = \Sigma_{ij} \frac{q_i q_j}{4 \pi \varepsilon_0 r_{ij}} \tag{A.6}$$

where,

r_{ij} is the distance generated by the interaction of two atoms (i and j) due to the attractive-repulsive forces (Å); ε_0 is the permittivity of vacuum (e); and q_i and q_j are the partial atomic charges of the given atom pair i and j (e).

APPENDIX B. MOLECULAR STRUCTURES OF N_2O AND ZIF-8

B.1. Nitrous oxide (N_2O)
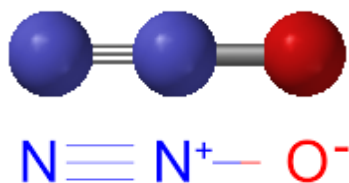
Figure A.1 Molecular structure of N_2O and its chemical structure. Nitrogen in blue; Oxygen in red.

B.2. Zeolitic Imidazolate Framework-8 (ZIF-8)
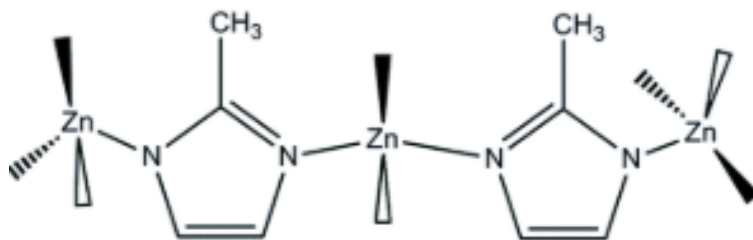
Figure A.2 Chemical structure of ZIF-8.
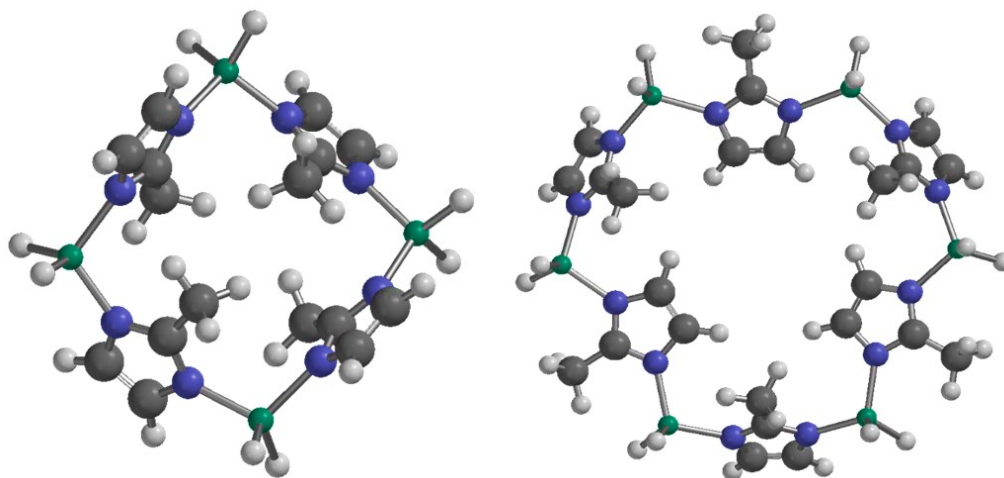
Figure A.3 Small pore (left) and big pore (right) of ZIF-8. Nitrogen in blue; Carbon in gray; Hydrogen in white; Zinc in green.

B.3. Segment of Zeolitic Imidazolate Framework-8 (ZIF-8)

a)

b)
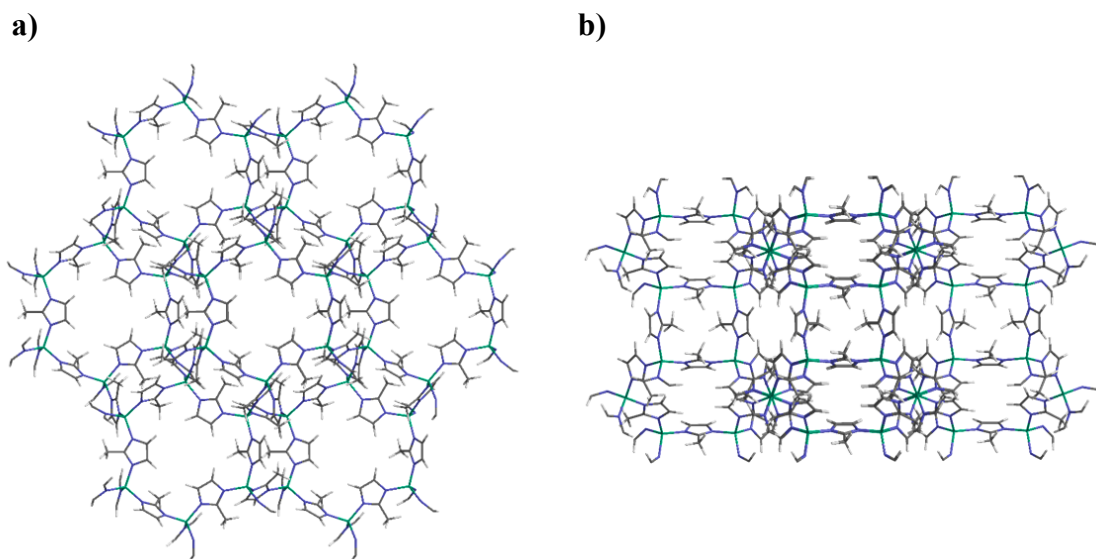
Figure A.4 Molecular structure of a ZIF-8 segment; (a) Front view, (b) Side view. Nitrogen in blue; Carbon in gray; Hydrogen in white; Zinc in green.

APPENDIX C. ADSORPTION CONFIGURATION AND SITES

C.1. N₂O adsorption configuration
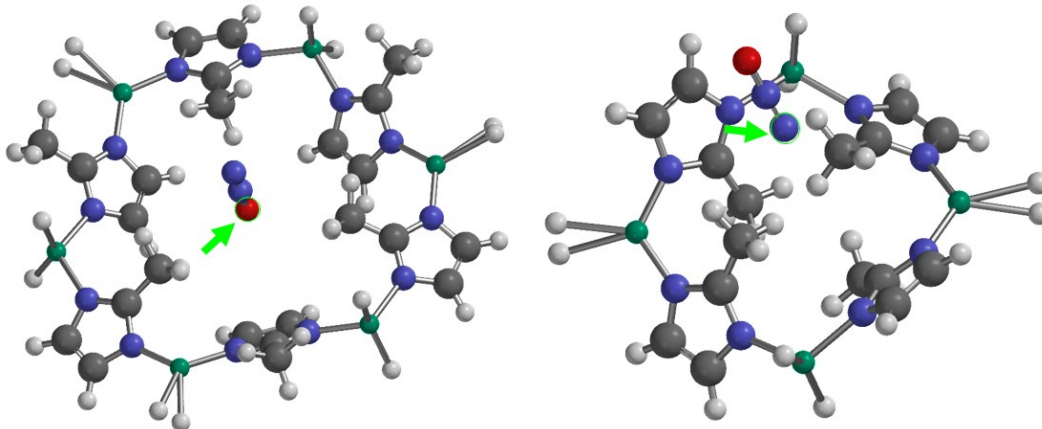
Figure A.5 Adsorption configuration of N_2O from –ONN end (left) or from –NNO end (right). The arrow indicates the atom by which the N_2O is adsorbed. Nitrogen in blue; Carbon in gray; Oxygen in red; Hydrogen in white; Zinc in green.

C.2. Adsorption sites in small and big pore of ZIF-8
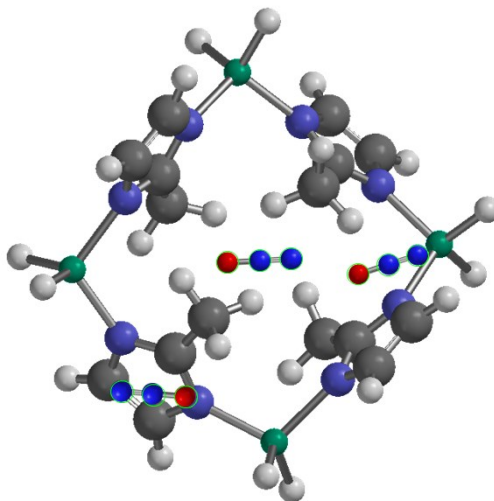
Figure A.6 Adsorption sites in small pore of ZIF-8: Center, Side and Methylcenter. Nitrogen in blue; Carbon in gray; Oxygen in red; Hydrogen in white; Zinc in green.
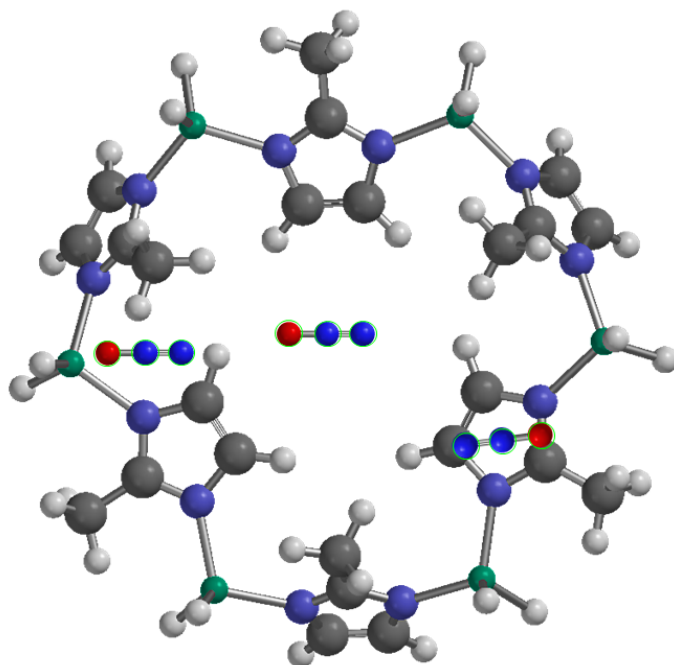
Figure A.7 Adsorption sites in big pore of ZIF-8: Center, Side and Methylcenter. Nitrogen in blue; Carbon in gray; Oxygen in red; Hydrogen in white; Zinc in green.

APPENDIX D. QUANTUM MECHANICS SIMULATION TOOLS

D.1. Define ligand point
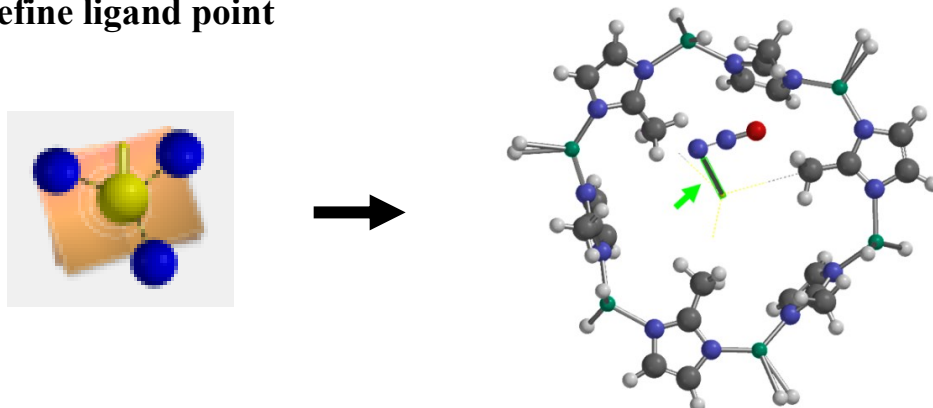
Figure A.8 Define ligand point tool (left) to simulate a physical adsorption and its application (right). The arrow indicates the ligan point.

D.2. Frozen atom
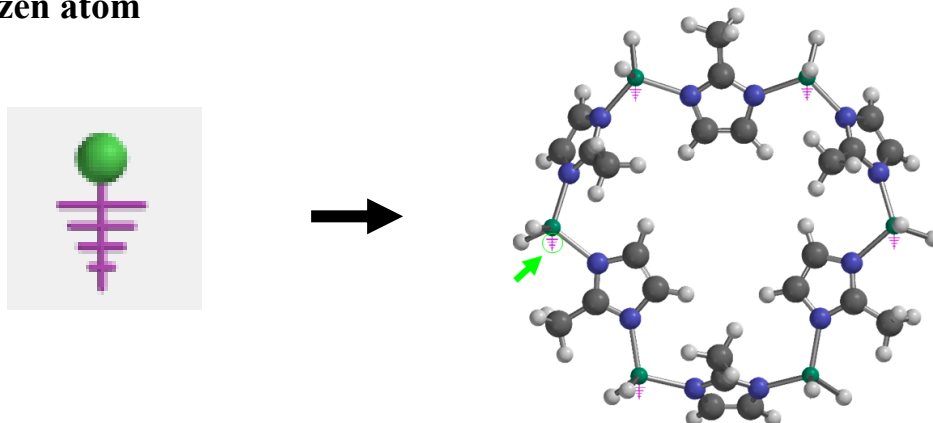
Figure A.9 Frozen atom tool (left) and its application during simulations (right). The arrow indicates how a frozen atom is identified.

D.3. Constraint distance and constraint angle
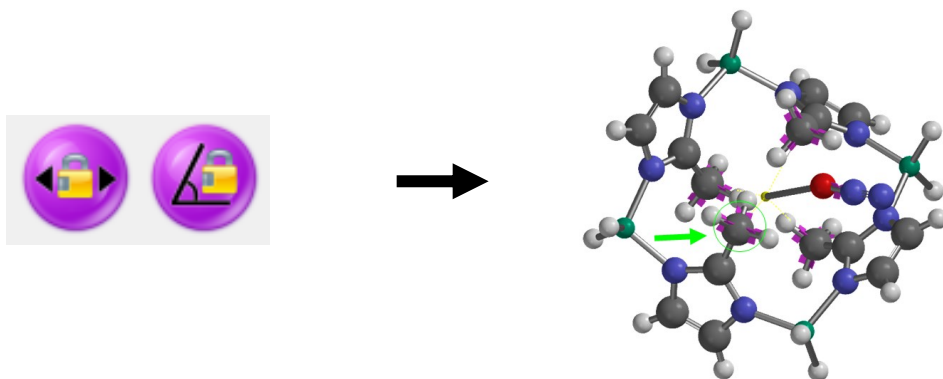
Figure A.10 Constraint distance and angle tools (left) and their application during simulations (right). The arrow indicates how a constraint atom is identified.

APPENDIX E. SYNTHESIS OF ZIF-8

E.1. Solvothermal synthesis of ZIF-8

Zinc nitrate hexahydrate (0.66 g of Zn $(NO_3)_2 \cdot 6H_2O$, 98 % Sigma-Aldrich) was dissolved by stirring in 28 ml of methanol (MeOH, 99.9 % Thermo Fisher Scientific). The compound 2-methylimidazole (1.20 g of 2-mIm, 97 % Sigma-Aldrich) was dissolved by stirring it in 28 ml of methanol. After 5 min, both solutions were mixed and stirred for 1 h (at a stirring rate of 640 rpm) and aging without stirring for 1 h at room temperature (298 ± 5 K). For solvothermal synthesis, the precursor solution was transferred in an autoclave and heated at 423 K for 5 h. ZIF-8 crystals were washed with MeOH and collected by centrifugation (4500 rpm for 20 min) three times. The crystals were dried at 353 K over-night [112].

APPENDIX F. FORCE FIELD PARAMETERS

F.1. MM3-MOF force field parameters for ZIF-8 [98]:

Table A.1 Atom type definition for ZIF-8.

Atom types		Atomic number	Atom mass (mol)	Valence electron
Zn	800	30	65.387	4
C3	801	6	12.000	4
H3	802	1	1.0080	1
H1	803	1	1.0080	1
N1	804	7	14.001	3
C2	805	6	12.000	3
C1	806	6	12.000	3
N2	814	7	14.001	2

Table A.2 Bond stretching parameters for ZIF-8.

Bond types		k_b (mdyne/Å)	r_b (Å)
C2-C3	805-801	5.293	1.489
C1-C1	806-806	7.392	1.386
C3-H3	801-802	4.998	1.100
N1-Zn	804-800	1.576	1.985
C1-N1	806-804	6.135	1.387
C1-H1	806-803	5.300	1.102
C2-N1	805-804	6.410	1.363
C1-C1	806-806	7.392	1.386
C1-N1	806-804	6.135	1.387
C2-N1	805-804	6.410	1.363

Table A.3 Angle bending parameters for ZIF-8.

Angle types		k_a (mdyne*Å/rad^2)	θ_a (°)
N1-C2-N1	804-805-804	1.507	122.584
N1-Zn-N1	804-800-804	0.208	109.471
H3-C3-H3	802-801-802	0.599	107.965
C2-N1-Zn	805-804-800	$6.252 \times 10^{-5} \approx 0$	114.814
C1-N1-Zn	806-804-800	0.065	154.547
C1-C1-H1	806-806-803	0.175	145.200
C1-C1-N1	806-806-804	1.485	105.865
C2-C3-H3	805-801-802	0.599	110.940
C3-C2-N1	801-805-804	0.599	124.160
H1-C1-N1	803-806-804	0.413	127.823
C1-N1-C2	806-804-805	1.282	106.203
N1-C2-N1	804-805-804	1.507	122.584
C1-C1-N1	806-806-804	1.485	105.865
C1-N1-C2	806-804-805	1.282	106.203

Table A.4 Dihedral torsions parameters for ZIF-8.

Dihedral types		V_1 (kcal/mol)	V_2 (kcal/mol)	V_3 (kcal/mol)
C1-C1-N1-C2	806-806-804-805	0.0	22.803	0.000
H1-C1-N1-C2	803-806-804-805	0.0	15.487	0.000
C3-C2-N1-C1	801-805-804-806	0.0	7.7450	0.000
N1-C1-C1-N1	804-806-806-804	0.0	25.692	0.000
N1-C2-N1-Zn	804-805-804-800	0.0	0.0060	0.000
H1-C1-C1-H1	803-806-806-803	0.0	0.2040	0.000
N1-C2-C3-H3	804-805-801-802	0.0	0.0000	0.000
H1-C1-N1-Zn	803-806-804-800	0.0	0.0270	0.000
C1-N1-Zn-N1	806-804-800-804	0.0	0.0000	-0.153
C2-N1-Zn-N1	805-804-800-804	0.0	0.0000	-0.900
C3-C2-N1-Zn	801-805-804-800	0.0	0.3400	0.000
N1-C2-N1-C1	804-805-804-806	0.0	10.010	0.000

C1-C1-N1-Zn	806-806-804-800	0.0	4.9210	0.000
H1-C1-C1-N1	803-806-806-804	0.0	1.0060	0.000
C1-N1-Zn-N2	806-804-800-814	0.0	0.0000	-0.153
C2-N1-Zn-N2	805-804-800-814	0.0	0.0000	-0.900
C1-C1-N1-C2	806-806-804-805	0.0	22.803	0.000
N1-C1-C1-N1	804-806-806-804	0.0	25.692	0.000
N1-C2-N1-C1	804-805-804-806	0.0	10.010	0.000

Table A.5 Out-of-plane angle parameters for ZIF-8.

Out-of-plane types		k_o (mdyne*Å/rad^2)	γ_o (°)
C2-C3-N1-N1	805-801-804-804	0.692	0.0
N1-C1-C2-Zn	804-806-805-800	$1.049\times10^{-3} \approx 0$	0.0
C1-C1-H1-N1	806-806-803-804	$2.640\times10^{-4} \approx 0$	0.0
N1-C1-C1-H1	804-806-806-803	$2.640\times10^{-4} \approx 0$	0.0
H1-C1-C1-N1	803-806-806-804	$2.640\times10^{-4} \approx 0$	0.0

Table A.6 Van der Waals potentials of ZIF-8.

Atom types		Leonard-Jones parameters	
		Radii r_{ij} (Å)	Energy ϵ (kcal/mol)
Zn	800	2.29	0.760
C3	801	2.04	0.027
H3	802	1.50	0.020
H1	803	1.50	0.020
N1	804	1.93	0.043
C2	805	1.96	0.056
C1	806	1.96	0.056
N2	814	1.93	0.043

Table A.7 Partial electron charges of ZIF-8.

Atom types		q (e)
Zn	800	0.7365
C3	801	-0.5201
H3	802	0.1448
H1	803	0.1695
N1	804	-0.3342
C2	805	0.5012
C1	806	-0.1848
N2	814	-0.3342

F.2. MM3-MOF force field parameters for cut-off ends of ZIF-8 [98]:

Table A.8 Atom type definition for the cut-off ends of ZIF-8.

Atom types		Atomic number	Atom mass (mol)	Valence electron
C4	816	6	12.000	2
H4	817	1	1.0080	1

Table A.9 Bond stretching parameters for the cut-off ends of ZIF-8.

Bond types		k_b (mdyne/Å)	r_b (Å)
C4-N1	816-804	6.272	1.375
C4-H4	816-817	5.300	1.102
N2-Zn	814-800	1.576	1.985
C4-N2	816-814	6.272	1.375

Table A.10 Angle bending parameters for the cut-off ends of ZIF-8.

Angle types		k_a (mdyne*Å/rad²)	θ_a (°)
C4-N1-Zn	816-804-800	0.032	134.680
H4-C4-N1	817-816-804	0.413	127.823
C4-N1-C4	816-804-816	1.282	106.203
N2-Zn-N1	814-800-804	0.208	109.471
C4-N2-Zn	816-814-800	0.032	134.680

H4-C4-N2	817-816-814	0.413	127.823
N2-Zn-N2	814-800-814	0.208	109.471

Table A.11 Dihedral torsions parameters for the cut-off ends of ZIF-8.

Dihedral types		V_1 (kcal/mol)	V_2 (kcal/mol)	V_3 (kcal/mol)
H4-C4-N1-Zn	817-816-804-800	0.0	0.0270	0.000
H4-C4-N1-C4	817-816-804-816	0.0	15.487	0.000
C4-N1-Zn-N1	816-804-800-804	0.0	0.0000	-0.153
H4-C4-N2-Zn	817-816-814-800	0.0	0.0270	0.000
C4-N2-Zn-N1	816-814-800-804	0.0	0.0000	-0.153
C4-N2-Zn-N2	816-814-800-814	0.0	0.0000	-0.153
C4-N1-Zn-N2	816-804-800-814	0.0	0.0000	-0.153

Table A.12 Out-of-plane angle parameters for the cut-off ends of ZIF-8.

Out-of-plane types		k_o (mdyne*Å/rad^2)	γ_o (°)
C2-C3-N1-N1	805-801-804-804	0.692	0.0

Table A.13 Van der Waals potentials for the cut-off ends of ZIF-8.

Atom types		Leonard-Jones parameters	
		Radii r_{ij} (Å)	Energy ϵ (kcal/mol)
C4	816	1.96	0.056
H4	817	1.50	0.020

Table A.14 Partial electron charges for the cut-off ends of ZIF-8.

Atom types		q (e)
C4	816	0.0075
H4	817	0.0075

F.3. TraPPE force field parameters for CO_2, CH_4 and N_2O [7], [100]:

Table A.15 Atom types for CO_2, CH_4 and N_2O.

Gas	Atom types		Atomic number	Atom mass (mol)	Valence electron
CO_2	O	607	8	15.999	1
	C	606	6	12.000	2
	O	607	8	15.999	1
CH_4	C	501	6	12.000	4
	H	505	1	1.0080	1
N_2O	N2	710	7	14.001	1
	N1	745	7	14.001	2
	O	769	8	15.999	1

Table A.16 Bond stretching parameters for CO_2, CH_4 and N_2O.

Gas	Bond types		k_b (mdyne/Å)		r_b (Å)
			MM3 FF	Calculated	
CO_2	O-C	607-606	10.500	-	1.160
CH_4	C-H	501-505	4.7401	-	1.0912
N_2O	N2-N1	710-745	17.330	19.253	1.1282
	N1-O	745-769	8.800	10.417	1.1842

Table A.17 Angle bending parameters for CO_2, CH_4 and N_2O.

Gas	Angle types		k_a (mdyne*Å/rad^2)	θ_a (°)
			MM3 FF	
CO_2	O-C-O	607-606-607	0.700	180.00
CH_4	H-C-H	505-501-505	0.550	109.47
N_2O	N2-N1-O	710-745-769	0.700	180.00

Table A.18 Van der Waals potentials of CO_2, CH_4 and N_2O.

Gas	Atom types		Leonard-Jones parameters	
			Radii r_{ij} (Å)	Energy ϵ (kcal/mol)
CO₂	O	607	3.050	0.1569
	C	606	2.800	0.0536
	O	607	3.050	0.1569
CH₄	C	501	-0.2400	-0.8940
	H	505	0.0600	0.2230
N₂O	N2	710	3.120	0.1573
	N1	745	2.800	0.0536
	O	769	3.050	0.1569

Table A.19 Partial electron charges of CO_2, CH_4 and N_2O.

Gas	Atom types		q (e)	
			Literature [7], [100]	Calculated
CO₂	O	607	-0.3500	-0.3680
	C	606	0.7000	0.7360
	O	607	-0.3500	-0.3680
CH₄	C	501	3.500	0.0660
	H	505	2.500	0.0300
N₂O	N2	710	-0.3630	-0.3370
	N1	745	0.7130	0.6990
	O	769	-0.3500	-0.3620

LIST OF REFERENCES

[1] A. Simsar and Y. Doğan, "Investigation of Preservice Preschool Teachers Views on Environmental Problems and Relevant Suggestions of Solution," *iejee*, vol. 11, no. 2, pp. 151–159, Jul. 2019, doi: 10.26822/iejee.2019248589.

[2] L. H. Udara Willhelm Abeydeera, J. Wadu Mesthrige, and T. I. Samarasinghalage, "Global Research on Carbon Emissions: A Scientometric Review," *Sustainability*, vol. 11, no. 14, p. 3972, Jul. 2019, doi: 10.3390/su11143972.

[3] A. E. Creamer and B. Gao, "Overview of Greenhouse Gases and Global Warming," in *Carbon Dioxide Capture: An Effective Way to Combat Global Warming*, Cham: Springer International Publishing, 2015, pp. 1–15. doi: 10.1007/978-3-319-17010-7_1.

[4] S. Piippo, M. Lauronen, and H. Postila, "Greenhouse gas emissions from different sewage sludge treatment methods in north," *Journal of Cleaner Production*, vol. 177, pp. 483–492, Mar. 2018, doi: 10.1016/j.jclepro.2017.12.232.

[5] World Meteorological Organization & Global Atmospheres Watch, "The State of Greenhouse Gases in the Atmosphere Based on Global Observations through 2019." *World Meteorological Organization and World Data Centre for Greenhouse Gases*, vol. 16, Nov. 2020.

[6] J. C. Groen, J. Pérez-Ramírez, and W. Zhu, "Adsorption of Nitrous Oxide on Silicalite-1," *J. Chem. Eng. Data*, vol. 47, no. 3, pp. 587–589, May 2002, doi: 10.1021/je015527l.

[7] N. Hansen, F. A. B. Agbor, and F. J. Keil, "New force fields for nitrous oxide and oxygen and their application to phase equilibria simulations," *Fluid Phase Equilibria*, vol. 259, no. 2, pp. 180–188, Oct. 2007, doi: 10.1016/j.fluid.2007.07.014.

[8] Q. Guo, L. Chen, S. Kutsuna, H. Quan, and J. Mizukado, "Atmospheric Chemistry of Perfluoronitriles: Environmental Impact and Experimental Evidence Related to N_2O and NO Formation," *Atmospheric Environment*, vol. 198, pp. 175–182, Feb. 2019, doi: 10.1016/j.atmosenv.2018.10.066.

[9] United Nations & Framework Convention on Climate Change, "National greenhouse gas inventory data for the period 1990–2016," *United Nations Climate Change*, 2018.

[10] D.-L. Chen, N. Wang, F.-F. Wang, J. Xie, Y. Zhong, W. Zhu, J. K. Johnson, and R. Krishna, "Utilizing the Gate-Opening Mechanism in ZIF-7 for Adsorption Discrimination between N_2O and CO_2," *J. Phys. Chem. C*, vol. 118, no. 31, pp. 17831–17837, Aug. 2014, doi: 10.1021/jp5056733.

[11] S. Hadi, M. Al-Mashhadani, and M. Eisa, "Optimization of Dye Adsorption Process for Albizia Lebbeck Pods as A Biomass Using Central Composite Rotatable Design Model," *CI&CEQ*, vol. 25, no. 1, pp. 39–46, 2019, doi: 10.2298/CICEQ180210021H.

[12] P. Pullumbi, F. Brandani, and S. Brandani, "Gas Separation by Adsorption: Technological Drivers and Opportunities for Improvement," *Current Opinion in Chemical Engineering*, vol. 24, pp. 131–142, Jun. 2019, doi: 10.1016/j.coche.2019.04.008.

[13] X. Gong, Y. Wang, and T. Kuang, "ZIF-8-Based Membranes for Carbon Dioxide Capture and Separation," *ACS Sustainable Chem. Eng.*, vol. 5, no. 12, pp. 11204–11214, Dec. 2017, doi: 10.1021/acssuschemeng.7b03613.

[14] D. J. Babu and J. J. Schneider, "Gas Adsorption Studies of CO_2 in Carbon Nanomaterials: A Case Study of Vertically Aligned Carbon Nanotubes," *Chemie Ingenieur Technik*, vol. 89, no. 10, pp. 1273–1287, 2017, doi: 10.1002/cite.201700099.

[15] S. Sircar, "Publications on Adsorption Science and Technology," *Adsorption*, vol. 6, pp. 359–365, 2000.

[16] S. Weinberger, A. Pellis, J. Comerford, T. Farmer, and G. Guebitz, "Efficient Physisorption of Candida Antarctica Lipase B on Polypropylene Beads and Application for Polyester Synthesis," *Catalysts*, vol. 8, no. 9, p. 369, Aug. 2018, doi: 10.3390/catal8090369.

[17] L. Sun, L. Yang, Y.-D. Zhang, Q. Shi, R.-F. Lu, and W.-Q. Deng, "Accurate Van Der Waals Force Field for Gas Adsorption in Porous Materials," *J. Comput. Chem.*, vol. 38, no. 23, pp. 1991–1999, Sep. 2017, doi: 10.1002/jcc.24832.

[18] T. Shimonishi, N. Nakatani, K. Furuya, and T. Hama, "Adsorption Energies of Carbon, Nitrogen, and Oxygen Atoms on the Low-Temperature Amorphous Water Ice: A Systematic Estimation from Quantum Chemistry Calculations," *ApJ*, vol. 855, no. 1, p. 27, Mar. 2018, doi: 10.3847/1538-4357/aaaa6a.

[19] A. Kiejna and T. Pabisiak, "Effect of Substrate Relaxation on Adsorption Energies: The Example of A-Fe$_2$O$_3$(0001) and Fe$_3$O$_4$(111)," *Surface Science*, vol. 679, pp. 225–229, Jan. 2019, doi: 10.1016/j.susc.2018.09.017.

[20] P. S. Schmidt and K. S. Thygesen, "Benchmark Database of Transition Metal Surface and Adsorption Energies from Many-Body Perturbation Theory," *J. Phys. Chem. C*, vol. 122, no. 8, pp. 4381–4390, Mar. 2018, doi: 10.1021/acs.jpcc.7b12258.

[21] B. Chen, Z. Yang, Y. Zhu, and Y. Xia, "Zeolitic Imidazolate Framework Materials: Recent Progress in Synthesis and Applications," *J. Mater. Chem. A*, vol. 2, no. 40, pp. 16811–16831, 2014, doi: 10.1039/C4TA02984D.

[22] A. Baldermann, A. C. Grießbacher, C. Baldermann, B. Purgstaller, I. Letofsky-Papst, S. Kaufhold, and M. Dietzel, "Removal of Barium, Cobalt, Strontium, and Zinc from Solution by Natural and Synthetic Allophane Adsorbents," *Geosciences*, vol. 8, no. 9, p. 309, Aug. 2018, doi: 10.3390/geosciences8090309.

[23] Y. Ban, Y. Li, Y. Peng, H. Jin, W. Jiao, X. Liu, and W. Yang, "Metal-Substituted Zeolitic Imidazolate Framework ZIF-108: Gas-Sorption and Membrane-Separation Properties," *Chem. Eur. J.*, vol. 20, no. 36, pp. 11402–11409, Sep. 2014, doi: 10.1002/chem.201402287.

[24] S. Bhattacharjee, M.-S. Jang, H.-J. Kwon, and W.-S. Ahn, "Zeolitic Imidazolate Frameworks: Synthesis, Functionalization, and Catalytic/Adsorption Applications," *Catal Surv Asia*, vol. 18, no. 4, pp. 101–127, Dec. 2014, doi: 10.1007/s10563-014-9169-8.

[25] G. D. Barbosa, L. Travalloni, F. W. Tavares, and M. Castier, "Adsorption of Gases on Zeolitic Imidazolate Frameworks: Modeling with Equations of State for Confined Fluids and Pore Size Distribution Estimation," *Ind. Eng. Chem. Res.*, vol. 58, no. 42, pp. 19702–19708, Oct. 2019, doi: 10.1021/acs.iecr.9b05221.

[26] A. Gotzias, "The Effect of gme Topology on Multicomponent Adsorption on Zeolitic Imidazolate Frameworks," *Phys. Chem. Chem. Phys.*, vol. 19, no. 1, pp. 871–877, 2017, doi: 10.1039/C6CP06036F.

[27] L. S. Lai, Y. F. Yeong, N. C. Ani, K. K. Lau, and A. M. Shariff, "Effect of Synthesis Parameters on the Formation of Zeolitic Imidazolate Framework 8 (ZIF-8) Nanoparticles for CO_2 Adsorption," *Particulate Science and Technology*, vol. 32, no. 5, pp. 520–528, Sep. 2014, doi: 10.1080/02726351.2014.920445.

[28] M. Askari and T.-S. Chung, "Natural Gas Purification and Olefin/Paraffin Separation Using Thermal Cross-Linkable Co-Polyimide/ZIF-8 Mixed Matrix Membranes," *Journal of Membrane Science*, vol. 444, pp. 173–183, Oct. 2013, doi: 10.1016/j.memsci.2013.05.016.

[29] H. Bux, F. Liang, Y. Li, J. Cravillon, M. Wiebcke, and J. Caro, "Zeolitic Imidazolate Framework Membrane with Molecular Sieving Properties by Microwave-Assisted

Solvothermal Synthesis," *J. Am. Chem. Soc.*, vol. 131, no. 44, pp. 16000–16001, Nov. 2009, doi: 10.1021/ja907359t.

[30] D. S. Sholl and J. A. Steckel, *Density Functional Theory*. Hoboken, NJ, USA: John Wiley & Sons, Inc., 2009. doi: 10.1002/9780470447710.

[31] R. Cantudo Agudo, *Preliminary approach to molecular simulation in the field of chemical engineering*. México: Fondo de Cultura Económica, 2018.

[32] D. C. Young, *Computational Chemistry: A Practical Guide for Applying Techniques to Real World Problems*. John Wiley & Sons, Inc., 2001.

[33] B. Zhang, G. He, Y. Shan, and H. He, "Experimental and DFT Study of The Adsorption of N_2O on Transition Ion-Exchanged ZSM-5," *Catalysis Today*, vol. 327, pp. 177–181, May 2019, doi: 10.1016/j.cattod.2018.05.008.

[34] S. Pabchanda, P. Pantu, D. Tantanak, and J. Limtrakul, "Structure and Energetics of Nitrous Oxide and Methane Adsorption on the Fe-ZSM-5 Zeolite: Oniom And Density Functional Studies," in *Studies in Surface Science and Catalysis*, vol. 154, Elsevier, 2004, pp. 1844–1848. doi: 10.1016/S0167-2991(04)80718-3.

[35] M. N. D. Boutarbouch, J. M. G. Cortés, M. S. E. Begrani, C. S. M. de Lecea, and J. Pérez-Ramírez, "Catalytic Conversion of N_2O Over Fezsm-5 Zeolite in the Presence of CO and NO," *Applied Catalysis B: Environmental*, vol. 54, no. 2, pp. 115–123, Dec. 2004, doi: 10.1016/j.apcatb.2004.06.013.

[36] V. N. Solkan, G. M. Zhidomirov, and V. B. Kazansky, "Density Functional Theory Studies of Nitrous Oxide Adsorption and Decomposition on Ga-ZSM-5," *Int. J. Quantum Chem.*, vol. 107, no. 13, pp. 2417–2425, 2007, doi: 10.1002/qua.21375.

[37] B. Zhang, Y. Lu, H. He, J. Wang, C. Zhang, Y. Yu, and L. Xue, "Experimental and Density Functional Theory Study of the Adsorption of N_2O on Ion-Exchanged ZSM-5: Part II. The Adsorption of N_2O on Main-Group Ion-Exchanged ZSM-5," *Journal of Environmental Sciences*, vol. 23, no. 4, pp. 681–686, Apr. 2011, doi: 10.1016/S1001-0742(10)60482-2.

[38] T. Maihom, S. Wannakao, B. Boekfa, and J. Limtrakul, "Density Functional Study of the Activity of Gold-Supported ZSM-5 Zeolites for Nitrous Oxide Decomposition," *Chemical Physics Letters*, vol. 556, pp. 217–224, Jan. 2013, doi: 10.1016/j.cplett.2012.11.058.

[39] Y. Wang, Z. Lei, R. Zhang, and B. Chen, "Adsorption of NO and N_2O on Cu-BEA Zeolite," *Journal of Molecular Structure: THEOCHEM*, vol. 957, no. 1–3, pp. 41–46, Oct. 2010, doi: 10.1016/j.theochem.2010.07.004.

[40] N. Liu, R. Zhang, B. Chen, Y. Li, and Y. Li, "Comparative Study on the Direct Decomposition of Nitrous Oxide Over M (Fe, Co, Cu)–BEA Zeolites," *Journal of Catalysis*, vol. 294, pp. 99–112, Oct. 2012, doi: 10.1016/j.jcat.2012.07.008.

[41] S.-Y. Wu, C.-H. Su, J.-G. Chang, H.-T. Chen, C.-H. Hou, and H.-L. Chen, "Adsorption and Dissociation of N_2O Molecule on Fe(111) Surface: A DFT Study," *Computational Materials Science*, vol. 50, no. 12, pp. 3311–3314, Dec. 2011, doi: 10.1016/j.commatsci.2011.06.021.

[42] J. Beheshtian, M. T. Baei, A. A. Peyghan, and Z. Bagheri, "Nitrous Oxide Adsorption on Pristine and Si-Doped AlN Nanotubes," *J Mol Model*, vol. 19, no. 2, pp. 943–949, Feb. 2013, doi: 10.1007/s00894-012-1634-6.

[43] M. Yoosefian, "Powerful Greenhouse Gas Nitrous Oxide Adsorption onto Intrinsic and Pd Doped Single Walled Carbon Nanotube," *Applied Surface Science*, vol. 392, pp. 225–230, Jan. 2017, doi: 10.1016/j.apsusc.2016.09.051.

[44] R. Hernández Huesca, J. Pérez Arcos, D. Vargas Hernández, and M. A. Pérez Cruz, "Adsorption Kinetics of N_2O on Natural Zeolites," *Rev. Int. Contam. Ambie.*, vol. 32, no. 2, pp. 237–242, May 2016, doi: 10.20937/RICA.2016.32.02.09.

[45] A. Shokuhi Rad, "DFT Study of Nitrous Oxide Adsorption on the Surface of Pt-Decorated Graphene," *PCR*, no. 4, Dec. 2016, doi: 10.22036/pcr.2016.16428.

[46] R. Gholizadeh, Y.-X. Yu, and Y. Wang, "N_2O Adsorption and Decomposition over Zno(0001) Doped Graphene: Density Functional Theory Calculations," *Applied Surface Science*, vol. 420, pp. 944–953, Oct. 2017, doi: 10.1016/j.apsusc.2017.05.235.

[47] D. Fairen-Jimenez, R. Galvelis, A. Torrisi, A. D. Gellan, M. T. Wharmby, P. A. Wright, C. Mellot-Draznieks, and T. Düren, "Flexibility and Swing Effect on the Adsorption of Energy-Related Gases on ZIF-8: Combined Experimental and Simulation Study," *Dalton Trans.*, vol. 41, no. 35, p. 10752, 2012, doi: 10.1039/c2dt30774j.

[48] Y. Hu, Z. Liu, J. Xu, Y. Huang, and Y. Song, "Evidence of Pressure Enhanced CO_2 Storage in ZIF-8 Probed by FTIR Spectroscopy," *J. Am. Chem. Soc.*, vol. 135, no. 25, pp. 9287–9290, Jun. 2013, doi: 10.1021/ja403635b.

[49] H. Huang, W. Zhang, D. Liu, B. Liu, G. Chen, and C. Zhong, "Effect of Temperature on Gas Adsorption and Separation in ZIF-8: A Combined Experimental and Molecular Simulation Study," *Chemical Engineering Science*, vol. 66, no. 23, pp. 6297–6305, Dec. 2011, doi: 10.1016/j.ces.2011.09.009.

[50] A. A. Jameh, T. Mohammadi, O. Bakhtiari, and M. Mahdyarfar, "Synthesis and Modification of Zeolitic Imidazolate Framework (ZIF-8) Nanoparticles as Highly Efficient Adsorbent for H_2S and CO_2 Removal from Natural Gas," *Journal of Environmental Chemical Engineering*, vol. 7, no. 3, p. 103058, Jun. 2019, doi: 10.1016/j.jece.2019.103058.

[51] C. L. Hobday, C. H. Woodall, M. J. Lennox, M. Frost, K. Kamenev, T. Düren, C. A. Morrison and S. A. Moggach, "Understanding the Adsorption Process in ZIF-8 Using High Pressure Crystallography and Computational Modelling," *Nat Commun*, vol. 9, no. 1, p. 1429, Dec. 2018, doi: 10.1038/s41467-018-03878-6.

[52] M. Fischer and R. G. Bell, "Interaction of Hydrogen and Carbon Dioxide with Sod-Type Zeolitic Imidazolate Frameworks: A Periodic DFT-D Study," *CrystEngComm*, vol. 16, no. 10, p. 1934, 2014, doi: 10.1039/c3ce42209g.

[53] J.-W. Wang, N.-X. Li, Z.-R. Li, J.-R. Wang, X. Xu, and C.-S. Chen, "Preparation and Gas Separation Properties of Zeolitic Imidazolate Frameworks-8 (ZIF-8) Membranes Supported on Silicon Nitride Ceramic Hollow Fibers," *Ceramics International*, vol. 42, no. 7, pp. 8949–8954, May 2016, doi: 10.1016/j.ceramint.2016.02.153.

[54] P. Kanthima, P. Puphasuk, and T. Remsungnen, "Intermolecular Force Field Parameters Optimization for Computer Simulations of CH_4 in ZIF-8," *Journal of Nanotechnology*, vol. 2016, pp. 1–6, 2016, doi: 10.1155/2016/3926089.

[55] Z. Zhang, S. Xian, Q. Xia, H. Wang, Z. Li, and J. Li, "Enhancement of CO_2 Adsorption and CO_2/N_2 Selectivity on ZIF-8 via Postsynthetic Modification," *AIChE J.*, vol. 59, no. 6, pp. 2195–2206, Jun. 2013, doi: 10.1002/aic.13970.

[56] J. Zhu, L. Jiang, C. Dai, N. Yang, and Z. Lei, "Gas Adsorption in Shaped Zeolitic Imidazolate Framework-8," *Chinese Journal of Chemical Engineering*, vol. 23, no. 8, pp. 1275–1282, Aug. 2015, doi: 10.1016/j.cjche.2015.01.015.

[57] K. Roy, S. Kar, and R. N. Das, "Computational Chemistry," in *Understanding the Basics of QSAR for Applications in Pharmaceutical Sciences and Risk Assessment*, Elsevier, 2015, pp. 151–189. doi: 10.1016/B978-0-12-801505-6.00005-3.

[58] J. Jiang and S. I. Sandler, "Separation of CO_2 and N_2 by Adsorption in C_{168} Schwarzite: A Combination of Quantum Mechanics and Molecular Simulation Study," *J. Am. Chem. Soc.*, vol. 127, no. 34, pp. 11989–11997, Aug. 2005, doi: 10.1021/ja0424575.

[59] J. Harvey, *Computational Chemistry*. Oxford University Press, no. 23, p. 139, 2018.

[60] M. Tuckerman, *Statistical Mechanics: Theory and Molecular Simulation*. Oxford University Press (OUP), p. 696, 2010.

[61] E. Paquet and H. L. Viktor, "Molecular Dynamics, Monte Carlo Simulations, and Langevin Dynamics: A Computational Review," *BioMed Research International*, vol. 2015, pp. 1–18, 2015, doi: 10.1155/2015/183918.

[62] D. Frenkel, Introduction to Monte Carlo Methods, *Computational soft matter: from synthetic polymers to proteins,* NIC, vol. 22, Jul. 2004.

[63] J. A. Bueren-Calabuig, "17 - Dinámica molecular," *Bioinformática con Ñ*. Zenodo, 2014, doi: 10.5281/zenodo.1066360

[64] W. J. Hehre, *A guide to molecular mechanics and quantum chemical calculations*. Irvine, CA: Wavefunction, Inc, 2003.

[65] J. J. P. Stewart, "Application of the PM6 Method to Modeling Proteins," *J Mol Model*, vol. 15, no. 7, pp. 765–805, Jul. 2009, doi: 10.1007/s00894-008-0420-y.

[66] O. Srihakulung, R. Maezono, P. Toochinda, W. Kongprawechnon, A. Intarapanich, and and L. Lawtrakul, "Host-Guest Interactions of Plumbagin with β-Cyclodextrin, Dimethyl-β-Cyclodextrin and Hydroxypropyl-β-Cyclodextrin: Semi-Empirical Quantum Mechanical PM6 and PM7 Methods," *Sci. Pharm.*, vol. 86, no. 2, p. 20, May 2018, doi: 10.3390/scipharm86020020.

[67] S. Bureekaew, S. Amirjalayer, M. Tafipolsky, C. Spickermann, T. K. Roy, and R. Schmid, "MOF-FF - A Flexible First-Principles Derived Force Field for Metal-Organic Frameworks: MOF-FF - A Force Field for Metal-Organic Frameworks," *Phys. Status Solidi B*, vol. 250, no. 6, pp. 1128–1141, Jun. 2013, doi: 10.1002/pssb.201248460.

[68] P. Dauber-Osguthorpe and A. T. Hagler, "Biomolecular Force Fields: Where Have We Been, Where Are We Now, Where Do We Need to Go and How Do We Get There?," *J Comput Aided Mol Des*, vol. 33, no. 2, pp. 133–203, Feb. 2019, doi: 10.1007/s10822-018-0111-4.

[69] J. K. Bristow, D. Tiana, and A. Walsh, "Transferable Force Field for Metal–Organic Frameworks from First-Principles: BTW-FF," *J. Chem. Theory Comput.*, vol. 10, no. 10, pp. 4644–4652, Oct. 2014, doi: 10.1021/ct500515h.

[70] J. P. Dürholt, G. Fraux, F.-X. Coudert, and R. Schmid, "Supporting Information: Ab Initio Derived Force fields for Zeolitic Imidazolate Frameworks: MOF-FF for ZIFs," *J. Chem. Theory Comput.*, vol. 15, no. 4, p. 16, Apr. 2019, doi: 10.1021/acs.jctc.8b01041.

[71] D. Dokur and S. Keskin, "Effects of Force Field Selection on the Computational Ranking of MOFs for CO_2 Separations," *Ind. Eng. Chem. Res.*, vol. 57, no. 6, pp. 2298–2309, Feb. 2018, doi: 10.1021/acs.iecr.7b04792.

[72] L. Hertaga, H. Buxb, J. Carob, C. Chmelikd, T. Remsungnenc, M. Knautha and S. Fritzschea, "Diffusion of CH_4 and H_2 in ZIF-8," *Journal of Membrane Science*, vol. 377, no. 1–2, pp. 36-41, Jul. 2011. doi:10.1016/j.memsci.2011.01.019.

[73] D. J. Hardy, J. E. Stone, K. L. Vandivort, D. Gohara, C. Rodrigues, and K. Schulten, "Fast Molecular Electrostatics Algorithms on GPUs," in *GPU Computing Gems Emerald Edition*, Elsevier, 2011, pp. 43–58. doi: 10.1016/B978-0-12-384988-5.00004-8.

[74] I. Dabo, B. Kozinsky, N. E. Singh-Miller, and N. Marzari, "Electrostatics in Periodic Boundary Conditions and Real-Space Corrections," *Phys. Rev. B*, vol. 77, no. 11, p. 115139, Mar. 2008, doi: 10.1103/PhysRevB.77.115139.

[75] T. Vasilevskaya and W. Thiel, "Periodic Boundary Conditions in QM/MM Calculations: Implementation and Tests," *J. Chem. Theory Comput.*, vol. 12, no. 8, pp. 3561–3570, Aug. 2016, doi: 10.1021/acs.jctc.6b00269.

[76] G. Palló, "The Advantage and Disadvantage of Peripheral Ignorance: The Gas Adsorption Controversy," *Ambix*, vol. 57, no. 2, pp. 216–230, Jul. 2010, doi: 10.1179/174582310X12719003720241.

[77] M. Mohamedali, H. Ibrahim, and A. Henni, "Incorporation of Acetate-Based Ionic Liquids into a Zeolitic Imidazolate Framework (ZIF-8) as Efficient Sorbents for Carbon Dioxide Capture," *Chemical Engineering Journal*, vol. 334, pp. 817–828, Feb. 2018, doi: 10.1016/j.cej.2017.10.104.

[78] World Meteorological Organization & Global Atmospheres Watch, "The State of Greenhouse Gases in the Atmosphere Based on Global Observations through 2018." *World Meteorological Organization and World Data Centre for Greenhouse Gases*, vol. 15, Nov. 2019.

[79] J. Saarenheimo, A. J. Rissanen, L. Arvola, H. Nykänen, M. F. Lehmann, and M. Tiirola, "Genetic and Environmental Controls on Nitrous Oxide Accumulation in Lakes," *PLoS ONE*, vol. 10, no. 3, p. e0121201, Mar. 2015, doi: 10.1371/journal.pone.0121201.

[80] C. Zellweger, R. Steinbrecher, O. Laurent, H. Lee, S. Kim, L. Emmenegger, M. Steinbacher, and B. Buchmann, "Recent Advances in Measurement Techniques for Atmospheric Carbon Monoxide and Nitrous Oxide Observations," *Atmos. Meas. Tech.*, vol. 12, no. 11, pp. 5863–5878, Nov. 2019, doi: 10.5194/amt-12-5863-2019.

[81] M. Askari and T.-S. Chung, "Natural Gas Purification and Olefin/Paraffin Separation Using Thermal Cross-Linkable Co-Polyimide/ZIF-8 Mixed Matrix Membranes," *Journal of Membrane Science*, vol. 444, pp. 173–183, Oct. 2013, doi: 10.1016/j.memsci.2013.05.016.

[82] S. O. Odoh, C. J. Cramer, D. G. Truhlar, and L. Gagliardi, "Quantum-Chemical Characterization of the Properties and Reactivities of Metal–Organic Frameworks," *Chem. Rev.*, vol. 115, no. 12, pp. 6051–6111, Jun. 2015, doi: 10.1021/cr500551h.

[83] R. Gholizadeh and Y.-X. Yu, "N_2O + CO Reaction over Si- And Se-Doped Graphenes: An Ab Initio DFT Study," *Applied Surface Science*, vol. 357, pp. 1187–1195, Dec. 2015, doi: 10.1016/j.apsusc.2015.09.163.

[84] Z.-Z. Qiu, Y.-X. Yu, and J.-G. Mi, "Adsorption of Carbon Monoxide on Ag(I)-ZSM-5 Zeolite: An Ab Initio Density Functional Theory Study," *Applied Surface Science*, vol. 258, no. 24, pp. 9629–9635, Oct. 2012, doi: 10.1016/j.apsusc.2012.05.162.

[85] M. F. Fellah and I. Onal, "C–H Bond Activation of Methane on M- and MO-ZSM-5 (M=Ag, Au, Cu, Rh And Ru) Clusters: A Density Functional Theory Study," *Catalysis Today*, vol. 171, no. 1, pp. 52–59, Aug. 2011, doi: 10.1016/j.cattod.2011.04.001.

[86] T. Y. Zakharian and S. R. Coon, "Evaluation of Spartan Semi-Empirical Molecular Modeling Software for Calculations of Molecules on Surfaces: CO Adsorption on Ni(111)," *Computers & Chemistry*, vol. 25, no. 2, pp. 135–144, Mar. 2001, doi: 10.1016/S0097-8485(00)00075-9.

[87] A. Uzun and S. Keskin, "Site Characteristics in Metal Organic Frameworks for Gas Adsorption," *Progress in Surface Science*, vol. 89, no. 1, pp. 56–79, Feb. 2014, doi: 10.1016/j.progsurf.2013.11.001.

[88] D. Polag and F. Keppler, "Global Methane Emissions from the Human Body: Past, Present and Future," *Atmospheric Environment*, vol. 214, p. 116823, Oct. 2019, doi: 10.1016/j.atmosenv.2019.116823.

[89] R. C. Braun and D. J. Bremer, "Nitrous Oxide Emissions in Turfgrass Systems: A Review," *Agronomy Journal*, vol. 110, no. 6, pp. 2222–2232, Nov. 2018, doi: 10.2134/agronj2018.02.0133.

[90] T. J. Griffis, Z. Chen, J. M. Baker, J. D. Wood, D. B. Millet, X. Lee, R. T. Venterea, and P. A. Turner, "Nitrous Oxide Emissions are Enhanced in a Warmer and Wetter World," *Proc Natl Acad Sci USA*, vol. 114, no. 45, pp. 12081–12085, Nov. 2017, doi: 10.1073/pnas.1704552114.

[91] H. A. Patel, J. Byun, and C. T. Yavuz, "Carbon Dioxide Capture Adsorbents: Chemistry and Methods," *ChemSusChem*, vol. 10, no. 7, pp. 1303–1317, Apr. 2017, doi: 10.1002/cssc.201601545.

[92] E. Mahmoud, "Mitigating Global Methane Emissions Using Metal-Organic Framework Adsorbents," *Applied Sciences*, vol. 10, no. 21, p. 7733, Oct. 2020, doi: 10.3390/app10217733.

[93] A. Awadallah-F, F. Hillman, S. A. Al-Muhtaseb, and H.-K. Jeong, "Adsorption Equilibrium and Kinetics of Nitrogen, Methane and Carbon Dioxide Gases onto ZIF-8, $Cu_{10\%}$/ZIF-8, and $Cu_{30\%}$/ZIF-8," *Ind. Eng. Chem. Res.*, vol. 58, no. 16, pp. 6653–6661, Apr. 2019, doi: 10.1021/acs.iecr.8b05892.

[94] H. Long, H.-F. Lin, M. Yang, Y. Bai, X. Tong, X.-G. Kong, and S.-G. Li, "Adsorption and Diffusion Characteristics of CH_4, CO_2, And N_2 in Micropores and Mesopores of Bituminous Coal: Molecular Dynamics," *Fuel*, vol. 292, p. 120268, May 2021, doi: 10.1016/j.fuel.2021.120268.

[95] B. Vujić and A. P. Lyubartsev, "Transferable Force-Field for Modelling of CO_2, N_2, O_2 and Ar in All Silica and Na^+ Exchanged Zeolites," *Modelling Simul. Mater. Sci. Eng.*, vol. 24, no. 4, p. 045002, May 2016, doi: 10.1088/0965-0393/24/4/045002.

[96] O. F. Speer, B. C. Wengerter, and R. S. Taylor, "Molecular Dynamics Simulations of Simple Liquids," *J. Chem. Educ.*, vol. 81, no. 9, p. 1330, Sep. 2004, doi: 10.1021/ed081p1330.

[97] J. Vekeman, N. Faginas-Lago, A. Lombardi, A. Sánchez de Merás, I. García Cuesta, and M. Rosi, "Molecular Dynamics of CH_4/N_2 Mixtures on a Flexible Graphene Layer: Adsorption and Selectivity Case Study," *Front. Chem.*, vol. 7, p. 386, Jun. 2019, doi: 10.3389/fchem.2019.00386.

[98] J. P. Dürholt, G. Fraux, F.-X. Coudert, and R. Schmid, "Ab Initio Derived Force Fields for Zeolitic Imidazolate Frameworks: MOF-FF for ZIFs," *J. Chem. Theory Comput.*, vol. 15, no. 4, pp. 2420–2432, Apr. 2019, doi: 10.1021/acs.jctc.8b01041.

[99] K. Sladekova, C. Campbell, C. Grant, A. J. Fletcher, J. R. B. Gomes, and M. Jorge, "The Effect of Atomic Point Charges on Adsorption Isotherms of CO_2 and Water in Metal Organic Frameworks," *Adsorption*, vol. 26, no. 5, pp. 663–685, Jul. 2020, doi: 10.1007/s10450-019-00187-2.

[100] P. Naeiji, F. Varaminian, and M. Rahmati, "The Kinetic Modeling of Methane Hydrate Growth by Using Molecular Dynamic Simulations," *International Journal of Heat and Mass Transfer*, vol. 142, p. 118356, Oct. 2019, doi: 10.1016/j.ijheatmasstransfer.2019.07.006.

[101] J. A. Rackers, Z. Wang, C. Lu, M. L. Laury, L. Lagardère, M. J. Schnieders, J.-P. Piquemal, P. Ren, and J. W. Ponder, "Tinker 8: Software Tools for Molecular Design," *J.*

Chem. Theory Comput., vol. 14, no. 10, pp. 5273–5289, Oct. 2018, doi: 10.1021/acs.jctc.8b00529.

[102] Q. Li, M. Ruan, B. Lin, M. Zhao, Y. Zheng, and K. Wang, "Molecular Simulation Study of Metal Organic Frameworks for Methane Capture from Low-Concentration Coal Mine Methane Gas," *J Porous Mater*, vol. 23, no. 1, pp. 107–122, Feb. 2016, doi: 10.1007/s10934-015-0060-4.

[103] M. Kharatha, A. Vaez, and A. S. Hasan Rozatian, "Molecular Dynamics Simulation of Gas Adsorption on Defected Graphene," *Molecular Physics*, vol. 111, no. 24, pp. 3726–3732, Dec. 2013, doi: 10.1080/00268976.2013.785609.

[104] D. Li, P. Zhang, Q. Kang, Y. Han, and D. Shen, "Investigation of the Effect of Energy Variation and Structure Change on the Adsorption of Volatile Organic Compounds in ZIF-8 by a DFT Approach," *Microporous and Mesoporous Materials*, vol. 248, pp. 84–90, Aug. 2017, doi: 10.1016/j.micromeso.2017.03.029.

[105] D. Lee, Y. Jin, N. Jung, J. Lee, J. Lee, Y. S. Jeong, and S. Jeon, "Gravimetric Analysis of the Adsorption and Desorption of CO_2 on Amine-Functionalized Mesoporous Silica Mounted on a Microcantilever Array," *Environ. Sci. Technol.*, vol. 45, no. 13, pp. 5704–5709, Jul. 2011, doi: 10.1021/es200680v.

[106] D. P. Bezerra, R. S. Oliveira, R. S. Vieira, C. L. Cavalcante, and D. C. S. Azevedo, "Adsorption of CO_2 on Nitrogen-Enriched Activated Carbon and Zeolite 13X," *Adsorption*, vol. 17, no. 1, pp. 235–246, Feb. 2011, doi: 10.1007/s10450-011-9320-z.

[107] M. Sarmah, B. P. Baruah, and P. Khare, "A Comparison Between CO_2 Capturing Capacities of Fly Ash Based Composites of MEA/DMA and DEA/DMA," *Fuel Processing Technology*, vol. 106, pp. 490–497, Feb. 2013, doi: 10.1016/j.fuproc.2012.09.017.

[108] S. Gadipelli, W. Travis, W. Zhou, and Z. Guo, "A Thermally Derived and Optimized Structure from ZIF-8 with Giant Enhancement in CO_2 Uptake," *Energy Environ. Sci.*, vol. 7, no. 7, pp. 2232–2238, 2014, doi: 10.1039/C4EE01009D.

[109] M. Kamruddin, P. K. Ajikumar, S. Dash, A. K. Tyagi, and B. Raj, "Thermogravimetry-Evolved Gas Analysis-Mass Spectrometry System for Materials Research," *Bull Mater Sci*, vol. 26, no. 4, pp. 449–460, Jun. 2003, doi: 10.1007/BF02711191.

[110] J. U. Keller, E. Robens, and C. du Fresne von Hohenesche, "Thermogravimetric and Sorption Measurement Techniques/Instruments," in *Studies in Surface Science and Catalysis*, vol. 144, Elsevier, 2002, pp. 387–394. doi: 10.1016/S0167-2991(02)80159-8.

[111] E. Levintal, M. I. Dragila, H. Zafrir, and N. Weisbrod, "The Role of Atmospheric Conditions in CO_2 and Radon Emissions from an Abandoned Water Well," *Science of The Total Environment*, vol. 722, p. 137857, Jun. 2020, doi: 10.1016/j.scitotenv.2020.137857.

[112] B. D. Cano, "Caractérisation des Matériaux Commerciaux et Synthétisés Destinés à Adsorber le Méthane et l'Oxyde Nitreux Présents dans des Émissions Gazeuses et Modélisation de l'Adsorption," p. 175.

[113] A. Schejn, L. Balan, V. Falk, L. Aranda, G. Medjahdi, and R. Schneider, "Controlling ZIF-8 Nano- And Microcrystal Formation and Reactivity Through Zinc Salt Variations," *CrystEngComm*, vol. 16, no. 21, pp. 4493–4500, 2014, doi: 10.1039/C3CE42485E.

[114] A. Guo, Y. Ban, K. Yang, and W. Yang, "Metal-Organic Framework-Based Mixed Matrix Membranes: Synergetic Effect of Adsorption and Diffusion for CO_2/CH_4 Separation," *Journal of Membrane Science*, vol. 562, pp. 76–84, Sep. 2018, doi: 10.1016/j.memsci.2018.05.032.

[115] M. U. A. Prathap and S. Gunasekaran, "Rapid and Scalable Synthesis of Zeolitic Imidazole Framework (ZIF-8) and its Use for the Detection of Trace Levels of Nitroaromatic Explosives," *Adv. Sustainable Syst.*, vol. 2, no. 10, p. 1800053, Oct. 2018, doi: 10.1002/adsu.201800053.

[116] Z. Abbasi, E. Shamsaei, S. K. Leong, B. Ladewig, X. Zhang, and H. Wang, "Effect of Carbonization Temperature on Adsorption Property of ZIF-8 Derived Nanoporous Carbon for Water Treatment," *Microporous and Mesoporous Materials*, vol. 236, pp. 28–37, Dec. 2016, doi: 10.1016/j.micromeso.2016.08.022.

[117] A. Jomekian, R. M. Behbahani, T. Mohammadi, and A. Kargari, "CO_2/CH_4 Separation by High Performance Co-Casted ZIF-8/Pebax 1657/PES Mixed Matrix Membrane," *Journal of Natural Gas Science and Engineering*, vol. 31, pp. 562–574, Apr. 2016, doi: 10.1016/j.jngse.2016.03.067.

[118] N. T. Tran, J. Kim, and M. R. Othman, "Microporous ZIF-8 Membrane Prepared from Secondary Growth for Improved Propylene Permeance and Selectivity," *Microporous and Mesoporous Materials*, vol. 285, pp. 178–184, Sep. 2019, doi: 10.1016/j.micromeso.2019.05.010.

[119] D. Roy, S. Neogi, and S. De, "Adsorptive Removal of Heavy Metals from Battery Industry Effluent Using MOF Incorporated Polymeric Beads: A Combined Experimental and Modeling Approach," *Journal of Hazardous Materials*, vol. 403, p. 123624, Feb. 2021, doi: 10.1016/j.jhazmat.2020.123624.

[120] M. Yahia, Q. N. P. Le, N. Ismail, M. Essalhi, O. Sundman, A. Rahimpour, M. M. Dal.Cin, and N. Tavajohi, "Effect of Incorporating Different ZIF-8 Crystal Sizes in the Polymer of Intrinsic Microporosity, PIM-1, For CO_2/CH_4 Separation," *Microporous and Mesoporous Materials*, vol. 312, p. 110761, Jan. 2021, doi: 10.1016/j.micromeso.2020.110761.

[121] C. Wu, Z. Xiong, C. Li, and J. Zhang, "Zeolitic Imidazolate Metal Organic Framework ZIF-8 with Ultra-High Adsorption Capacity Bound Tetracycline in Aqueous Solution," *RSC Adv.*, vol. 5, no. 100, pp. 82127–82137, 2015, doi: 10.1039/C5RA15497A.

[122] Y. Ding, Y. Xu, B. Ding, Z. Li, F. Xie, F. Zhang, H. Wang, J. Liu, and X. Wang, "Structure Induced Selective Adsorption Performance of ZIF-8 Nanocrystals in Water," *Colloids and Surfaces A: Physicochemical and Engineering Aspects*, vol. 520, pp. 661–667, May 2017, doi: 10.1016/j.colsurfa.2017.02.012.

[123] L. Wang, M. Fang, J. Liu, J. He, L. Deng, J. Li, and J. Lei, "The Influence of Dispersed Phases on Polyamide/ZIF-8 Nanofiltration Membranes for Dye Removal from Water," *RSC Adv.*, vol. 5, no. 63, pp. 50942–50954, 2015, doi: 10.1039/C5RA06185G.

[124] M. Jian, B. Liu, G. Zhang, R. Liu, and X. Zhang, "Adsorptive Removal of Arsenic from Aqueous Solution by Zeolitic Imidazolate Framework-8 (ZIF-8) Nanoparticles," *Colloids and Surfaces A: Physicochemical and Engineering Aspects*, vol. 465, pp. 67–76, Jan. 2015, doi: 10.1016/j.colsurfa.2014.10.023.

[125] M. Thomas, B. N. Nair, G. M. Anilkumar, A. P. Mohamed, K. G. K. Warrier, and U. S. Hareesh, "Processing of thermally stable 3D hierarchical ZIF-8@ZnO structures and their CO2 adsorption studies," *Journal of Environmental Chemical Engineering*, vol. 4, no. 2, pp. 1442–1450, Jun. 2016, doi: 10.1016/j.jece.2016.01.043.

[126] J. McEwen, J.-D. Hayman, and A. Ozgur Yazaydin, "A Comparative Study of CO_2, CH_4 and N_2 Adsorption in ZIF-8, Zeolite-13X and BPL Activated Carbon," *Chemical Physics*, vol. 412, pp. 72–76, Feb. 2013, doi: 10.1016/j.chemphys.2012.12.012.